

UNIVERSITY OF CINCINNATI

Date: _____

I, _____,

hereby submit this original work as part of the requirements for the degree of:

in _____

It is entitled:

Student Signature: _____

This work and its defense approved by:

Committee Chair: _____

Approval of the electronic document:

I have reviewed the Thesis/Dissertation in its final electronic format and certify that it is an accurate copy of the document reviewed and approved by the committee.

Committee Chair signature: _____

Interactions with topoisomerase II α enhance the unwinding activity of the BLM helicase on recombination substrates and are necessary for preventing chromosome breakage

A dissertation submitted to the

Graduate School

of the University of Cincinnati

in partial fulfillment of the

requirement for the degree of

Doctor of Philosophy

In the Department of Molecular Genetics, Biochemistry & Microbiology

of the College of Medicine

by

Beatriz Russell

M.A. Boston University

April 2002

Committee Chair: Joanna Groden, Ph.D.

ABSTRACT

The BLM helicase is a member of the RecQ-like family of 3'-5' ATP- and Mg²⁺-dependent helicases. Cells deficient in BLM are characterized by increased sister chromatid exchanges, quadriradial structures and chromosome breaks, chromosome structures that suggest the disruption of normal mechanisms that resolve recombination intermediates and maintain chromosome stability. Previously identified interactions between yeast RecQ-like helicases and topoisomerases suggest cooperation in DNA transactions such as recombination repair and chromosome segregation. This work demonstrates that human BLM and topoisomerase II α interact directly. BLM and topoisomerase II α co-immunoprecipitate from human cells and co-localize in a cell cycle-specific manner. Their association and co-localization increases in S- and G₂/M- and is predominant in M-phase. *In vitro* binding assays demonstrate that amino acids 489-587 within the N-terminus of BLM are required for this interaction. *In vitro* biochemical analysis of the decatenation activity of topoisomerase II α in the presence of BLM revealed no effect by BLM. On the other hand, BLM helicase activity is enhanced approximately three- and five-fold by topoisomerase II α on a 3' overhang duplex and bubble substrates, respectively, but not an X-junction substrate. These data suggest that BLM and topoisomerase II α may be involved in the processing of early homologous replication intermediates, but not structures that form later. *In vivo*, *siRNA* mediated knock-down of either BLM, topoisomerase II α , or both in combination increased chromosome breakage to the same extent compared to a scrambled control knock-down, suggesting a common pathway that requires BLM and topoisomerase II α for protecting the integrity of genomic DNA.

In order to determine the importance of the BLM-topoisomerase II α interaction, a mutant BLM protein lacking the topoisomerase II α interaction domain (aa 489-587) was generated, EGFP-BLM ^{Δ 489-587}. The mutant protein was unable to co-immunoprecipitate topoisomerase II α , although it still localized to nuclear PML foci and the nucleolus as wild-type BLM. To determine the significance of their interaction on chromosome breakage, the ability of this mutant to reduce the high endogenous levels of γ H2AX foci of BS cells was tested. Transfection BS cells line with the EGFP-BLM ^{Δ 489-587} mutant protein did not reduce γ H2AX foci formation to the levels of transfection with a wild-type BLM protein, but exacerbated the number of γ H2AX foci in cells compared to untransfected cells. We propose that in the presence of BLM, cells commit to a BLM dependent pathway of double strand break repair and the inability of EGFP-BLM ^{Δ 489-587} mutant to bind topoisomerase II α locks the cells in such pathways without being able to correctly finish the repair. Taken together, these data suggest an involvement of BLM and topoisomerase II α in a pathway that prevents chromosome breakage. The *in vitro* biochemical data suggest that this pathway may involve the regulation of homologous recombination through the processing of DNA intermediates occurring at early stages of repair.

Acknowledgements

I would like to thank all the member of the Groden laboratory, both past and present, for generating reagents used in this work. Special thanks to some current members, Jeremy Keirse, April Sandy and Patrick Grierson, for their help in finishing experiments during my long commutes home. Dr. Samir Acharya, for his training on protein purification, and last but not least Joanna Groden for being such a supportive mentor and always encouraging me to think independently.

Finally, I would like to thank my family especially my husband, Casey Russell, for always being supportive of me pursuing a Ph.D. and for his constant help and support during the last four years complicated by a long daily commute.

Table of Contents

Abstract	iii
Acknowledgements	vi
Table of Contents	vii
List of Tables	xi
List of Figures	xi
Abbreviations	xii

CHAPTER ONE. Literature Review.

Introduction.	1
RecQ-like helicases.	5
Biochemical properties of BLM.	7
Cell cycle regulation and localization of BLM.	12
Protein binding partners of BLM.	12
Post-translational modifications of BLM and response to DNA damaging agents.	16
Role of BLM in DSB repair and replication fork restart.	17
Homologous recombination.	18
Anti-recombinogenic and anti-crossover roles of BLM in DSB repair.	19
Replication fork lesion bypass activity of BLM.	20
Pro-recombinogenic roles of BLM in DSB repair.	21
Role of BLM in non-homologous end-joining.	22
Role of BLM in telomere maintenance.	25

Role of BLM in chromosome segregation.	26
Conclusions.	27
CHAPTER TWO. Thesis Rationale and Research Objectives.	28
CHAPTER THREE. The interaction of BLM and topoisomerase IIα enhances BLM unwinding activity on recombination substrates.	
I. Introduction.	31
II. Materials and Methods.	
Cell lines, tissue culture and cell synchronization.	34
Immunoprecipitations.	35
Immunofluorescence.	36
In vitro transcription-translation (IVTT).	36
Pull-down assays.	37
Protein expression and purification.	38
Helicase assays.	38
Decatenation assays.	40
III. Results.	
BLM and topoisomerase II α co-immunoprecipitate and co-localize in human cells.	41
The association of BLM and topoisomerase II α is cell cycle-dependent.	42
BLM directly interacts with topoisomerase II α through amino acids 489-587 of BLM.	46

BLM does not alter topoisomerase II α decatenation activity.	49
Topoisomerase II α enhances the <i>in vitro</i> unwinding activity of BLM using DNA substrates representing early homologous recombination intermediates.	53
IV. Conclusions.	64

CHAPTER FOUR. BLM and topoisomerase II α interaction is necessary to prevent chromosome breaks.

I. Introduction.	65
II. Materials and Methods.	
Cell lines and synchronization.	66
Knock-down and comet assays.	67
Generation of pEGFP-BLM ^{Δ489-587} .	68
Immunoprecipitations.	69
Immunofluorescence.	69
III. Results.	
BLM and topoisomerase II α prevent chromosome breakage in a common pathway.	69
Amino acids 489-587 are necessary for binding topoisomerase II α .	72
The topoisomerase II α interaction domain of BLM is required for correction of increased chromosome breakage in BS cells.	74
IV. Conclusions.	77

CHAPTER FIVE. Thesis Summary and Discussion. 78

CHAPTER SIX. Bibliography. 87

List of Tables.

Table 1. BLM Interacting Proteins.	15
Table 2. Specific activity of BLM and BLM/TOPO II α on recombination substrates.	63

List of Figures.

Figure 1. Phenotypic and cytological properties of Bloom's syndrome.	4
Figure 2. Family of RecQ-like helicases.	6
Figure 3. <i>In vitro</i> DNA structures recognized and processed by BLM.	10
Figure 4. <i>In vitro</i> biochemical function of BLM on homologous recombination intermediates.	11
Figure 5. Pathways of homologous recombination.	23
Figure 6. Anti-recombinogenic and anti-crossover roles of BLM.	24
Figure 7. BLM and topoisomerase II α associate in asynchronous cells.	44
Figure 8. The association of BLM and topoisomerase II α is cell cycle-specific.	45
Figure 9. The interaction of BLM with topoisomerase II α occurs within the amino-terminus of BLM.	48
Figure 10. Purification scheme and validation of purified 6xHis-tagged BLM protein.	51
Figure 11. BLM does not affect the decatenation activity of topoisomerase II α .	52
Figure 12. Unwinding activity of BLM using recombination substrates.	57,58
Figure 13. Topoisomerase II α does not have unwinding activity.	59
Figure 14. BLM unwinding activity is enhanced by topoisomerase II α using a 3' overhang, bubble and a model replication fork substrates, but not with an X-junction substrate.	60-62

Figure 15. Comet tail size does not change following <i>siRNA</i> -mediated knock-down of BLM, topoisomerase II α , and both in combination.	71
Figure 16. Amino acids 489-587 of BLM are necessary for topoisomerase II α binding.	73
Figure 17. The interaction of BLM and topoisomerase II α is necessary to revert the breakage phenotype of BS cells.	76
Figure 18. Model for BLM and topoisomerase II α possible involvement in double strand break repair.	86

Abbreviations

ALT	Alternative lengthening of telomeres
ATLD	ataxia telangiectasia-like disorder
ATM	Ataxia telangiectasia mutated protein
ATR	ATM and Rad3-related protein
BASC	BRCA1-associated genome surveillance complex
BLAP	BLM-associated polypeptide
BS	Bloom's syndrome
BTB	BLM-topoisomerase III α -BLAP75-BLAP18 complex
CAF-1	Chromatin assembly factor 1
D-loop	Displacement loop
DSB	Double strand breaks
DSBR	Double strand break repair
EXO1	Exonuclease 1
FA	Fanconi anemia
FBS	Fetal bovine serum
FEN1	Flap endonuclease-1
FPLC	Fast protein liquid chromatography
HR	Homologous recombination
HRDC	Helicase and RNase D C-terminal
HSP90	Heat shock protein 90
HU	Hydroxyurea
IR	Ionizing radiation

IVTT	<i>In vitro</i> transcription-translation
LOH	Loss of heterozygosity
MMS	Methyl methanesulfonate
MPS1	Monopolar spindle kinase 1
MRN	MRE11/RAD50/NBS1 complex
NHEJ	Non-homologous end-joining
NLS	Nuclear localization sequence
PBS	phosphate buffered saline
PLK1	Polo-like Kinase 1
PML	Promyelocytic leukemia protein
Qr	Quadriradial structure
RFC	Replication factor C
RPA	Replication protein A
RQC	RecQ C-terminal
RT	Rothmund-Thomson syndrome
SCE	Sister chromatid exchange
SDSA	Synthesis-dependent strand annealing
SSA	Single strand annealing
SSB	Single stranded DNA-binding
TA	Telomere association
TEP1	Telomerase-associated protein 1
TRF	TTAGGG repeat factor 2
UV	Ultraviolet

WS

Werner's syndrome

CHAPTER ONE. Literature Review.

Introduction.

Bloom's syndrome (BS) was first described by Dr. David Bloom in 1954 [1]. Approximately 10 years later, the increased chromosomal breakage and cytological characteristics of BS cells were reported [2]. BS is a rare autosomal recessive disorder in which affected individuals show pre- and post-natal growth retardation, sun-sensitive facial erythema, immunodeficiency, male infertility and female subfertility (Figure 1A). BS individuals are predisposed to a plethora of cancers often occurring by the age of 25 [3]. These are not limited to, but most often include, leukemias and lymphomas, colon, breast and skin cancers [4]. Immunodeficiency may be associated with, although mutational events may also be related to, the increased incidence of non-Hodgkin's lymphomas, acute lymphocytic leukemia and acute non-lymphocytic leukemia in younger BS individuals [5]. Adaptive immunity is compromised in BS, as a decrease in IgM secretion has been observed in some BS persons [6,7]. Ear and upper respiratory tract infections are common, making pulmonary disease the second highest cause of death in BS individuals [7].

Cytogenetically, the hallmark of BS cells is excessive sister chromatid exchange (SCE) (Figure 1B, Panel a.), approximately 5-10 fold higher than in normal cells [8]. Quadri-radial structures (Qrs) (Figure 1B, Panel b.) formed by unresolved somatic recombination events between homologous chromosomes are observed in 1% of BS cells [8]; they are extremely rare in normal cells. These structures represent intra- and inter-chromosomal recombination, respectively, suggesting that BLM plays a role in regulating recombination events. Increased somatic recombination can lead to loss of heterozygosity (LOH), the consequence of which is

associated with increased tumor formation. Telomere associations (TAs) (Figure 1B, Panel c.) are also visible in metaphases of BS cells, a subset of which appear as end-to-end fusions [9]. Finally, chromosome breaks (Figure 1B, Panel d.) and gaps occur in high frequency in BS cells [2,10]. The appearance of micronuclei is elevated in BS cells and is an indirect measure of chromosome breaks or inappropriate replication [11]. A retarded rate of DNA chain elongation is also characteristic of BS cells suggesting defective replication [12]. In total, these observations provided the first insight into the molecular mechanisms that leads to the chromosomal instability, hyper-mutability and increased cancer predisposition observed in BS individuals.

Increased recombination rates of BS cells led to the identification of the gene responsible for BS [13]. Although the diagnostic feature of BS is high SCE, some individuals possess a small population of lymphocytes with low SCE. The low SCE lymphocytes were proposed to have arisen from a recombination event in compound heterozygotes that led to the correction of one *BLM* allele through intragenic recombination of two mutant alleles. *BLM* was identified using an approach referred to as somatic crossover point mapping in which comparison of regions of heterozygosity in high SCE cells that were reduced to homozygosity in the low SCE cells were used to pin-point the position of the *BLM* locus [13]. *BLM* was mapped to chromosome 15q26.1 [14-16].

To date, numerous mutations (64) have been found throughout *BLM* in BS individuals [4]. Fifty-four of the mutations are nonsense mutations, generating transcripts degraded by nonsense-mediated mRNA decay. One such mutation, the *Blm^{Ash}* allele, consists of a 6 bp deletion and 7 bp insertion creating a nonsense codon; it has been extensively used in human population studies since it occurs in high frequency among Ashkenazi Jews due to a founder

effect [13,17]. The remaining ten mutant alleles include missense mutations, some of which affect the nuclear localization of BLM, although the protein remains enzymatically active (helicase activity), and others that completely abrogate enzymatic activity. Interestingly, these mutations are grouped in the helicase and RQC domains of BLM [4]. The domains of RecQ-like helicases are discussed below.

A.



B.

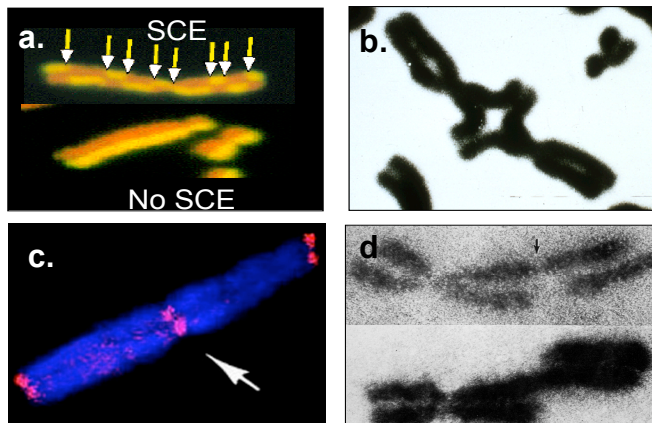


Figure 1. Phenotypic and cytological properties of Bloom's syndrome. A. Photograph depicting the small stature of a young BS male (right) next to an average size male (left). B. Panel a. Sister chromatid exchanges representative of recombination between sister chromatids. Panel b. Quadriradial structures representative of recombination between homologous chromosomes. Panel c. Telomere associations. Panel d. Double strand breaks and gaps in BS metaphase chromosomes. Photographs courtesy of Dr. James L. German.

RecQ-like helicases.

The cloning of *BLM* revealed a gene with sequence homology to the *Escherichia coli* (*E. coli*) RecQ helicase [13]. The RecQ family of helicases is highly conserved throughout evolution. The *E. coli* RecQ protein, which functions in the RecF pathway of recombination, is the prototypical member of this family and the sole *E. coli* RecQ helicase. *Saccharomyces cerevisiae* (*S. cerevisiae*) and *Schizosaccharomyces pombe* (*S. pombe*) have only one RecQ-like gene, *Sgs1* and *Rqh1*, respectively [18,19]. In contrast to bacteria and yeast, multiple RecQ-like helicases are found in multicellular organisms; *Homo sapiens* have five [20] (Figure 2).

Members of the human RecQ-like family of helicases include BLM, mutations in which lead to Bloom's syndrome; WRN, the protein mutated in Werner's syndrome (WS); RecQL4, the protein mutated in Rothmund-Thomson (RT), RAPADILINO and Baller-Gerold syndromes [21]; and RecQL1 and RecQL5, neither of which has been associated with a genetic disorder. Individuals with WS show accelerated aging and have an elevated incidence of sarcomas [5]. Individuals with RT have poikiloderma of the face and develop osteogenic sarcomas [22]. Individuals with RAPADILINO syndrome are characterized by short stature, radial ray defects and other malformations, but have not been reported to have cancer predisposition [23]. Baller-Gerold syndrome is characterized by radial aplasia/hypoplasia and craniosynostosis [21].

The enzymatic activity of RecQ-like helicases is ATP- and Mg²⁺-dependent with 3'-5' directionality. Most need a 3' overhang to initiate their activity [24], although this is not a structural requirement for unwinding by some RecQ-like helicases [25]. The helicase domain spans approximately 350-400 amino acids (blue box in Figure 2) and it is often centrally located in the protein.

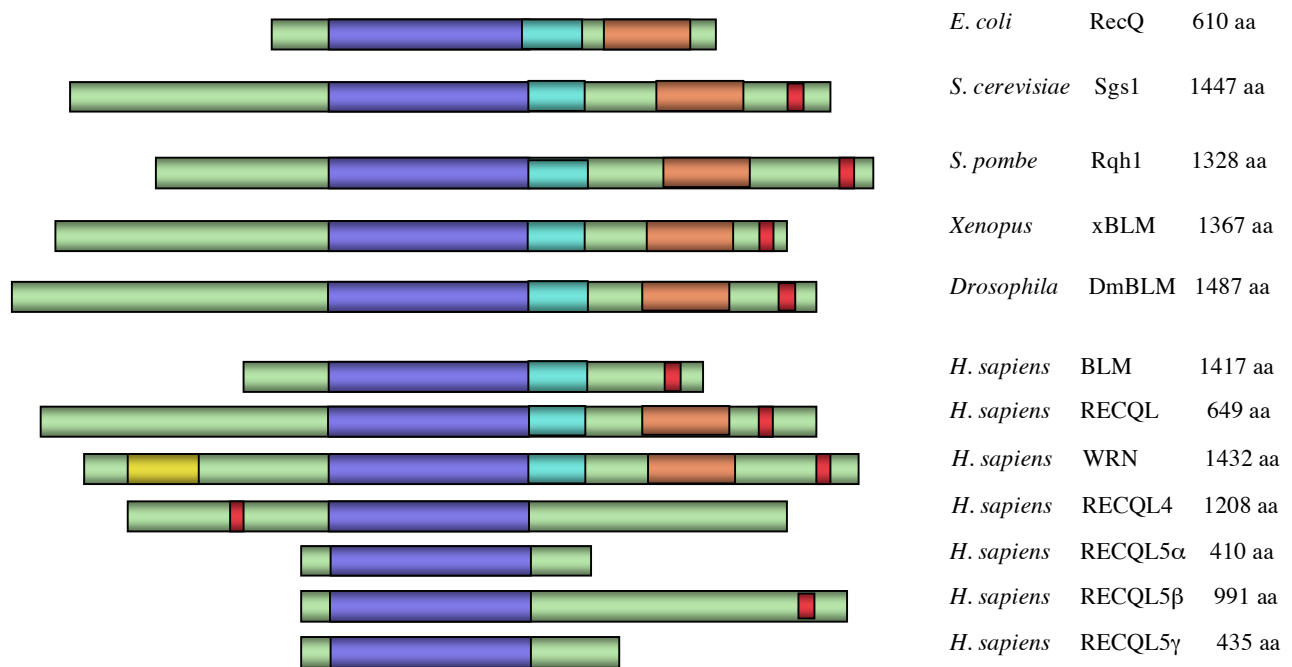


Figure 2. Family of RecQ-like helicases. Schematic representation of RecQ helicases from bacteria, yeast, xenopus, drosophila and humans. The blue box represents the conserved helicase domain, the cyan box represents the RQC (RecQ C-terminal) domain, the orange box represents the HRDC (Helicase and RNase D C-terminal) domain, the red box represents the nuclear localization signal, and the yellow box represents the exonuclease domain of WRN.

The helicase domain of BLM contains seven motifs conserved among RecQ helicases; I, Ia, II, III, IV, V, and VI. Motifs I and II contain Walker A and B boxes, characteristic of ATPases needed for ATP binding and hydrolysis [24]. Motif Ia and III to VI code for conserved protein structures unique to RecQ helicases presumably used in substrate binding and unwinding [5]. Carboxy-terminal to the helicase domain is the conserved RQC (RecQ C-terminal) domain that defines this family [26]; further toward the C-terminus is the HRDC domain (Helicase and RNase D C-terminal), common to RNA helicases although BLM is not categorized as an RNA helicase, it can unwind RNA-DNA duplexes [27]. In BLM, this domain is necessary for the specific recognition and binding to a double Holliday junction [28], a function of BLM that will be discussed later. Also found in the C-terminus of the majority of RecQ-like helicase is a nuclear localization sequence (NLS) [26,29]. RecQL4 contains the NLS within the N-terminus and splice variants of RecQL5, α and γ , do not possess a NLS. RecQ helicases have little homology outside of the central helicase domain, and their N- and C-termini vary greatly in length [30] (Figure 2). WRN contains an exonuclease domain at the N-terminus. This activity is not common to RecQ-like helicases. It has been proposed that the Ku heterodimer allows WRN exonuclease to digest through regions that contain 8-oxoadenine and 8-oxoguanidine modifications, suggesting a role for both WRN and the Ku heterodimer in a common DNA repair pathway [31].

Biochemical properties of BLM.

The helicase activity of BLM is ATP- and Mg^{2+} - dependent with 3'-5' directionality [32]. Size exclusion chromatography and electron microscopy demonstrate that BLM forms predominantly hexameric ring structures with a diameter of 13 nm and a central hole of 3.5 nm. The most enzymatically active form of BLM has an apparent molecular mass of > 700 kDa [33].

This is consistent with the observation that the majority of helicases work as dimers or hexamers [34]. BLM does not unwind blunt-ended double helices [25,32], and has poor processivity on dsDNA with a 3' tail (Figure 3A). RPA can enhance its processivity two-fold, presumably by stabilizing regions of single strandedness [35], an enhancement that is specific, as SSB (single-stranded DNA-binding) protein from *E. coli* does not have the same effect [35,36].

Other BLM substrates include G4 DNA, or G tetraplex DNA [37], (Figure 3B), a structure that can form *in vivo* in regions of the genome with an abundance of G-tracks, such as telomeres and rDNA gene clusters [37]. Triple helices (Figure 3C) that form when a third DNA strand binds in the major groove of duplex DNA containing polypurine:polypyrimidine sequences are also disrupted *in vitro* by BLM [38].

Most importantly, BLM is proficient in the unwinding of a number of DNA substrates observed during recombination, including duplex DNA containing a bubble [25] (Figure 3D and Figure 4A), displacement loops (D-loops) [39] (Figure 3E and Figure 4B) and X-junctions [40] (Figure 3F and Figure 4C). Double Holliday junctions [41] (Figure 3G and Figure 4D) can be processed in order to eliminate crossovers by the action of the BTB complex composed of BLM-topoisomerase III α -BLAP75-BLAP18 (BLM-associated polypeptide) [41-43] (Figure 4D). It is proposed that BLM is able to allow lesion bypass of a stalled replication fork. Biochemical assays on a model replication fork [44] (Figure 3H and Figure 4E) suggest that BLM is able to carry out fork regression [44], followed by reverse branch migration thus facilitating the bypass of DNA damage without initiation of homologous recombination (HR) [40] (Figure 4E). *In vitro* substrate processing, therefore, strongly suggests that BLM is able to disrupt structures that form during HR perhaps to shift the repair of damaged DNA towards mechanisms that do not use

recombination. Additionally, if HR takes place, the BTB complex is able to process double Holliday junctions eliminating the production of crossovers.

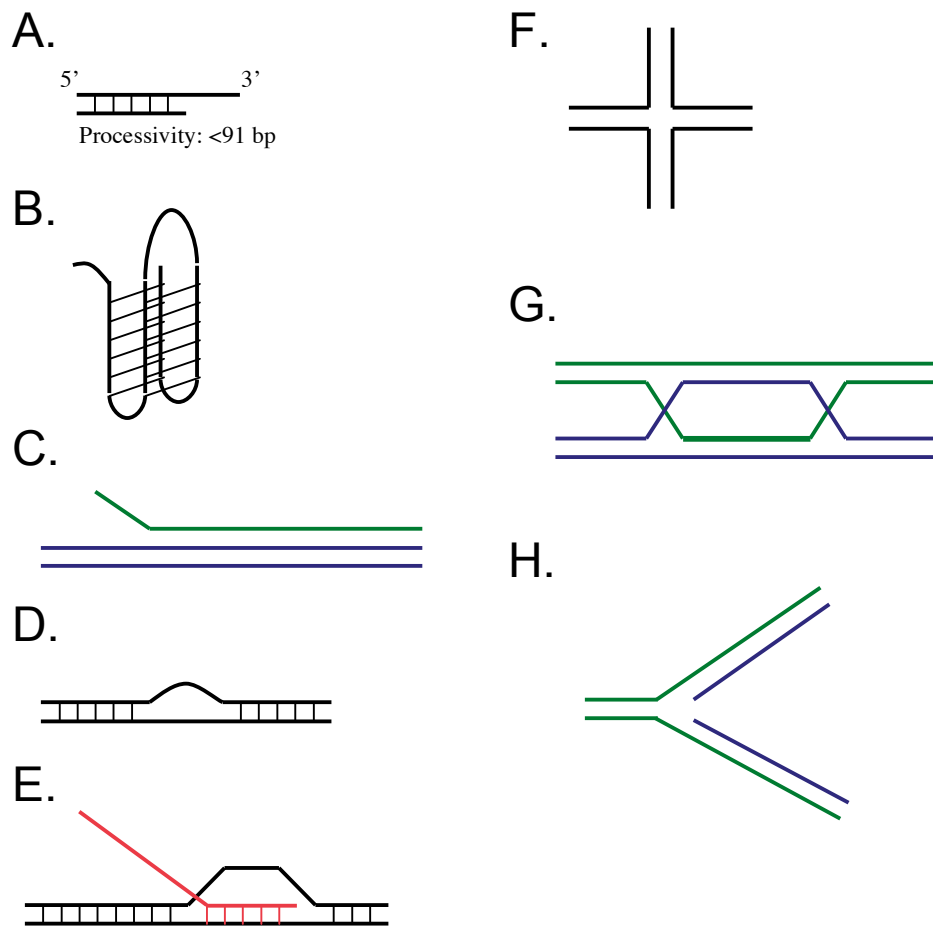


Figure 3. *In vitro* DNA structures recognized and processed by BLM. A. BLM unwinds double stranded duplexes with a 3' overhang, B. G-tetraplex or G4 DNA, which form in G rich sequences and C. triple helices. DNA structures representing early HR intermediates processed by BLM include D. a duplex with an internal bubble and E. a D-loop. DNA structures representing late HR intermediates processed by BLM include F. Holliday junctions or X-junctions and G. double Holliday junctions, which are resolved *in vitro* by the concerted action of BLM-topoisomerase III α -BLAP75-BLAP18. H. Model replication forks representing stalled replication forks can be subject to reverse branch migration by BLM generating a "chicken foot" structure.

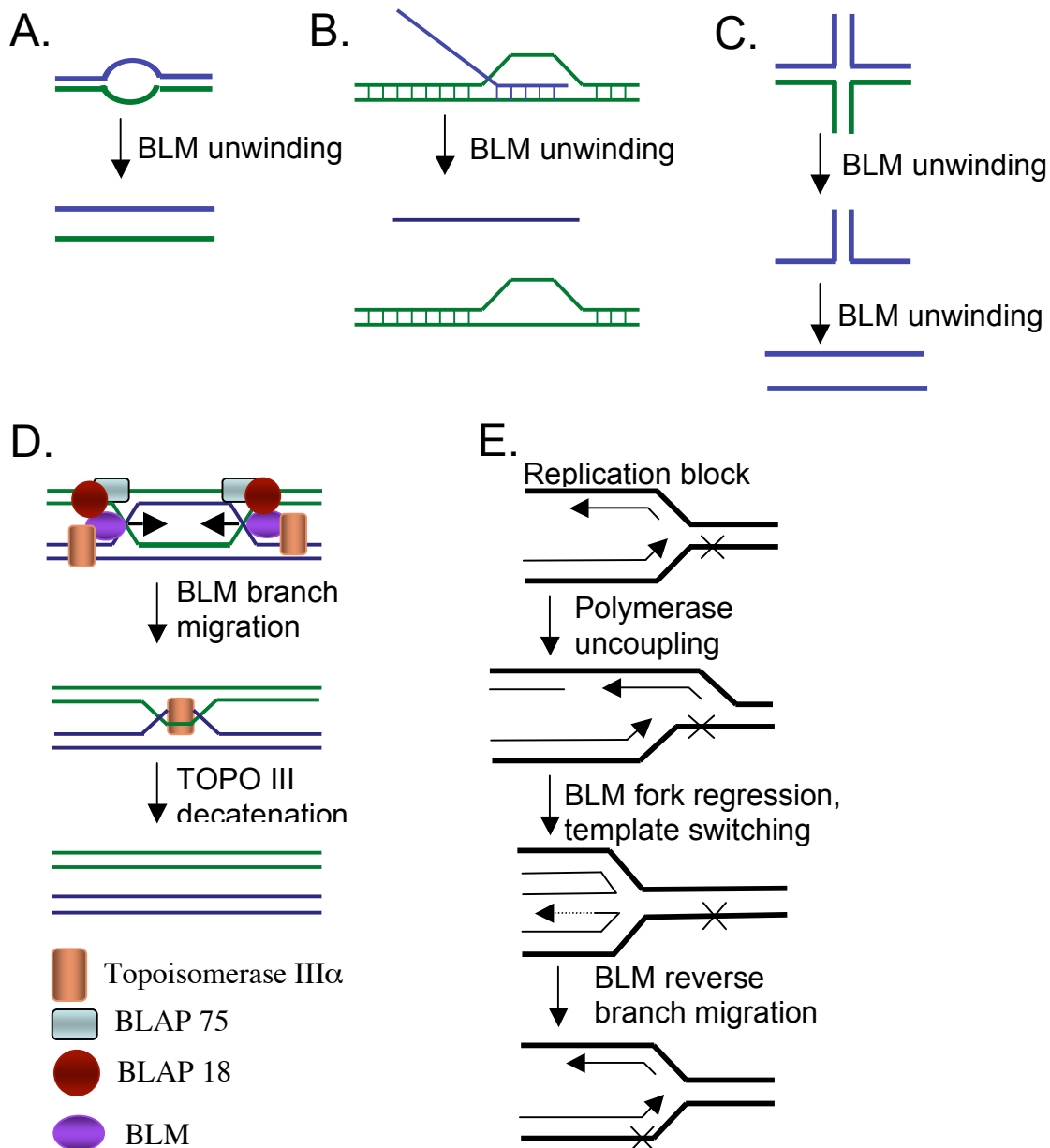


Figure 4. *In vitro* biochemical functions of BLM on homologous recombination intermediates. A. BLM is able to unwind a bubble substrate. B. BLM can remove the invading strand of a D-loop leaving a bubble. C. A Holliday junction can be processed *in vitro* by BLM in a two step reaction. First, BLM is responsible for unwinding of two of the four strands and second BLM is able to process the two strand leading to single stranded products. D. A double Holliday junction is processed by the action of the BTB complex composed of BLM-topoisomerase III α -BLAP75-BLAP18 to yield non-crossover products exclusively. E. Lesions in DNA can lead to polymerase uncoupling from the replication fork. In order to reestablish the fork, BLM promotes fork regression leading to a “chicken foot” structure that allows template switching. Following replication, BLM initiates reverse branch migration restoring the replication fork.

Cell cycle regulation and localization of BLM.

The expression of BLM is cell cycle-regulated and limited to highly proliferative tissues, such as lymphoid tissues, skin and gut epithelium [45]. Accumulation of BLM begins in early S-phase, with protein levels peaking in late S-phase and G2; high levels of BLM persist until mitosis followed by a dramatic drop in G1 [46]. BLM is a nuclear protein containing a bipartite NLS in its C-terminus [47]. It is distributed in bright foci in promyelocytic leukemia (PML) bodies throughout the cell cycle except in S-phase where it is localized the nucleolus [11,48]. PML bodies, also called ND10, are nuclear matrix-associated protein depots where localized RNA transcription and splicing, DNA replication and DNA repair are reported to take place. In G1/S-synchronized cells, BLM localizes in the nuclear fraction and the matrix [49]. In S/G2, BLM is found in the matrix, co-localized with RAD51 and RPA [48]. Mitotic BLM is highly phosphorylated and retains helicase activity, but is excluded from the nuclear matrix [46]. Dutertre *et al.* have suggested that mitotic exclusion of BLM from the NP-40 insoluble fraction (chromatin and matrix) detains BLM from interfering with processes such as chromosome condensation [50]. On the other hand, in response to DNA damage, BLM is recruited to the NP-40 insoluble sites to aid in DNA repair [46], increasing the number of BLM foci per cell [48].

Protein binding partners of BLM.

BLM is reported to be a member of two protein super-complexes. BASC (BRCA1-associated genome surveillance complex) is composed of BRCA1, BLM, the mismatch repair proteins MSH2, MSH6 and MLH1, the checkpoint kinase ataxia telangiectasia mutated (ATM), the homologous recombination complex, MRE11, RAD50 and NBS1, and Replication Factor C (RFC) [51]. This complex is proposed to patrol the genome, mediating repair at the sites of

damage. The second super-complex termed BRAFT, includes BLM, RPA, the Fanconi anemia (FA) core complex (FANCA, C, E, F and G proteins) and topoisomerase III α . This complex possesses DNA unwinding activity and is thought to function in the processing of aberrant structures resulting from DNA replication or repair [52]. The isolation of this complex provided the first evidence that FA proteins are involved in DNA repair and established a link between BS and FA, two chromosome instability disorders.

BLM physically interacts with topoisomerase III α ; their interaction is necessary for the *in vitro* processing of double Holliday junctions in a manner leading exclusively to non-crossover products [41] (Figure 4D). Two other proteins were later identified as integral components of the double Holliday junction dissolvasome, BLAP75 and BLAP18 [43,53,54]. These four proteins comprise the BTB complex. BLAP75 and BLAP18 enhance the BLM/topoisomerase III α dissolution of double Holliday junctions *in vitro*. *In vivo*, depletion of BLAP75 by *siRNA* leads to an increase in SCE similar to BS cells [55]. Depletion of BLAP18 lead to destabilization of the BTB complex, chromosome breaks, and sensitivity to methyl methanesulfonate (MMS).

Recently, double immunoprecipitation assays in cells that employ an alternative lengthening of telomeres (ALT) pathway, showed that BLM and the TTAGGG repeat factor 2 protein (TRF2) reside in a complex with the telomerase-associated protein 1 (TEP1), heat shock protein 90 (HSP90) and topoisomerase II α . These three proteins co-localize with BLM and TRF2 during late S- G2/M phases when ALT is proposed to take place and at sites of on-going replication. *In vitro*, HSP90 inhibited the helicase activity of BLM using a telomeric substrate, while TEP1 and topoisomerase II α slightly inhibited the initial unwinding kinetics [56]. Future

experiments will determine the molecular mechanism employed by these proteins and perhaps others in the maintenance of telomere ends using ALT.

Many other proteins bind directly or associate with BLM (Table 1). These include replication protein A (RPA), which stimulates the processivity of BLM [35,36]; RAD51, involved in the start of HR [57]; FANCD2, involved in replication blocks due to cross-linking agents [58]; chromatin assembly factor 1 (CAF-1), necessary for chromatin assembly-coupled DNA damage repair or replication blockade [59]; p12, the smallest subunit of DNA polymerase δ recruits BLM to sites of stalled DNA replication and BLM enhances the activity of polymerase δ by allowing the continuation of replication past forked structures [60]; DNA polymerase η synthesis on substrates that resemble one end of the D-loop is stimulated by BLM [61]; the mismatch repair proteins MSH2/6 and MLH1, for possible regulation of fidelity during recombination events [62-65]; TRF1 and TRF2 [66-68], proteins that modulate the activity of BLM on telomeric substrates; p53, for proper localization of p53 to sites of stalled replication forks and interaction with RAD51 [69]; WRN, its exonuclease activity is inhibited by BLM [70]; flap endonuclease-1 (FEN1), suggested to process intermediates of DNA replication and repair [71]; exonuclease 1 (EXO1), for which BLM enhances nuclease activity leading to the generation of a 3' overhang then used by RAD51 [72]; ATM, to phosphorylate BLM upon radiation-induced damage on residue T99 [73]; 53BP1, to recruit BLM to sites of HU-induced replication arrest [74] and CHK1, phosphorylates BLM on residue T99 in order to mediate the interaction with 53BP1 [75].

Table 1. BLM Interacting Proteins.

Interacting protein	Function of complex with BLM	Reference
RPA	Replication/DNA repair	[35]
BASC	Genome surveillance	[51]
FANC core complex	Replication repair	[52]
FANCD2	Replication repair	[58]
RAD51	Replication repair via HR	[57]
53BP1	Replication repair via HR	[75]
ATM	Replication repair via HR	[73]
CHK1	Replication repair via HR	[75]
γ H2AX	Replication repair	[74]
EXO1	Replication repair via HR	[72]
CAF-1	Replication repair via HR	[59]
p12	Replication repair via HR	[60]
DNA polymerase η	Replication repair	[61]
FEN1	Replication repair	[71]
p53	Recombination/ Apoptosis	[69]
MLH1	Fidelity of end joining events	[63,64]
MSH2/6	Fidelity of end joining events	[62,65]
WRN	Recombination?	[70]
TRF1	Telomere maintenance	[68]
TRF2	Telomere maintenance	[66]
TEP1	Telomere maintenance	[56]
HSP90	Telomere maintenance	[56]
TOPO II α	Telomere maintenance	[56]
Top2p (yeast)	Chromosome segregation	[76]
PLK1	Chromosome segregation	[77]
TOPO III	Double Holliday junction resolution	[41]
BLAP75	Double Holliday junction resolution	[53]
BLAP18	Double Holliday junction resolution	[43]

Post-translational modifications and response to DNA damaging agents.

Post-translational modifications of proteins further control the activity of proteins via their localization, association with protein partner(s), or through degradation. These modifications include phosphorylation, ubiquitination, acetylation, and sumoylation. Phosphatase assays indicate that a change in electrophoretic mobility of mitotic BLM compared to non-mitotic BLM is due primarily to phosphorylation [46]. Three kinases have been implicated in the mitotic phosphorylation of BLM. Western blot analysis of wild type and ATM-deficient cells arrested in mitosis revealed that ATM is partially responsible for the mitotic phosphorylation of BLM [73], although the specific residues phosphorylated by ATM were not identified. Also, mitosis arrested cells treated with roscovitine, a specific inhibitor of Cdc2, display a complete reversal of mitotic BLM phosphorylation [50], suggesting that Cdc2 is also responsible mitotic phosphorylation events on BLM. Additionally, the monopolar spindle 1 kinase (MPS1) phosphorylates BLM during mitosis [77] at S144 to allow interaction with Polo-like kinase 1 (PLK1), a mitotic kinase. Disruption of this interaction, tested via a phosphorylation mutant (BLM^{S144A}), leads to disruption of chromosome numbers, suggesting that mitotic phosphorylation and interaction with PLK1 are necessary for accurate chromosome segregation.

BLM is phosphorylated in response to different types of DNA-damaging agents by the ATM and ATR (ATM and Rad3-related) kinases, upstream kinases in DNA damage checkpoints [73,78-82]. Both kinases are members of the phosphatidylinositol-3 kinase family. ATM is primarily involved in checkpoint activation following damage by ionizing radiation (IR) and radiomimetic agents, while ATR is involved in the response to ultraviolet light (UV) and hydroxyurea (HU) [83].

In response to stalled replication forks induced by treatment of cells with HU, BLM is phosphorylated at residues T99 and T122 in an ATR-dependent manner [80,82]. This phosphorylation event is important for the recruitment of other repair proteins, as a BLM double phosphorylation mutant, $BLM^{T99A/T122A}$, is unable to recruit the MRE11/RAD50/NBS1 complex to RAD51 foci following HU treatment [11,80].

Following exposure to IR and other agents leading to double strand breaks (DSB), *BLM* mRNA levels increase about four-fold leading to a ten-fold increase in BLM protein that localizes to RAD51 foci [57], presumed sites of HR-mediated repair. The increase in protein levels and localization is concomitant with an ATM-dependent phosphorylation at residue T99 [73,78]. BS cells are sensitive to IR during S- and G2-phases, and show increased chromosome breaks following irradiation [84]. Interestingly an ATM phosphorylation mutant, BLM^{T99A} , is unable to rescue IR sensitivity of BS cells, suggesting that the phosphorylation status of BLM is important for its role in IR-induced damage [73].

Finally, BLM is modified by SUMO-1 and SUMO-2 at residues K317, K331, K334 and K374. Eladad et al. showed that BLM sumoylation was needed for BLM recruitment to PML bodies. A BLM SUMO-binding mutant, containing arginine mutations at residues 317 and 331 did not accumulate in PML bodies and induced the formation of DNA damage foci containing BRCA1 and γ H2AX. Therefore, lack of BLM sumoylation and exclusion from PML bodies leads to constitutively active DNA damage signaling [85].

Role of BLM in DSB repair and replication fork restart.

Accurate replication and repair of DNA is essential to maintain genome integrity. Double strand breaks (DSB) are the most deleterious lesions encountered by the genome [86-88]. If not

repaired, exposed DNA ends are subject to degradation by nucleases leading to deletions. DSB also lead to loss of chromosome fragments, duplications and translocations, events associated with tumor formation. DSBs can be generated by endogenous and exogenous agents, such as by-products of metabolism and IR, respectively. Eukaryotic cells have evolved two distinct mechanisms to repair DSB. HR is an error-free pathway that uses the information of a homologous sister chromatid or chromosome to repair the break (Figure 5). This method of repair is mostly used during S- and G2-phases of the cell cycle due to the availability of a sister chromatid. Non-homologous end-joining (NHEJ) is an error-prone pathway that leads to deletions and is mainly employed in G1.

Homologous recombination.

HR is carried out by the proteins encoded by the RAD52 epistasis group and include RAD51, RAD52, RAD54 and the MRE11/RAD50/NBS1 (MRN) complex [89]. There are two models of HR, each of which begins with the formation of a 3' end that invades the homologous DNA strand [90]. The action of the MRN complex may be used to resect the 5' strand leading to a 3' overhang. *In vitro* evidence though, suggests that an exonuclease other than MRE11 may be involved in the resection since in order to generate a 3' overhang, exonuclease activity in the 5' to 3' direction is necessary and MRE11 has 3' to 5' exonuclease activity. EXO1 has been proposed to function as the exonuclease that fulfills this role [91]. Nevertheless, the MRN complex is necessary to tether the two ends of the breaks. The generated 3' overhang is quickly coated with RPA [92]. RAD52 binds to the 3' overhang, protecting the overhang from further exonuclease digestion. Binding of BRCA2 to RAD51 facilitates RAD51-mediated strand invasion of the homologous sister chromatid generating a D-loop. The invading 3' overhang primes the start of replication using the donor duplex as a template (Figure 4, top panel). In

synthesis-dependent strand annealing (SDSA), resection, strand invasion, priming and replication occur in the same manner. Following extension of the invading strand, this strand is displaced and can anneal to its complementary strand at the other side of the break. The remaining gap is filled and ligated. This process leads to non-crossover products [93] (Figure 4, left panel).

According to the double-strand break-repair (DSBR) model, the other end of the break is free to anneal to the displaced donor strand that can also prime replication. The resulting intermediate, a double Holliday junction, is then resolved to crossover or non-crossover products [93] (Figure 4, right panel).

HR is also employed in the recovery of stalled replication forks from single strand breaks. During replication restart, resection, strand invasion, priming and replication occur as previously described. In this model, if repair begins before the upstream replication fork meets the single strand break generating a DSB, a second strand to anneal to the displaced donor strand does not exist, therefore, the recombination intermediate is known as a Holliday junction [94]. Resolution of the Holliday junction leads to a crossover product (SCE) half the time.

Anti-recombinogenic and anti-crossover roles of BLM in DSB repair.

BS cells show two cytological signs of deregulated HR: Qrs, pairs of homologous chromosomes undergoing recombination [8]; and SCE, inter-chromosomal exchanges between sister chromatids [6]. These observations suggest that BLM prevents excessive recombination and crossover events from taking place. DSBs are processed by the action of the proteins involved in HR leading to the generation of a 3' overhang that is coated by RAD51. Biochemical evidence shows that BLM promotes RAD51 filament disruption, to establish repair by non-recombination mechanisms such as single strand annealing (SSA) or non-homologous end joining (NHEJ) (Figure 6A). Evidence also shows that BLM can melt the RAD51-associated D-

loop [95], freeing the 3' overhang for repair by SSA or NHEJ [91] (Figure 6B). In SSA the ends of the break are processed by a 5' to 3' exonuclease, exposing regions of complementarity that anneal. DNA synthesis fills in the gaps followed by ligation [90]. The process of NHEJ is discussed below.

The ability of BLM to carry out RAD51 filament disruption is only possible when RAD51 is in its inactive ADP-bound form. Once the activation of RAD51 takes place, repair of the break will proceed through a recombination mediated pathway [96] (Figure 6C). At this stage, BLM is proposed to melt the D-loop structure after replication has taken place. Following displacement, BLM pairs this strand with the complementary strand at the other side of the break through its strand annealing activity [97], restoring the duplex DNA molecule without further processing by resolvases [91] (Figure 6D). Biochemical evidence also suggests that in the event that second strand capture and branch migration takes place, the BTB complex can process double Holliday junction in a manner exclusively leading to non-crossover products (Figure 6E) [41].

Replication fork lesion bypass activity of BLM.

Slow fork progression, abnormal distribution of DNA intermediates [98], and high sensitivity to HU and other replication inhibiting drugs [82] in BS cells suggest a role for BLM in the restart of DNA replication during S-phase. Additionally, the replication forks of BS cells do not properly recover from HU treatment, leading to an accumulation of DSB [99]. A role in lesion bypass of stalled replication forks for BLM is supported by biochemical assays on a model replication fork [44] in which BLM was able to carry out fork regression allowing template switching and polymerase extension. BLM then carries out reverse branch migration

reestablishing the replication fork. This biochemical activity bypasses the DNA lesion without initiating HR [40] (Figure 4E).

Other evidence implicates BLM in S-phase checkpoint arrest. BLM localization to repair foci permits its association with the ATR/CHK1/53BP1 complex [74], proteins necessary for checkpoint signaling. ATR-mediated phosphorylation of BLM on T99 is required for binding 53BP1. BLM binding to 53BP1 is also enhanced by CHK1-mediated phosphorylation of 53BP1. BLM then enhances the interaction between 53BP1 and RAD51 disrupting RAD51 filament formation [61,75]. Under low replication stress, BLM then attempts to reestablish the fork via fork regression and reverse branch migration. It has been proposed that under high replication stress conditions, BLM transmits the signals from the ATR/CHK1/53BP1 complex to RAD51 allowing repair to take place via HR [74].

Pro-recombinogenic roles of BLM in DSB repair.

The localization of BLM at sites of replication stress with γ H2AX occurs within minutes of treatment with HU suggesting that BLM is one of the first responders to stalled replication forks [80,100]. BLM is partially responsible for the co-localization of the MRN complex and BRCA1 to the repair foci [69,100,101], proteins that initiate the DNA processing for HR. Once cells commit to damage repair via HR, BLM is still able to reduce the amount of crossovers generated by acting in the later stages of HR as described above.

Biochemical evidence also suggests a pro-recombinogenic role for BLM in the processing of early HR intermediates. An interaction between BLM and EXO1 has been reported to stimulate EXO1 resection of DNA ends to enable DNA strand exchange by RAD51 [72]. Additionally, BLM stimulates DNA Pol η DNA synthesis on substrates that resemble one end of the D-loop [61] and was also reported to interact with p12, the small subunit of DNA Pol

δ. The latter interaction enhances DNA Pol δ strand displacement activity, allowing replication within structures that are forked [60].

Role of BLM in non-homologous end-joining.

When the homologous sister chromatid is not available, DSB repair proceeds through NHEJ. In this pathway, the two ends of the break are processed to expose areas of microhomology by the action of the Ku70/Ku86 heterodimer and DNA-PKcs. XRCC4 and DNA ligase IV ligate the two ends. This pathway of repair is error-prone leading to small deletions [87]. NHEJ is most prevalent in G1-phase when it is difficult to find a homologous chromosome for homologous recombination [89].

NHEJ is highly error-prone in BS cells. Langland et al. found that BS cell extracts were unable to align areas of nearby microhomology, which in turn led to small deletions [102]. Similarly, Gaymes et al. observed aberrant NHEJ in BS cells in which ligation took place at distant sites of microhomology resulting in very large deletions [103]. Such studies suggest a role for BLM in the alignment of microhomologies in NHEJ.



Figure 5. Pathways of homologous recombination. Double strand breaks arising from ionizing radiation or single strand breaks during replication are repaired by homologous recombination by resection of the break leading to a 3' overhang. The 3' overhang is used in strand invasion of the homologous sister chromatid generating a displacement loop (D-loop). In synthesis-dependent strand annealing (SDSA), the invading strand is displaced and can anneal to its complementary strand at the other side of the break. The remaining gap is filled and ligated leading to non-crossover product. According to the double-strand break-repair (DSBR) model, the other end of the break is free to anneal to the displaced donor strand that can also prime replication. The resulting intermediate, a double Holliday junction, is then resolved to crossover or non-crossover products. Figure modified from [90].

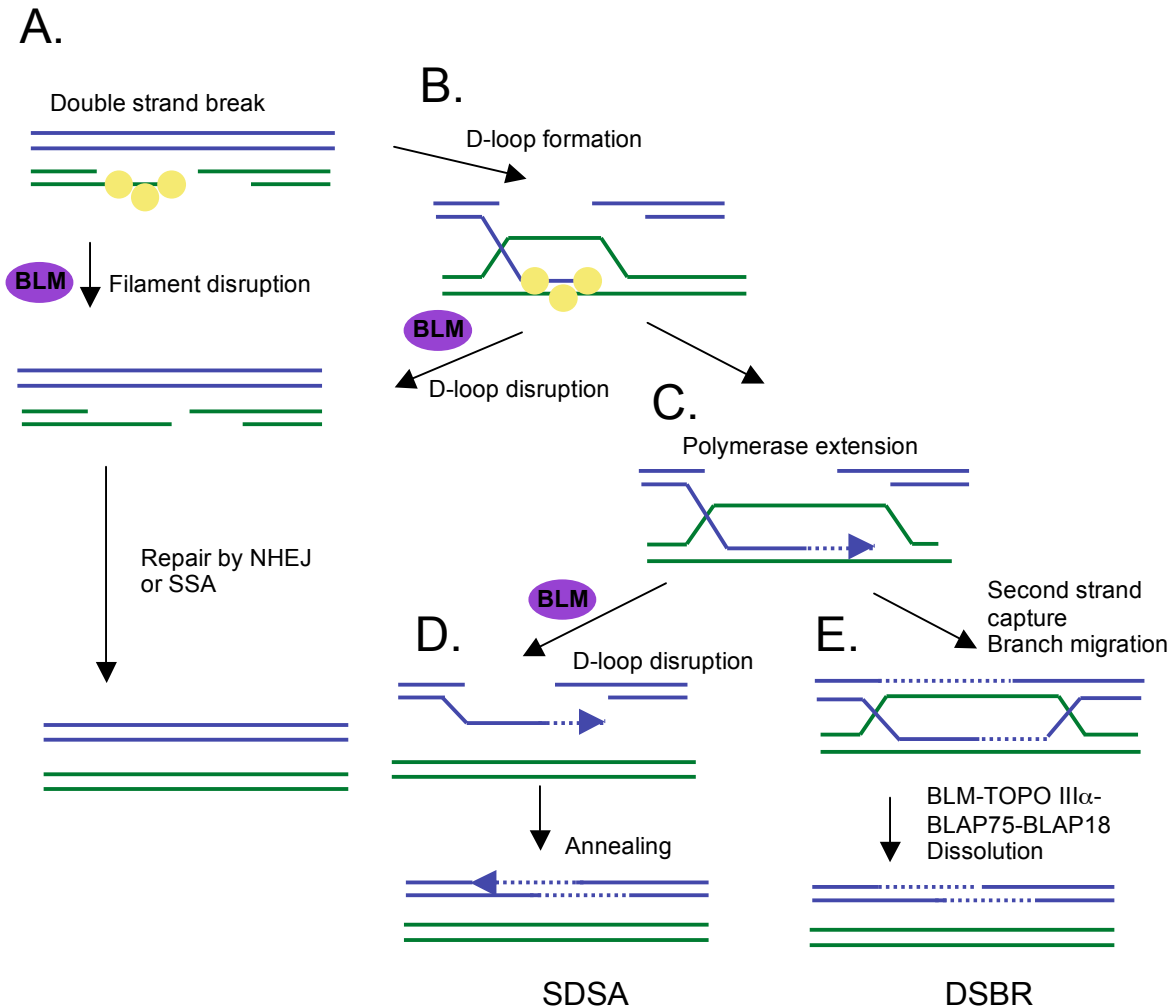


Figure 6. Anti-recombinogenic and anti-crossover roles of BLM. A. BLM promotes RAD51 (yellow circles) filament disruption allowing the break to be repaired by SSA or NHEJ. B. BLM can melt the RAD51-associated D-loop, freeing the 3' overhang for repair by SSA or NHEJ. C. Activation of RAD51 commits repair via HR allowing polymerase extension. D. BLM can melt the D-loop structure after replication has taken place and use its strand annealing activity to pair this strand with the complementary strand at the other side of the break. This action restores the duplex DNA molecule without further processing by resolvases (SDSA). E. If second strand capture and branch migration takes place, the BTB complex can process double Holliday junction in a manner exclusively leading to non-crossover products (DSBR). Figure modified from [61].

Role of BLM in telomere maintenance

Cells lacking telomerase activity maintain telomere length through a recombination-mediated mechanism known as ALT, or alternative lengthening of telomeres [104]. In budding yeast, ALT mechanisms are characterized by the generation of two types of cells: type I survivors with amplification of subtelomeric Y' elements or short telomere repeat tracts at the termini; and type II survivors with abrupt additions of long tracts of telomere repeats. Both mechanisms are dependent on RAD52 [105]; type I is also dependent on RAD51; type II is dependent on RAD50 and Sgs1 [66,106].

Various lines of evidence suggest that in humans, BLM, much like Sgs1, plays a role in telomere lengthening via an ALT pathway. A small subset of sub-telomere probes co-localize with BLM and chromatin immunoprecipitation, or ChIP, localizes BLM to telomeric DNA repeats [107] suggesting the presence of BLM at telomeres. More specifically as it pertains to the ALT mechanism, transient over-expression of BLM increases ALT-specific telomeric DNA [66]. *In vivo* and *in vitro* experiments with both TRF1 and TRF2, proteins involved in telomere maintenance, show that these proteins physically interact with BLM to regulate its helicase activity [67]. This evidence suggests a model in which RPA binding to BLM permits the unwinding of long telomere duplex regions prebound by TRF2, where TRF2 binding to BLM enhances its helicase activity [67]. TRF1 binding to BLM, in contrast to TRF2, selectively inhibits DNA unwinding by BLM at telomeric repeat sequences *in vitro* even in the presence of TRF2 [68] suggesting a dynamic regulation of BLM by the TRF proteins in order to maintain telomere length in cells that use ALT. Recently, other ALT-specific BLM interacting proteins have been identified and include TEP1, HSP90 and topoisomerase II α , although the precise role of these interactions remains to be elucidated [56].

Role of BLM in chromosome segregation.

Topoisomerases belong to two families: type I and type II. Type I topoisomerases create a transient single stranded break on one DNA strand allowing passage of the unbroken strand through the break to relieve supercoiling. In humans, type I topoisomerases include topoisomerase I, III α and III β . Type II topoisomerases, functioning as homodimers, cleave both strands of a DNA duplex to allow passage of another double stranded DNA molecule through the break, unknotting or decatenating the DNA molecules. In humans, type II topoisomerases include topoisomerase II α and II β [108,109].

The interaction between helicases and topoisomerases is not surprising, since unwinding by helicases leads to tension upstream of the DNA strand that can be released by the action of topoisomerases. As discussed above, BLM interaction with the type I topoisomerase, topoisomerase III α , promotes the dissolution of double Holliday junctions. The interaction between type II topoisomerases and RecQ-like helicases is also documented. In yeast, Sgs1 interacts directly with Top2p, an interaction required for faithful chromosome segregation [76]. A temperature-sensitive mutant of Top2 (CH1110 strain) grown at the semipermissive temperature shows a 10-fold increase in chromosome missegregation, measured by red sectoring in yeast colonies. The Δ *sgs1* strain showed similar levels of missegregation. Crossing of the Δ *sgs1* strain to CH1110 strain followed by growth at the semipermissive temperature did not increase chromosome missegregation over that seen in the CH1110 strain, suggesting that Sgs1 and Top2 may function in the same segregation pathway.

In mammalian cells, BLM is localized to fine anaphase bridges with topoisomerase III α and BLAP75. The PICH protein, which links centromeric regions of DNA, is also contained in these BLM-DNA bridges. BS cells display excessive levels of anaphase bridging and lagging

chromosomes [110]. These structures represent incompletely segregated chromosomes and could give rise to chromosome breaks generated by the mitotic spindle forces [96]. Additionally, as mentioned earlier, the mitotic phosphorylation of BLM by MPS1 at residue S144 allows BLM interaction with PLK1, and this event is necessary for BLM's interaction with PLK1 and perhaps accurate chromosome segregation [77]. These observations suggest that BLM may also have a role in chromosome segregation in mammalian cells.

Conclusions.

BS cells are characterized by hyper-recombination in the form of increased SCE and Qrs, chromosome instability observed as DSB, and sensitivity to genotoxic agents. BLM appears to exert its genome-stabilizing effect via multiple mechanisms including its lesion bypass activity in order to reset a stalled replication fork, through interactions with proteins involved in DSBR including HR and NHEJ, chromosome segregation and telomere maintenance. The work presented here will focus on determining reasons why BS cells have increased chromosome breaks. Therefore, this thesis will investigate the interaction of BLM with a type II topoisomerase, topoisomerase II α , in order to understand the processing of DNA structures found in mitosis (i.e. catenated DNA) and those representing HR intermediates that when inappropriately processed could result in DSB. This work will also investigate if the interaction of BLM and topoisomerase II α is needed in order to prevent the increased chromosome breakage observed in BS cells.

CHAPTER TWO. Thesis Rationale and Research Objectives.

Double strand breaks are one of the most deleterious insults to DNA and can lead to point mutations, small and large deletions, chromosome loss, duplication and translocation [93]. Such events are also associated with tumors in humans, underlining the importance of proper double strand break (DSB) repair [87]. All cells have evolved DSB repair mechanisms to maintain the integrity of DNA via two distinct mechanisms, homologous recombination (HR) and non-homologous end-joining (NHEJ) [86-88]. Increasing evidence suggests a role for BLM in the repair of DSBs through either of these pathways. The involvement of BLM in HR ensures that intermediates are processed in a manner leading to non-crossovers [41]. Immunofluorescence evidence suggests that BLM is one of the first proteins that co-localize to DSB and that its presence aids in the recruitment of other repair and checkpoint proteins to the damage site [69,74,75,80,100] ensuring proper processing of DSBs. In the NHEJ mechanism, BLM is suggested to be important in the alignment of microhomology [102,103].

Chromosome breakage was one of the first distinguishing cytological characteristics of cells from individuals with BS [10]. These abnormalities included isochromatid breaks and associated displaced acentric fragments, or apparently telocentric chromosomal fragments, dicentric chromosomes, triradials, asymmetric quadriradial configurations and abnormal monocentric chromosomes. Such chromosome breaks are highly reminiscent of those in cells where the activity of topoisomerase II α is inhibited [111]. BS cells display excessive levels of anaphase bridging and lagging chromosomes [110], structures that represent incompletely segregated chromosomes and could give rise to chromosome breaks generated by the mitotic spindle forces [96]. This observation suggests that BLM may be involved in chromosome segregation and its

function may be necessary to prevent breakage. In *Saccharomyces cerevisiae*, the BLM ortholog Sgs1, binds to a type II topoisomerase and their action is required for proper chromosome segregation [76]. These observations suggested that we test whether the BLM helicase interacts directly or indirectly with the mammalian type II topoisomerase, topoisomerase II α , and whether the increased chromosome breakage of BS cells results from the disrupted interaction of BLM and topoisomerase II α .

The interaction of a RecQ-like helicase with a type II topoisomerase had not been demonstrated in mammalian cells, but had been reported in *S. cerevisiae* [76] and therefore, posed an interesting line of investigation. This work focuses on determining reasons why BS cells have increased chromosome breaks. We reasoned there could be at least two possible explanations as to why. First, as stressed above, defects in HR lead to accumulation of DSB, and BLM is proposed to function at multiple stages of DSBR. Second, residual tanglement in chromosomes leads breakage as the chromosomes attempt to migrate to opposite poles during mitosis. We asked whether BLM and topoisomerase II α interact in mammalian cells and if this interaction was direct. In order to establish a potential mechanism of action, we not only assayed the effect of BLM on the ability of topoisomerase II α to decatenate DNA substrates, but we also assayed the effect of topoisomerase II α on the helicase activity of BLM on several of its DNA substrates representing HR intermediates.

This work tests the hypothesis that the interaction of BLM and topoisomerase II α is necessary for proper processing of DNA structures in order to prevent chromosomes breaks. *In vivo* and *in vitro* binding assays were employed to determine the association characteristics of the two proteins and the mapping of the interaction domain within BLM. Biochemical assays determined the *in vitro* effects on the catalytic activities of each protein in the presence of the

other. Finally, somatic cell genetic approaches determined the cytological and cell cycle consequences of the loss or disruption of the BLM and topoisomerase II α interaction.

CHAPTER THREE. The interaction of BLM and topoisomerase II α enhances BLM unwinding activity on early recombination substrates.

I. Introduction.

Homologous recombination (HR) is a process by which cells repair double strand breaks (DSBs) with the use of a homologous sister chromatid or homologous chromosome. This process is highly regulated in cells, as the exchange or loss of genetic material contributes to genetic variation in daughter cells that may lead to tumor formation. DSBs can be created by endogenous and exogenous cellular agents such as by-products of metabolism or ionizing radiation (IR), respectively.

The importance of properly recognizing and processing DSBs is underscored by the fact that mutations in the genes involved in HR lead to genomic instability and cancer in humans. The proteins encoded by *NBS1*, *MRE11* and *BRCA2* perform important functions in the process of HR. The proteins MRE11, RAD50 and NBS1 associate to form the MRN complex. This complex functions as a tether between the two ends of the double strand break and it has been proposed to be necessary for the generation of the 3' overhang [91]. Mutations in the *NBS1* gene lead to Nijmegen breakage syndrome [112]. This syndrome is characterized by increased cancer incidence, defects in cell cycle checkpoints, radiation sensitivity and immunodeficiency [113]. Mutations in *MRE11* lead to an ataxia telangiectasia-like disorder (ATLD). The BRCA2 protein serves its function in HR by facilitating RAD51 strand invasion [94]. Fanconi anemia, also characterized by genomic instability and cancer predisposition, results from mutations in the *BRCA2* (*FANCD1*) gene, or other genes in the Fanconi anemia complementation groups, (A, B, C, D2, E, F, G, I, J, L, M and N) [114,115].

Mutations in the *BLM* gene lead to excessive HR manifested as elevated levels of sister chromatid exchanges (SCE), suggesting the importance of BLM in the process of HR [8]. Loss of BLM leads to Bloom's syndrome (BS), a recessive disorder in which affected individuals are predisposed to a plethora of cancers including those epithelial in nature; colon, breast and skin cancers, and leukemias and lymphomas [4].

The precise role of BLM in DSBR is not yet fully understood. Several lines of evidence suggest its involvement at multiple stages of repair that either promote or inhibit HR. The proposed roles of BLM in DSBR are described in detail in Chapter 1 Figure 6. Briefly, in the early stages of DSBR, BLM is proposed to disrupt RAD51 filament formation, either before or after D-loop formation, shifting the equilibrium away from recombination repair and towards SSA or NHEJ [116]. Following polymerase extension of the invading strand, D-loop disruption by BLM allows repair via the SDSA branch of HR. If second strand capture takes place, DSBR branch, the BTB complex dissolves the double Holliday junction leading to non-crossovers [41,43,53].

The evidence presented above suggests an anti-recombinogenic role, but recent biochemical data propose that BLM could be playing a positive role in HR. BLM is reported to interact with EXO1, an interaction that stimulates EXO1 resection of DNA ends *in vitro*, presumably enabling DNA strand exchange by RAD51 [72]. Additionally, purified BLM is able to stimulate DNA Pol η DNA synthesis on substrates that resemble one end of the D-loop [61], and BLM also interacts with p12, the small subunit of DNA Pol δ . The latter interaction enhances DNA Pol δ strand displacement activity, allowing replication past forked DNA structures such as bubbles and D-loops [60].

BLM carries out its biochemical activities alongside its protein-binding partners. An interaction of BLM with topoisomerase III is conserved throughout evolution. The interaction between a type II topoisomerase and a RecQ-like helicase is documented in the budding yeast where an interaction of Sgs1 and Top2p is required for faithful chromosome segregation [76]. This interaction, not previously reported in mammalian cells until recently in ALT cells by our laboratory [56], prompted the question as to whether or not this interaction is also conserved in mammalian cells. Additionally, a similarity in cellular phenotypes in the form of chromosome breakage in both BS cells [10] and in cells in which the enzymatic activity of topoisomerase II α is inhibited [111] further warranted this question and whether or not these proteins are involved in a pathway that regulates the integrity of DNA.

The work in this chapter focuses on determining if an interaction of BLM with a type II topoisomerase is conserved in mammalian cells and the biochemical consequences this interaction might have. We began by asking whether BLM and topoisomerase II α interact in mammalian cells and if this interaction was direct and if so, what is the biochemical consequence of their interaction. This work shows that BLM and topoisomerase II α associate in mammalian cells in a cell cycle-dependent manner. Their association is enhanced in S- and G₂-phases and is most prominent during mitosis. *In vitro* pull-down assays show that the association occurs through physical interaction via amino acids 489-587 of BLM. *In vitro* decatenation assays with human purified topoisomerase II α showed that BLM did not have an effect on the decatenation activity of topoisomerase II α . Interestingly, *in vitro* BLM helicase activity is enhanced approximately three- and five-fold by equimolar topoisomerase II α using early HR intermediates such as 3' overhangs and bubble substrates, respectively. On the other hand, topoisomerase II α had a mild but inhibitory effect on BLM processing of an X-junction substrate, an intermediate

observed at later stages. These biochemical data suggest that BLM and topoisomerase II α could be involved in the early processing of HR intermediates, but perhaps not those occurring at later stages of repair.

II. Materials and Methods.

Cell lines, tissue culture and cell synchronization- Cell lines used in this study include 293T (human embryonic kidney cell line), HeLa (cervical cancer cell line), MCF7 (breast cancer cell line) and HCT116 (colorectal cancer cell line). Cells were obtained from the American Tissue Culture Collection (Rockville, MD). 293T, HeLa and MCF7 were cultured in Dulbecco's Modified Eagle Medium (DMEM) (Invitrogen) containing 10% fetal bovine serum (FBS) (Hyclone). HCT116 cells were cultured in McCoy's Eagle Medium with 10% FBS. All cells were grown at 37°C in 5% CO₂. To obtain cell extracts for cell cycle specific co-immunoprecipitations, 293T and HCT116 cells were first synchronized with a double-thymidine block. Cells were treated with 2mM thymidine (Sigma) in DMEM or McCoy's Eagle Medium, respectively, for 16 hours followed by removal of the thymidine containing media and two washes with phosphate buffered saline (PBS) (Invitrogen). The cells were allowed to continue growth for 8 hours, at which time, thymidine-containing media was added. Following 16 hours of treatment, the cells were washed with PBS and released into fresh media. To obtain cells at S- and G₂/M-phases, cells were harvested at 1 and 6 hours post-release, respectively. To obtain cells in G₁- or M-phases, 293T and HCT116 cells were treated with 200 μ g/mL nocodazole (Sigma) for 16 hours, released into fresh media and harvested 16 or 6 hours post-release, respectively.

Immunoprecipitations- Asynchronous or synchronized 293T and HeLa cells were treated using hypotonic solution A (10 mM HEPES pH 7.9, 10 mM KCl, 1.5 mM MgCl₂, 0.3 M sucrose, 10% glycerol, 10 mM NaF, 1 mM PMSF, 1 mM NaVO₄ and protease inhibitor cocktail (Sigma)) for 10 minutes on ice in order to lyse the cytoplasmic membrane. Intact nuclei were separated from cytoplasm by centrifugation at 3,400 rpm for 4 minutes at 4°C. Nuclei were lysed in hypotonic solution A on ice for 10 minutes and sonicated with two 10 second pulses of a Fisher Scientific 550 model sonic dismembrator with the wave amplitude set at 40%. Broken nuclei were further treated with 500 units of Micrococcal nuclease (USB) and 10 mM CaCl₂ for 1 hour on ice to digest the DNA. Proteins were further extracted from remaining chromatin by treatment with 300 mM NaCl and 0.1% triton X-100 on ice for 10 minutes. Lysed nuclei were cleared by centrifugation at 13,000 rpm for 20 minutes at 4°C. Nuclear extracts (4 mg) were pre-cleared with protein A/G agarose beads (Santa Cruz Biotechnology) for 1 hour at 4°C with rotation in Buffer Z (50 mM Tris HCl pH 8, 20% glycerol, 150 mM NaCl, 1 mM DTT, 0.1% NP-40, 500 mM KCl, 1 mM PMSF and protease inhibitor cocktail). The pre-cleared extracts were used in immunoprecipitations with 10 µg of BLM antibody (A300-110A, Bethyl Laboratories) overnight at 4°C with rotation. Protein-antibody complexes were bound to protein A/G agarose beads by incubation at 4°C with rotation for 45 minutes. Agarose beads were precipitated by centrifugation at 2,000 rpm for 1 minute and washed 2X Buffer Z for 10 minutes at 4°C with rotation followed by one final wash with 200 mM NaCl (final concentration) for the same amount of time. Proteins were separated using 4-12% Tris-glycine polyacrylamide gel electrophoresis (Invitrogen), transferred to PVDF membrane (Millipore) and visualized by western blotting using antibodies specific for BLM (A300-110A, Bethyl Laboratories, Inc.),

topoisomerase II α (Ab-1, Calbiochem), or topoisomerase III α (N-20, Santa Cruz Biotechnology).

Immunofluorescence- MCF7 and HCT116 cells were cultured on glass cover-slips in 6 well plates to 50% confluency. Cells were transfected with 4 μ g of *pEGFP-BLM* expression vector using Lipofectamine 2000 (Invitrogen) in Opti-MEM media for 5 hours at 37°C and 5% CO₂. Following transfection, cells were synchronized as described above. At appropriate times following release from synchronization, cells were fixed with 4% formalin for 20 minutes and washed 3 times with PBS. The cells were then permeabilized with PBT (0.1% Triton X-100 in PBS) for 10 minutes and blocked for 1 hour in 5% BSA, 6% goat serum in PBT. Cells were stained for one hour at 37°C and 5% CO₂ with an antibody against topoisomerase II α (Ab-1, Lab Vision) used at 1:500 in 2% BSA in PBT. Following three 10 minute washes with PBS, the cells were stained with a Rhodamine conjugated secondary antibody (Jackson ImmunoResearch) used at 1:700 in 2% BSA in PBT for 30 minutes at 37°C and 5% CO₂. Nuclei were stained with DAPI after three 5 minutes washes with PBS and viewed using an Axiovert 200M Zeiss microscope with Axio Vision 4.5 software.

In vitro transcription-translation (IVTT)- IVTT reactions with BLM segments, N (aa 1-587), H (aa 588-1000) and C (aa 996-1417) were carried out using *pET*-vectors containing the indicated BLM segments (*pET24D-BLM-N*, *pET24D-BLM-H* and *pET30A-BLM-C*, generated and characterized in [63]) and Rabbit reticulocyte IVTT reaction kit (Promega) according to manufacturer's instructions with [³⁵S]-methionine (Perkin Elmer). IVTT BLM-N-terminal segments, 1-587, 101-587, 203-587, 301-587, 401-587 and 1-488 were generated using the TNT

T7 Quick for PCR DNA kit (Promega) following manufacture's instructions with [³⁵S]-methionine. PCR products for the BLM-N-terminal segments were obtained from the *pET-BLMN* vector using the following primers. Segment 1-587, primers BLM N1 (5'-AAGCTGGATCCTAATACGACTCACTATAGGGAGCCACCATGGCTGCTGTTCCCTC-3') and BLM NR587 (5'-GATCTTTACTTGATGGGTTGATAGGC-3'); segment 101-587, primers BLM N101 (5'-AAGCTGGATCCTAATACGACTCACTATAGGGAGCCACCATG GGTGGATCAAATC-3') and BLM NR587; segment 203-587, primers BLM N203 (5'-AAGCT GGATCC TAATACGACTCACTATAGGGAGCCACCATGGTAAAGACTGATTTGC-3') and BLM NR587; segment 301-587, primers BLM N301 (5'-AAGCTGGATCC TAATACGACTCACTATAGGG AG CCACCATGCCACCTTCTCCAGAAG-3') and BLM NR587; segment 401-587, primers BLM N401 (5'-AAGCT GGATCC TAATACGACTCACTATAGGG AG CCACCATGCTTCAGCAGCGGAAC-3') and BLM NR587; and segment 1-488, primers BLM N1 and BLM NR488 (5'-GATCTTTACCTTTCAAAAAGATTCTTCC-3').

Pull-down assays- In vitro pull-down assays with BLM protein segments were carried out with 400 ng of human topoisomerase II α (USB) and 30 μ L of each IVTT reaction in topoisomerase II α assay buffer (10 mM Tris pH 7.9, 50 mM NaCl, 50 mM KCl, 5 mM MgCl₂, 0.1 mM EDTA, 1 mM ATP, with additional 0.05% Triton X-100, 1 mM PMSF and protease inhibitor cocktail) (USB). Following binding for 2 hours at 4°C, topoisomerase II α was immunoprecipitated with 3 μ g of topoisomerase II α -specific antibody (ab2987, Abcam), followed by binding to Protein A/G agarose beads (Santa Cruz Biotechnology). Rabbit IgG was used as a control (Jackson ImmunoResearch). Proteins were separated using 4-12% Tris-glycine polyacrylamide gel electrophoresis (Invitrogen) and visualized by autoradiography.

Protein expression and purification- The *pYES* expression vectors containing 6xHis-tagged-BLM, BLM^{D795A} (helicase-dead mutant) or β -galactosidase were overexpressed in the *S. cerevisiae* strain JEL1. Transformed yeast were grown in 1L of -Ura DO + minimal base and 2% glucose in an orbital shaker at 30°C. Protein expression was induced at an OD₆₀₀ of 1.2-1.4 by switching cells to growth in media containing 2% galactose. Cells were grown for an additional 16 hours, pelleted and resuspended in 30 mL of lysis buffer (50 mM KPO₄ pH 7.0, 500 mM KCl, 10% glycerol, 1 mM PMSF and protease inhibitor cocktail (Sigma)). Cells were lysed using a french press at 20K psi, cleared by ultracentrifugation and purified by FPLC on nickel resin, Ni-NTA (Qiagen). An initial 35 mM imidazole wash was followed by a 50 mL gradient from 35 mM to 250 mM imidazole. All 6xHis-tagged proteins eluted off the nickel resin at 121-185 mM imidazole. Fractions containing desired protein were pooled and dialyzed (50 mM Tris pH 7.5_{RT}, 10 % glycerol, 100 mM NaCl, 1 mM PMSF and protease inhibitor cocktail). Dialyzed fractions were loaded on a Q-sepharose column (Sigma) and washed at 100 mM NaCl followed by a 10 mL gradient from 150 mM to 1 M NaCl. Pure 6xHis-tagged proteins eluted at 221-351 mM NaCl. Fractions containing proteins were dialyzed in final storage buffer (25 mM Tris pH 7.5_{RT}, 20% glycerol, 1 mM DTT, 1 mM EDTA, 200 mM NaCl, 1 mM PMSF and protease inhibitor cocktail) and snap-frozen at -80°C.

Helicase assays- The 3' overhang substrate was generated by radiolabeling NT38 (5'-ATGAGAAGCAGCCGTATCAGGAAGAGGGAAAGGAAGAA-3') at the 5' terminus with [γ -³²P]ATP and T4 polynucleotide kinase prior to annealing to NT68 (5'-TTCTTCCTTTCCT

CTTCCTGATACGGCTGCTTCTCATCTACAACGTGATCCGTCATGGTTCGGAGTG-3').

The bubble substrate was generated by radiolabeling BT (5'-GACGCTGCCGAATTCTGGCTTGCTCGGACATCTTTGCCCACGTTGACCCG-3') at the 5' terminus with [γ -³²P]ATP and T4 polynucleotide kinase prior to annealing to BB (5'-CGGGTCAACGTGGGCAAAGCCAATGC GATCGGCCAGAATTCGGCAGCGTC-3'). The X-junction substrate was generated by radiolabeling X12-1 (5'-GACGCTGCCGAATTCTGGCTTGCTAGGACATCTTTGCCCACGT TGACCCG-3') at the 5' terminus with [γ -³²P]ATP and T4 polynucleotide kinase prior to annealing to X12-2 (5'-CGGGTCAACGTGGGCAAAGATGTCCTAGCAATGTAATCGTC TATGACGTC-3') and annealing X12-3 (5'-GACGTCATAGACGATTACATTGCTAGGACA TGCTGTCTAGAGACTATCGC-3') to X12-4 (5'-GCGATAGTCTCTAGACAGCATGTCCTA GCAAGCCAGAATTCGGCAGCGTC-3'). X12-1/2 was then annealed to X12-3/4 at 4°C overnight as described in Mohagheh et al. [25]. Oligonucleotides for the fork substrate were a kind gift from Dr. David Orren, and this substrate was generated by annealing 70lead (5'-CGTGACTTGATGTTAACCCTAACCCTAAGAATTCGGCTTAAGTGAGTGTGAGGATAT CATGTACGATAGC-3') to 5' terminus [γ -³²P]ATP labeled 27lead (5'-GCTATCGTACATGA TATCCTCACACTC-3') and 5' terminus [γ -³²P]ATP labeled 70lag (5'-GCTATCGTACATGAT ATCCTCACACTCTGAATAGCCGAATTCTTAGGGTTAGGGTTAACATCAAGTCACG-3') to 27lag (5'-GAGTGTGAGGATATCATGTACGATAGC-3'). The annealed leading and lagging duplexes were then annealed to each other at 4°C overnight as described in Machwe et al. [44]. All substrates were separated from un-annealed products using native 8% PAGE. The correct size band was excise the gel and transferred to a microfuge tube. The radiolabeled substrate was eluted from the gel with 150-300 μ l of 10 mM Tris 8.0, 10 mM NaCl, depending on the size of the gel slice, with rotation overnight at room temperature. Helicase assays were

carried out with the indicated amounts of BLM and topoisomerase II α (USB) with 2 fmoles of substrate, unless otherwise indicated, in 1X helicase buffer (20mM Tris-HCl pH 7.5, 0.1 mg/mL BSA, 2mM MgCl₂, 2mM ATP and 1 mM DTT), at 37°C for the indicated times. In reactions with topoisomerase II α , the substrate was pre-incubated with topoisomerase II α for 5 minutes prior to adding BLM. Reactions were terminated with helicase stop buffer (30% glycerol, 50mM EDTA pH 8, 0.9% SDS, 0.25% bromophenol blue and 0.25% xylene cyanol) and the products of the reactions were separated using native 12% PAGE for the 3' overhang and bubble substrates, and native 10% PAGE for the X-junction and model replication fork substrates. All assays were performed at least three times.

Decatenation assays- Decatenation assays were carried out with the Topoisomerase II Assay Kit as per manufacturer's directions (TopoGEN). Catenated DNA was used at 100 ng per reaction with indicated amounts of topoisomerase II α and BLM, BLM^{D795A}, or β -galactosidase for 30 minutes at 37°C. Assays were terminated with supplied stop-dye and treated with proteinase K (50 μ g/mL) for 30 minutes at 37°C before separation using 1% agarose gel electrophoresis and visualization using ethidium bromide-staining.

III. Results.

BLM and topoisomerase II α co-immunoprecipitate and co-localize in human cells.

To determine whether BLM and topoisomerase II α associate in mammalian cells, co-immunoprecipitation experiments were carried out using nuclear extracts prepared from asynchronous 293T and HeLa cells. The anti-BLM antibody co-immunoprecipitated BLM and topoisomerase II α from both cell lysates as shown by subsequent western analysis with antibodies specific for BLM and topoisomerase II α (Figure 7A). The inverse co-immunoprecipitation with an antibody specific to topoisomerase II α did not yield detectable levels of BLM protein by western blotting (data not shown). This is likely a result of the great differences in protein levels of BLM and topoisomerase II α . A negative control, IgG, did not precipitate either protein (Figure 7A).

These immunoprecipitation data were validated using co-immunofluorescence to determine whether BLM and topoisomerase II α co-localize. MCF7 cells were transfected with a vector expressing an EGFP-tagged BLM fusion protein. GFP fluorescence of transfected MCF7 cells demonstrates expression of BLM (Figure 7B, Panel A.). An antibody specific for topoisomerase II α identifies immunostaining of topoisomerase II α distributed throughout the nucleus and in discrete brighter foci (Figure 7B, Panel B.). Merged images of Figure 7B Panels A and B along with DAPI nuclear staining, show co-localization of EGFP-BLM and topoisomerase II α within the nucleus, confirming immunoprecipitation and western analysis data (Figure 7B, Panel C.). A rhodamine-labeled IgG control shows that rhodamine signal is specific to topoisomerase II α staining and it does not coincide with EGFP expression (Figure 7B, Panel D.).

The association of BLM and topoisomerase II α is cell cycle-dependent.

The independent expression patterns of BLM and topoisomerase II α are cell cycle regulated, with low expression in G₁-phase that follows an increase during S-phase and peaks at G₂/M-phases [46,117]. To test whether the association of BLM and topoisomerase II α also varies during the cell cycle, 293T cells were synchronized by double thymidine block and collected one-hour post-release to obtain cells in S-phase or six-hours post-release to obtain cells in G₂/M-phase. 293T cells were arrested with nocodazole and harvested six-hours post-release in order to obtain M-phase cells. FACS analysis confirmed cell synchronization of harvested cells (Figure 8A). Nuclear extracts from asynchronous and synchronized cells were used for BLM immunoprecipitation. Inputs (Figure 8B, left panel) represent 2.5% of the extracts used for immunoprecipitation. Consistent with our initial experiments, western blotting demonstrated the association of BLM and topoisomerase II α in asynchronous cells. Following cell cycle synchronization, the association of the two protein increased in S- and G₂/M-phases and, most dramatically, in M-phase (Figure 8B, right panel). As a positive control, the inputs and immunoprecipitations were blotted with topoisomerase III α , a protein documented to associate and physically bind to BLM (Figure 8B). In order to provide further evidence of the cell cycle dependent association co-immunofluorescence of BLM and topoisomerase II α was assayed in HCT116 cells. Cells were transfected with an EFGP-tagged BLM expression vector. For this experiment MCF7 cells were not used due to difficulty with synchronization, which did not yield at least 65% of the cells in the desired cell cycle phase. Association was scored as one or more co-localizing focus/foci. The histogram in Figure 8C shows that 39.1% of the cells score positive for BLM-topoisomerase II α association. This number decreases to 23.3% in G₁, most likely because of minimal expression of both proteins in G₁. The co-localization increases to

55.2%, 63.2% and 81.1% at S, G₂/M and M-phases, respectively. Low levels of background association reaching 8.9% were observed with a rhodamine labeled IgG control. The co-localization data obtained support the immunoprecipitation data suggesting that an increase in BLM and topoisomerase II α association in S and G₂ phases, that becomes more prominent in mitosis.

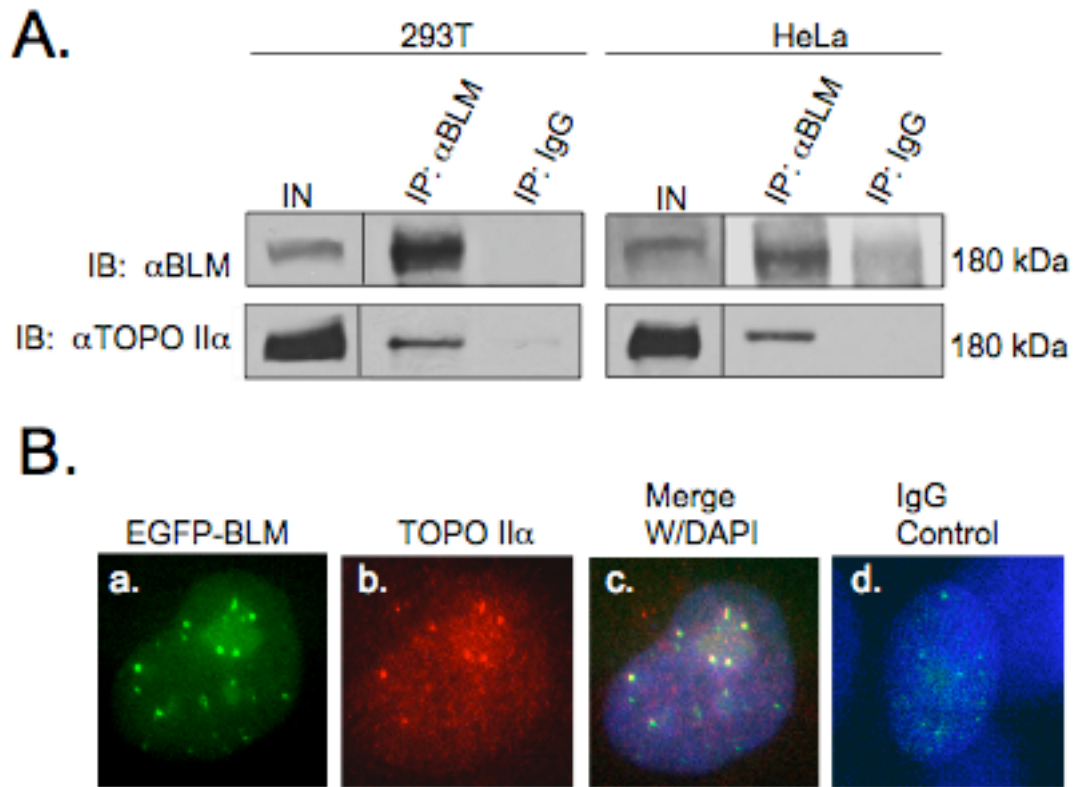


Figure 7. BLM and topoisomerase II α associate in asynchronous cells. A. BLM was immunoprecipitated from nuclear extracts prepared from 293T and HeLa cells with rabbit anti-BLM antibody or rabbit IgG. Immunoprecipitated proteins were separated using SDS-PAGE and analyzed by western blotting with anti-BLM or anti-topoisomerase II α antibodies. B. MCF7 cells were transfected with *pEGFP-BLM*. Forty-eight hours post-transfection, cells were fixed and stained with anti-topoisomerase II α antibodies, and DAPI for nuclear staining. Panel a. shows EGFP-BLM-positive foci; Panel b. shows topoisomerase II α staining; Panel c. shows merged EGFP-BLM, topoisomerase II α and DAPI staining; Panel d. shows staining with rhodamine-labeled mouse anti-rabbit IgG (m α IgG) as a negative control.

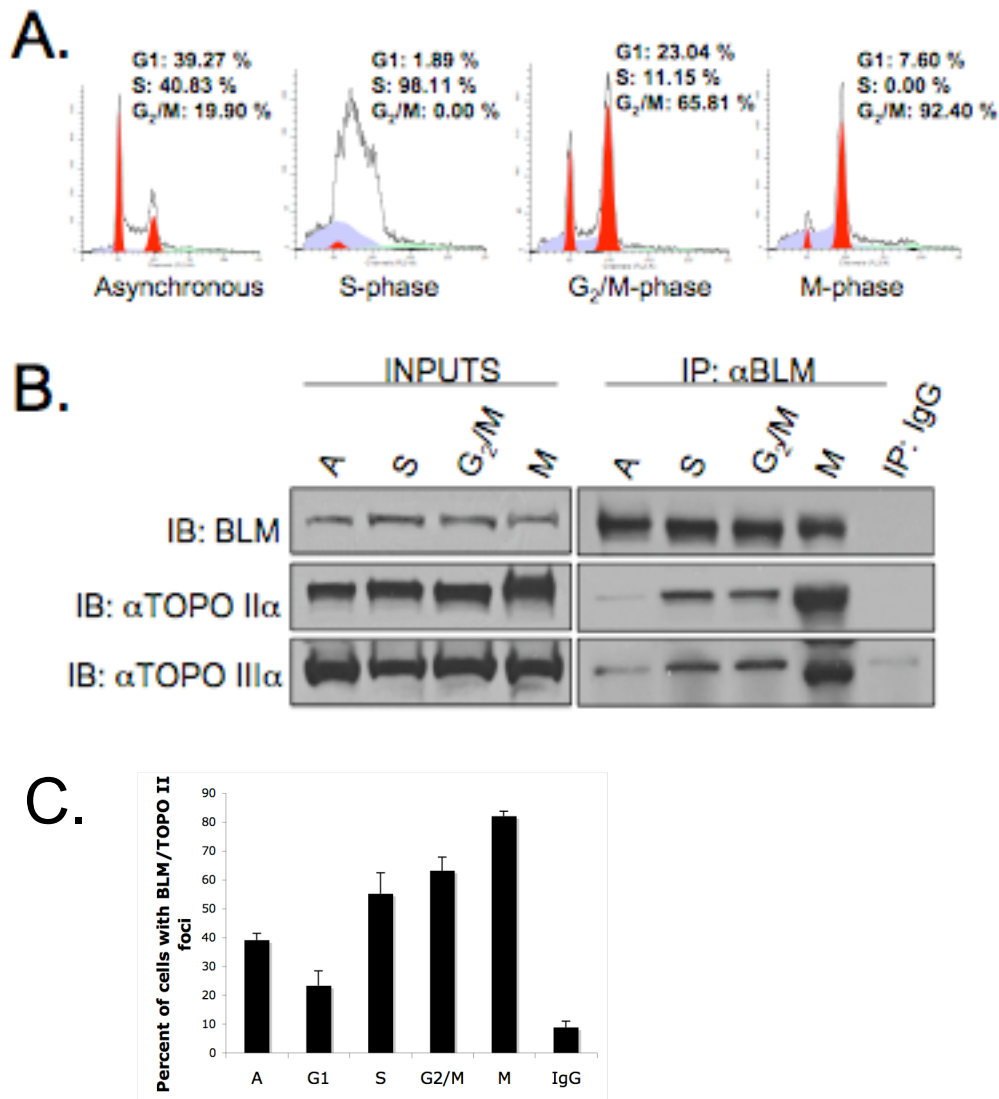


Figure 8. The association of BLM and topoisomerase II α is cell cycle-specific. A. FACS analysis of representative 293T cells synchronized at different phases of the cell cycle and used for immunoprecipitations. Cell cycle stage was analyzed by ModFit. B. Nuclear extracts from 293T synchronized cells were used in immunoprecipitations with anti-BLM antibody or rabbit IgG. Immunoprecipitated proteins were separated using SDS-PAGE and analyzed by western blotting with anti-BLM, anti-topoisomerase II α or anti-topoisomerase III α antibodies. C. Histogram shows the percentage of cells with BLM and topoisomerase II α co-localized foci at different phases of the cell cycle. HCT116 cells transfected with *pEGFP-BLM*. Twenty-four hours post-transfection, cells were synchronized similarly to the 293T cells and used for immunofluorescence with anti-topoisomerase II α antibodies. Histogram shows the average of at least 100 cells analyzed per cell cycle phase from three different experiments.

BLM directly interacts with topoisomerase II α through amino acids 489-587 of BLM.

To test whether BLM and topoisomerase II α interact directly, three segments of BLM were *in vitro* transcribed and translated (IVTT): BLM N, extending from the start of translation to the start of the helicase domain (aa 1-587), BLM H, covering the helicase domain and a small part of the recQ-like C-terminal domain (RQC) (aa 588-1000), and BLM C, containing the majority of the RQC domain, the helicase and RNase D C-terminal domain (HRDC) and the nuclear localization signal (NLS) (aa 996-1417) (Figure 9A). The three [³⁵S]-labeled segments were used in *in vitro* immunoprecipitation assays with human recombinant topoisomerase II α protein and an antibody specific to topoisomerase II α . Topoisomerase II α immunoprecipitates with the BLM N segments consisting of amino acids 1-587, but not the helicase domain (BLM H) or the C-terminal domain (BLM C) (Figure 9B).

To define the topoisomerase II α interaction domain more specifically, the BLM N-terminal segment was further broken down into five segments by sequentially removing approximately 100 amino acids from the start of translation, and one segment from which the last 98 most amino acids were removed (Figure 9C). [³⁵S]-labeled IVTT products of the six segments were subject to immunoprecipitations with a Topoisomerase II α specific antibody. The input panel of Figure 9D shows the expected sizes of IVTT products for all the segments. Most of the products of the IVTT reactions show smaller protein products most likely due to incomplete transcription or translation. Topoisomerase II α immunoprecipitated five of the segments, each of which contained the last 98 amino-terminal amino acids (489-587). The sixth segment (aa 1-488) lacking the region 489-587 did not immunoprecipitate with topoisomerase II α , suggesting that amino acids 489-587 of BLM are necessary for the interaction with topoisomerase II α (Figure 9D). This region falls within the much larger segment previously

mapped for *S. cerevisiae* Sgs1 and Top2 interaction [76]. An IgG control immunoprecipitation with all six segments showed background immunoprecipitation of all segments. Although visually less than the amounts immunoprecipitated with the topoisomerase II α specific antibody, we often observed that the BLM protein or its fragments had a tendency to immunoprecipitate with the IgG control, an issue that we were unable to resolve in these particular immunoprecipitations.

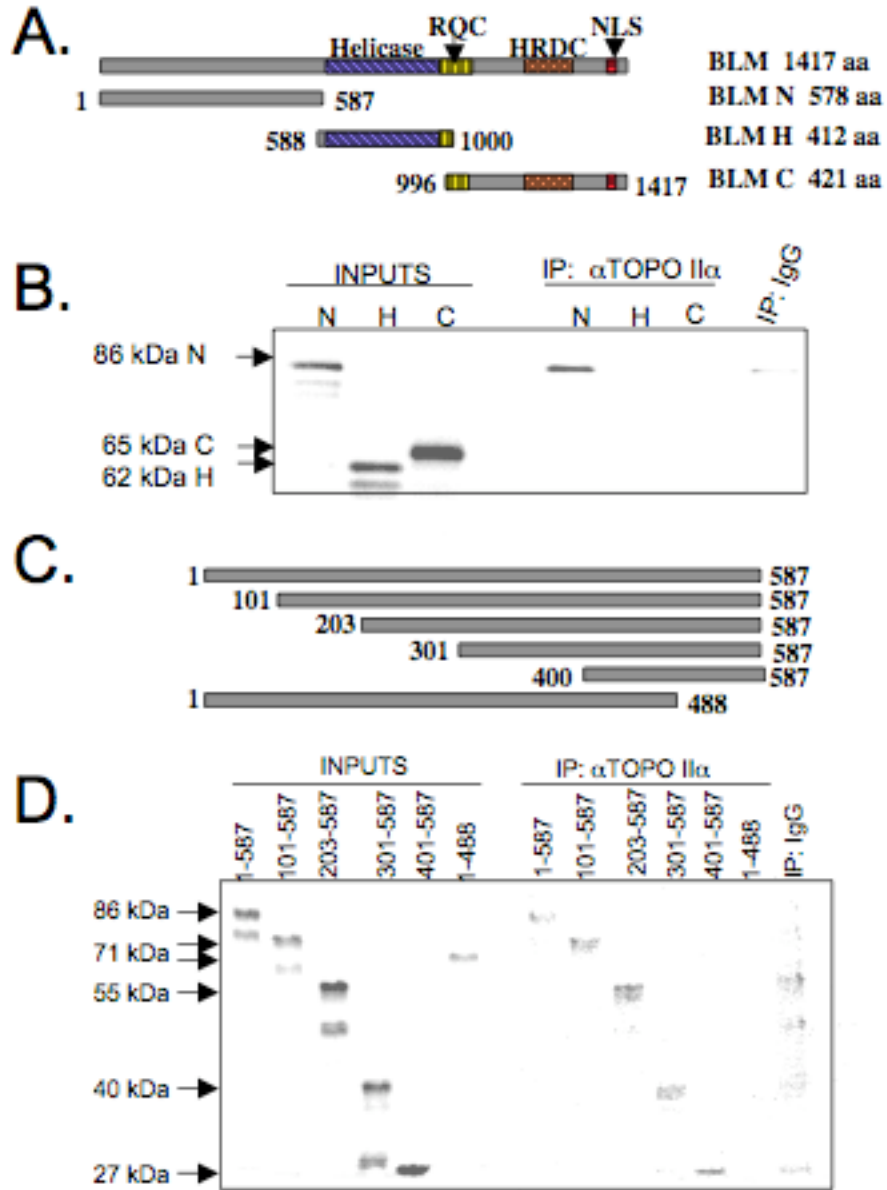


Figure 9. The interaction of BLM with topoisomerase II α occurs within the amino-terminus of BLM. A. Schematic representation of the BLM protein and smaller segments tested for topoisomerase II α binding. B. [35 S]-methionine-labeled IVTT proteins representing the amino-terminal (N), helicase (H) and carboxy-terminal (C) segments were incubated with purified topoisomerase II α and immunoprecipitated (IP) with a topoisomerase II α -specific antibody. The input lanes represent 1 μ L of each IVTT reaction. Control reactions were carried out by immunoprecipitating all three segments with mIgG. C. Schematic representation of N-terminal segments. D. N-terminal segments were generated via IVTT and tested for their ability to bind topoisomerase II α as described in B. Input lanes represent 10 μ L of each IVTT reaction; immunoprecipitations (IP) were carried out with 40 μ L of each IVTT reaction.

BLM does not alter topoisomerase II α decatenation activity.

The direct interaction of BLM and topoisomerase II α suggested that BLM may modulate the decatenation activity of topoisomerase II α or that topoisomerase II α may modulate the helicase activity of BLM. We first test the *in vitro* effect of BLM on the ability of topoisomerase II α to decatenate DNA.

To carry out these experiments we developed a new purification scheme for BLM that yields approximately 95% pure protein. This new scheme relies on two purification steps using fast protein liquid chromatography (FPLC) through a nickel resin followed by a second purification step through a Q-sepharose resin (Figure 10A). Yeast expression vectors (*pYES*) containing 6xHis-tagged BLM, 6xHis-tagged BLM^{D795A}, a helicase dead mutant, and 6xHis-tagged β -galactosidase, used as a negative control, were used to transform JEL1 yeast. Figure 10B shows a coomassie blue-stained gel of the first purification step loaded with crude yeast cell lysates (C), the column flow through (F) and the column washes (W) followed by fractions from the imidazole gradient corresponding to 35-195 nM imidazole. The arrow indicates a protein of the predicted size for BLM that elutes between 121-185 nM imidazole. All 6xHis-tagged proteins eluted at this range (data not shown). This round of purification removes two of the three most prevalent protein contaminants of 86 and 64 kDa in size. The coomassie blue-stained gel in Figure 10C shows the final purification step through a Q-sepharose column loaded with the pooled and dialyzed fractions from Figure 10B (D), the column washes (W) and fractions from the NaCl gradient corresponding to 140-700 mM NaCl. This step concentrated fractions obtained from the previous column and removed the third protein contaminant of 45 kDa. The arrow indicates protein bands of the predicted size for BLM eluting between 221-351 nM NaCl. All 6xHis-tagged proteins eluted at this range (data not shown). Figure 10D (left) shows a

Coomassie blue-stained gel demonstrating the purity of a protein slightly larger than 180 kDa; western blotting with an anti-BLM antibody confirmed the identity of this band as BLM (Figure 10D, right).

To determine whether binding of BLM to topoisomerase II α altered the decatenation activity of topoisomerase II α , a range of purified 6xHis-tagged BLM was used with purified human topoisomerase II α (USB) and kinetoplast DNA, the genome from the insect *Crithidia fasciculata* composed of catenated DNA micro circles approximately 2.5 Kb in size. To explore the possibility that the helicase activity of BLM might be required to mediate any change observed, a helicase dead mutant, BLM^{D795A}, was used. Also, to show that our purification scheme did not contain any protein contaminants affecting the activity of topoisomerase II α , bacterial β -galactosidase was used as a negative control. Two units of topoisomerase II α demonstrate almost full decatenation (84.8%) of kinetoplast DNA into its nicked and circular products that separate during electrophoresis (Figure 11A and B). The size and level of catenation of kinetoplast DNA prevents it from leaving the well of a 1% agarose gel. The effect of the 6His-tagged proteins on topoisomerase II α decatenation were carried out with 0.1U of topoisomerase II α , an amount that generates approximately 20% decatenation (22.8%) (Figure 11A and B). Addition of BLM, BLM^{D795A} or β -galactosidase, ranging from 0.1 nM to 100 nM, did not alter the average percent decatenation of 0.1U topoisomerase II α (Figure 11A and B). None of the 6His-tagged proteins by themselves had an affect on kinetoplast DNA (Figure 11A). Figure 11B shows a histogram of the decatenation activity as an average of three independent experiments. These data suggest that in these *in vitro* assays, BLM is unable to alter the decatenation activity of topoisomerase II α .

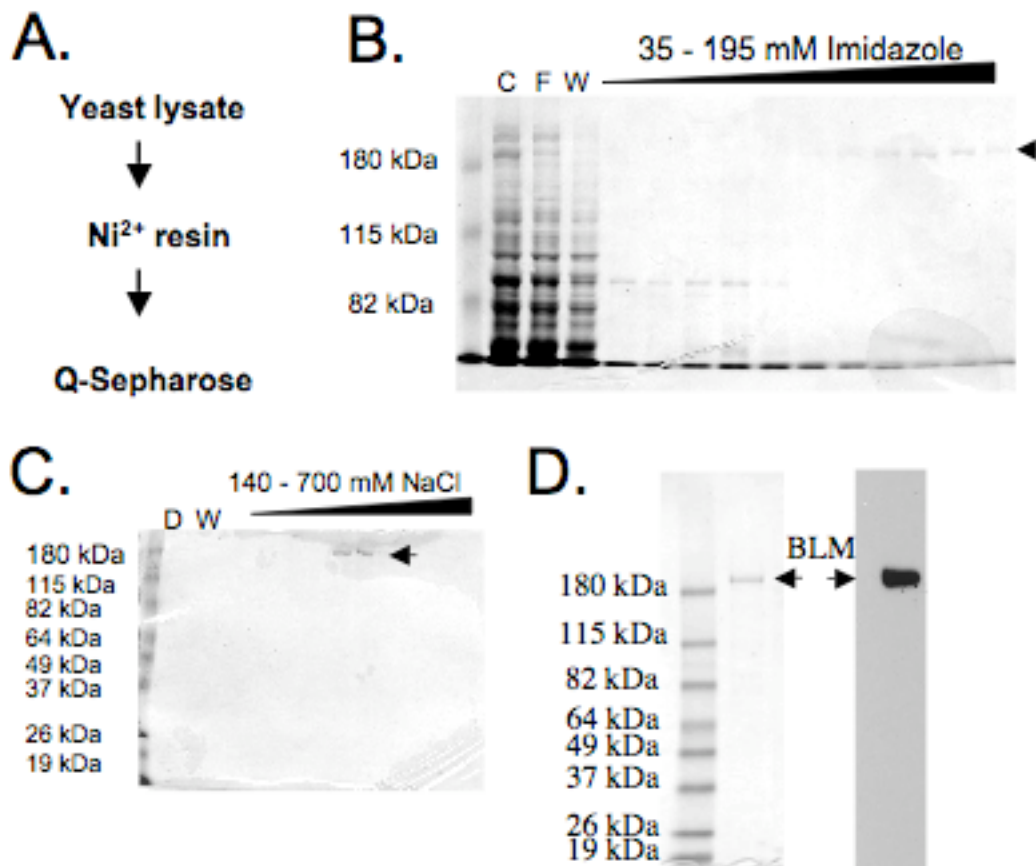


Figure 10. Purification scheme and validation of purified 6xHis-tagged BLM protein. A. Purification scheme used for 6xHis-tagged proteins from yeast. Yeast lysates were obtained by French pressure. SixHis-tagged BLM was purified using FPLC on Ni²⁺ resin followed by Q-sepharose. B. Coomassie blue stained polyacrylamide gel of protein fractions from Ni²⁺ column. C: crude extract; F: flow through; W: wash. Fractions from 35 - 195 mM imidazole are shown. Arrow shows protein of expected size for BLM. C. Coomassie blue stained polyacrylamide gel of protein fractions from Q-sepharose column. D: dialized fraction; W: wash. Fractions from 140 - 700 mM NaCl are shown. Arrow shows protein of expected size for BLM. D. Coomassie blue stained polyacrylamide gel of purified recombinant 6xHis-tagged BLM (100 ng) used in helicase assays (left arrow) and western blot analysis of purified protein with an antibody specific for BLM (right arrow).

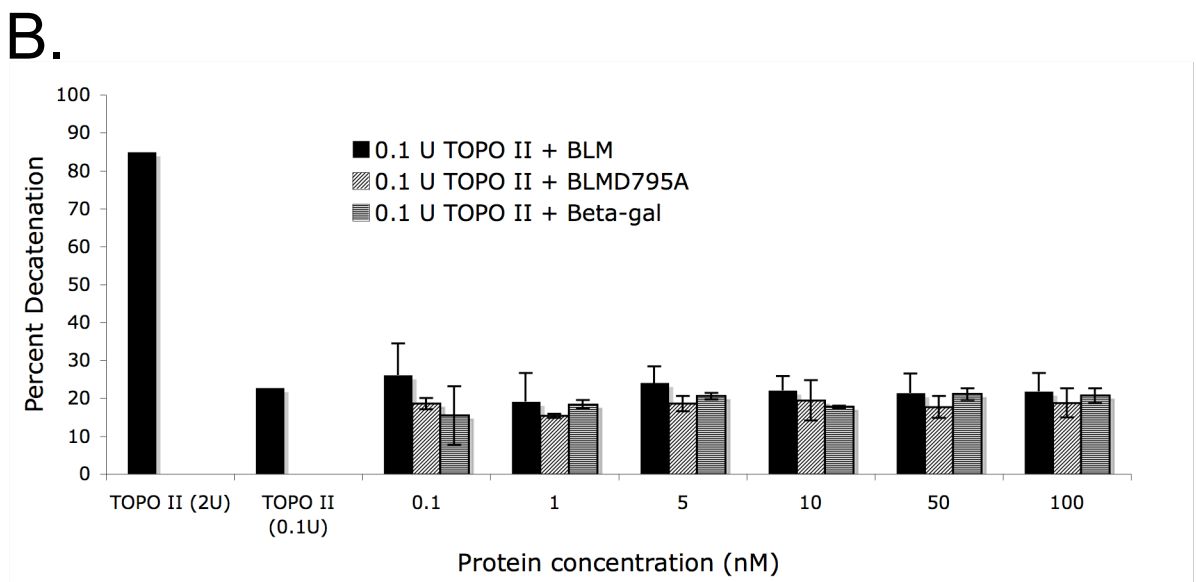
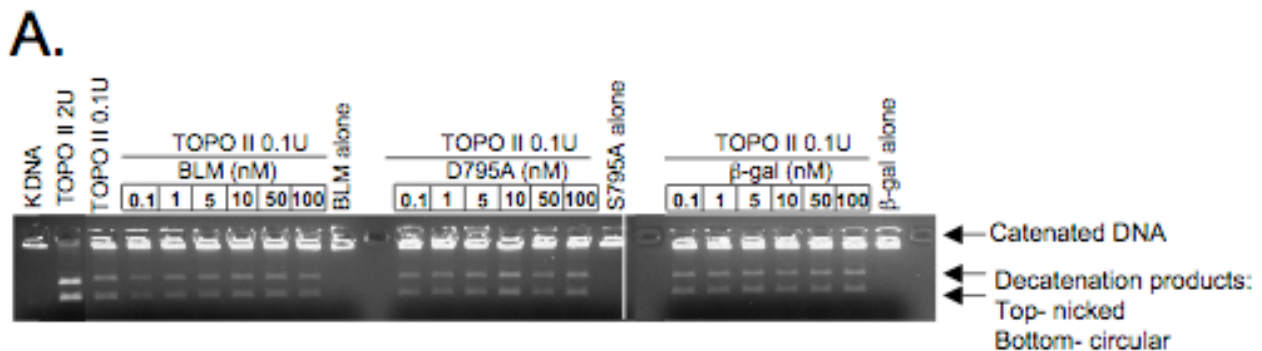


Figure 11. BLM does not affect the decatenation activity of topoisomerase II α . A. Decatenation assays were carried out with 100 ng of catenated DNA, the indicated units of topoisomerase II α (USB) and increasing amounts of purified 6His-tagged BLM proteins (or β -galactosidase as a negative control). Decatenation products were separated using gel electrophoresis with 1% agarose gels. A catenated DNA control (KDNA) demonstrates the mobility of fully catenated DNA. A decatenated control (TOPO II 2U) demonstrates the migration of both decatenation products. A decatenation reaction containing 0.1 units of topoisomerase II α (TOPO II 0.1U) demonstrates approximately 20% decatenation and is the starting topoisomerase II α concentration for all other reactions containing either wt BLM, the helicase dead mutant, BLM^{D792A} or β -galactosidase (β -gal). Control reactions with BLM, BLM^{D795A} and β -gal alone are indicated. B. Graphical representation of results of decatenation assays as an average of three independent experiments.

Topoisomerase II α enhances the *in vitro* unwinding activity of BLM using DNA substrates representing early homologous recombination intermediates.

As our decatenation assays did not show a change in the decatenation activity of topoisomerase II α in the presence of BLM, we now assayed the effect of topoisomerase II α on the helicase activity of BLM. Four *in vitro*-generated DNA structures were chosen that include early HR intermediates such as a 3' overhang and a bubble; an X-junction, a late intermediate of HR and a model replication fork, in order to determine if topoisomerase II α could aid BLM in processing of a stalled replication fork inhibiting the start of HR. The purified 6xHis-tagged BLM protein was used in helicase assays at increasing concentrations with 2 fmoles of each of the aforementioned substrates in order to determine if this protein behaved similarly to previously published work. BLM concentrations ranging from 0.005-10 nM were used in helicase assays as stated in Figure 12A-D. BLM was effective at processing all of the substrates, but showed preference for the model replication fork (Figure 12C and E) requiring 0.5 nM BLM to process one half of the total substrate. The BLM concentration needed to process half of the bubble substrate was 1 nM (Figure 12B and E), the X-junction was 2.1 nM (Figure 12D and E) and finally half of the 3' overhang substrate was processed by 2.5 nM BLM (Figure 12A and E). A graphical representation of substrate unwinding preference of purified BLM is shown in Figure 12E. These data corroborate previously published findings that a model replication fork, bubble substrates and X-junction substrates are more attractive substrates to BLM than a 3' overhang [25].

The ability of topoisomerase II α to alter the kinetics of BLM unwinding was examined on the same substrates. Control experiments were performed to determine if topoisomerase II α alone had any significant unwinding effect on any of the substrates. Helicase assays were

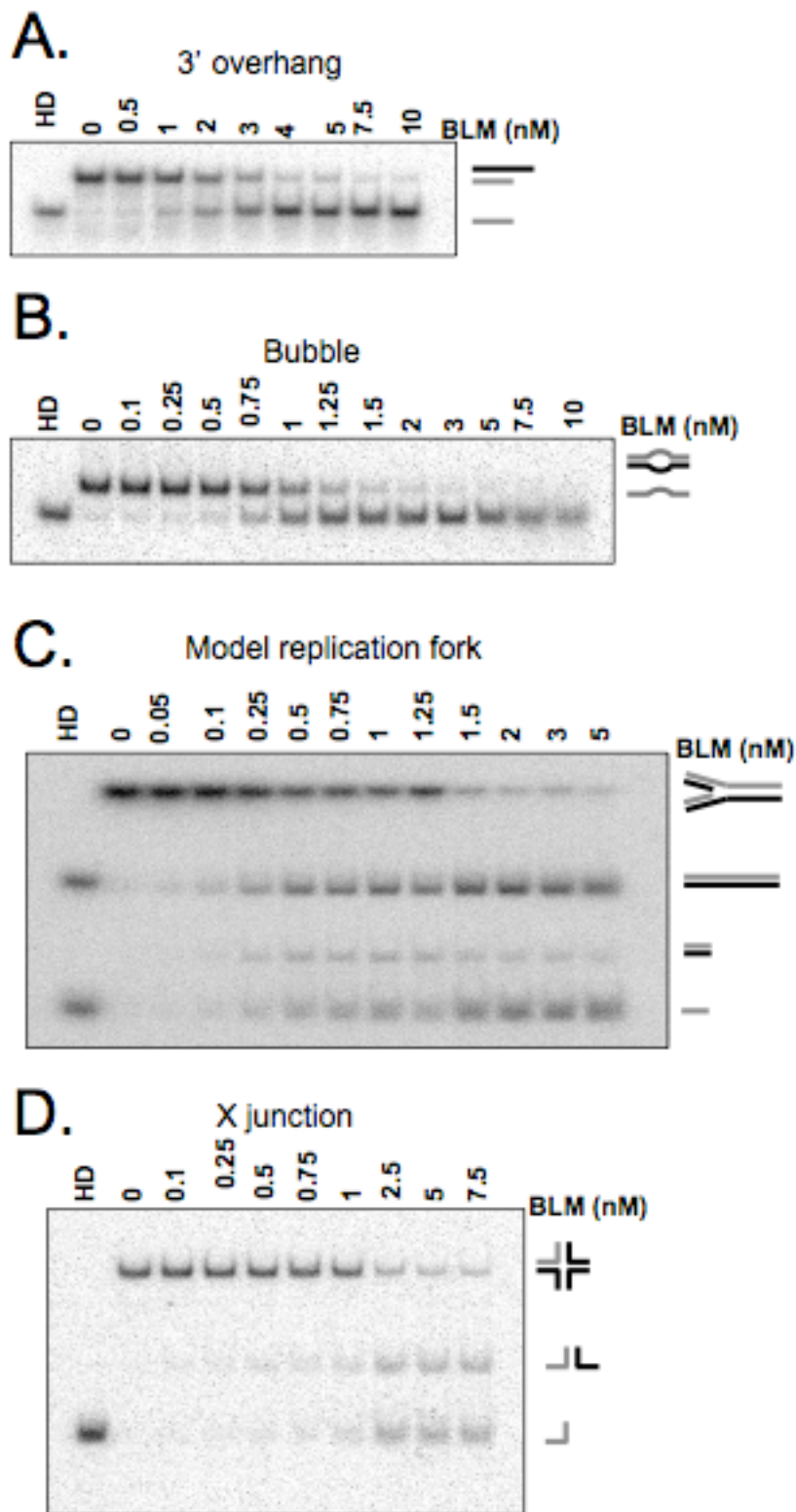
performed in the presence of 4 nM topoisomerase II α and 2 fmoles of each substrate. All reactions were allowed to proceed for 15 minutes at 37°C. Figure 13A-D shows the autoradiographs of the reaction for which a heat denatured control was loaded to show the migration of the released labeled strand(s) and a no protein control (0) is loaded to enable subtraction of any spontaneous substrate dissociation. Quantification of the percent unwinding by topoisomerase II α for each substrate is plotted in Figure 13E and amounts to 2.08% for the 3' overhang, 2.58% for the bubble, 1.26% for the model replication fork and 0.56% for X-junction substrates.

Data from Figure 12 were used to calculate the concentrations of BLM needed to achieve approximately 10% unwinding for each of the substrates and was used as the starting concentration in time-dependent helicase assays. From these time-dependent assays, the specific activity of BLM for each substrate was calculated, which is defined as the femtomoles of substrate unwound per minute per nanomolar concentration of BLM ($\text{fmol}\cdot\text{min}^{-1}\cdot\text{nM}^{-1}$). The nanomolar concentrations of BLM leading to approximately 10% unwinding for each substrate were then used in a separate set of reactions with equimolar amounts of topoisomerase II α and a new specific activity for BLM was calculated. Figure 14 shows representative autoradiographs of these assays where the radiolabeled strand(s) are colored grey, along with the graphical representation of the percent unwinding in the absence and presence of topoisomerase II α . The percent unwinding of the 3' overhang substrate with 1 nM BLM in the presence of equimolar amounts of topoisomerase II α changed from 16.6 to 52.7% leading to a change in specific activity from 0.02768 to 0.08787 $\text{fmol}\cdot\text{min}^{-1}\cdot\text{nM}^{-1}$, a 3.17 fold increase (Figure 14A and E, and Table 2). For the bubble substrate, 0.5 nM BLM lead to 13.1% unwinding which increased to 60.7% in the presence of equimolar amounts of topoisomerase II α leading to a change in specific

activity from 0.04374 to 0.20245 $\text{fmol}\cdot\text{min}^{-1}\cdot\text{nM}^{-1}$, a 4.6 fold increase (Figure 14B and E, and Table 2). Topoisomerase II α inhibited BLM unwinding of the X-junction substrate from 7.9% to 3.2% changing the specific activity of BLM from 0.01774 to 0.00725 $\text{fmol}\cdot\text{min}^{-1}\cdot\text{nM}^{-1}$, leading to a 2.4-fold decrease of BLM specific activity in the presence of topoisomerase II α .

For the model replication fork, 0.5 nM BLM unwound 13.7% of the total substrate, an activity that was increased to 47.7% in the presence of equimolar topoisomerase II α . This led to an increase in specific activity of BLM from 0.22976 to 0.79583 $\text{fmol}\cdot\text{min}^{-1}\cdot\text{nM}^{-1}$ in the presence of topoisomerase II α , a 3.4 fold increase (Figure 14C and E, and Table 2). The pattern of substrate appearance in Figure 14C is not in accordance with the proposed substrate appearance in a reverse branch migration reaction. Model replication fork substrates may undergo reverse branch migration through a “chicken foot” intermediate or a Holliday junction (as in Figure 4E) [118]. This is supported biochemically through the exclusive release of a 70 lead/70 lag annealed product and the 27 lead/27 lag annealed product that could only be released if reverse branch migration proceeded through the “chicken foot” intermediate. Fork regression assays in Figure 12C show the appearance of both of these products, suggesting that reverse branch migration is taking place. The release of a single stranded 27 lead oligonucleotide has been attributed to spontaneous melting of the 27 lead/27 lag product, as BLM does not have activity on blunt ended double helices [25,32]. The time-dependent assays in Figure 14C, do not show the appearance of the 27 lead/ 27 lag annealed product suggesting that fork regression has not taken place. This pattern of product appearance suggests a biochemical activity in which BLM unwinds the 70 lead/ 70 lag strands with the short complementary fragments still annealed to them. This activity results in the release of 70 lead/27 lead and 70 lag/27 lag annealed products. The free 27 mer results from BLM unwinding of the 70 mer/27 mer with a 3’ overhang, although

less efficiently since BLM has lower preference of this substrate. Due to this technical complication a role for BLM and topoisomerase II α in reverse branch migration cannot be suggested.



E.

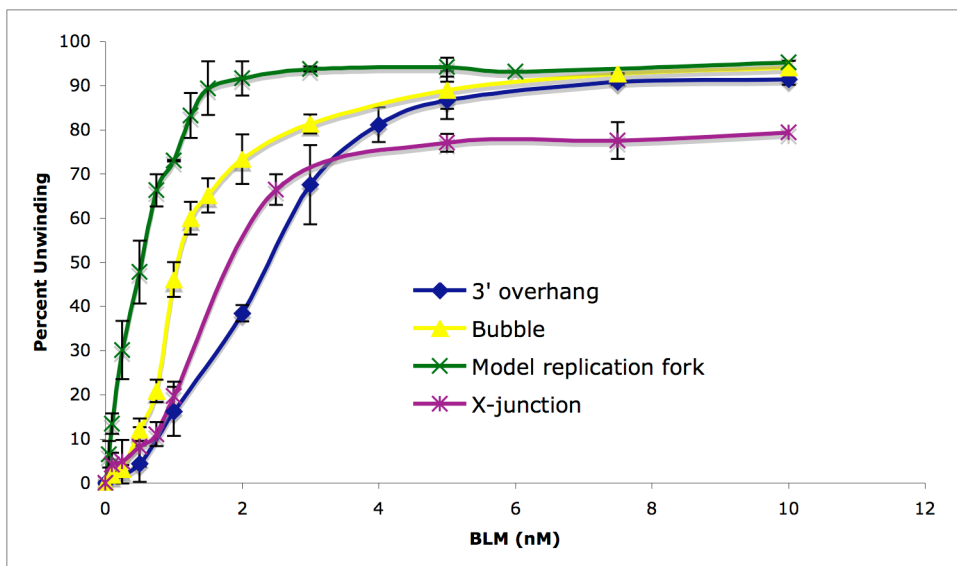


Figure 12. Unwinding activity of BLM using recombination substrates. Autoradiographs of BLM (concentrations as shown) with 2 fmoles of each substrate. A. 3' overhang; B. bubble; C. model replication fork; or D. X-junction substrates. Helicase reactions were terminated after 15 minutes at 37°C. Resulting DNA products were resolved using non-denaturing PAGE. A heat-denatured control (HD) shows migration of the released radiolabeled strand(s) (gray). E. Percent unwinding was quantitated with each of the different substrates.

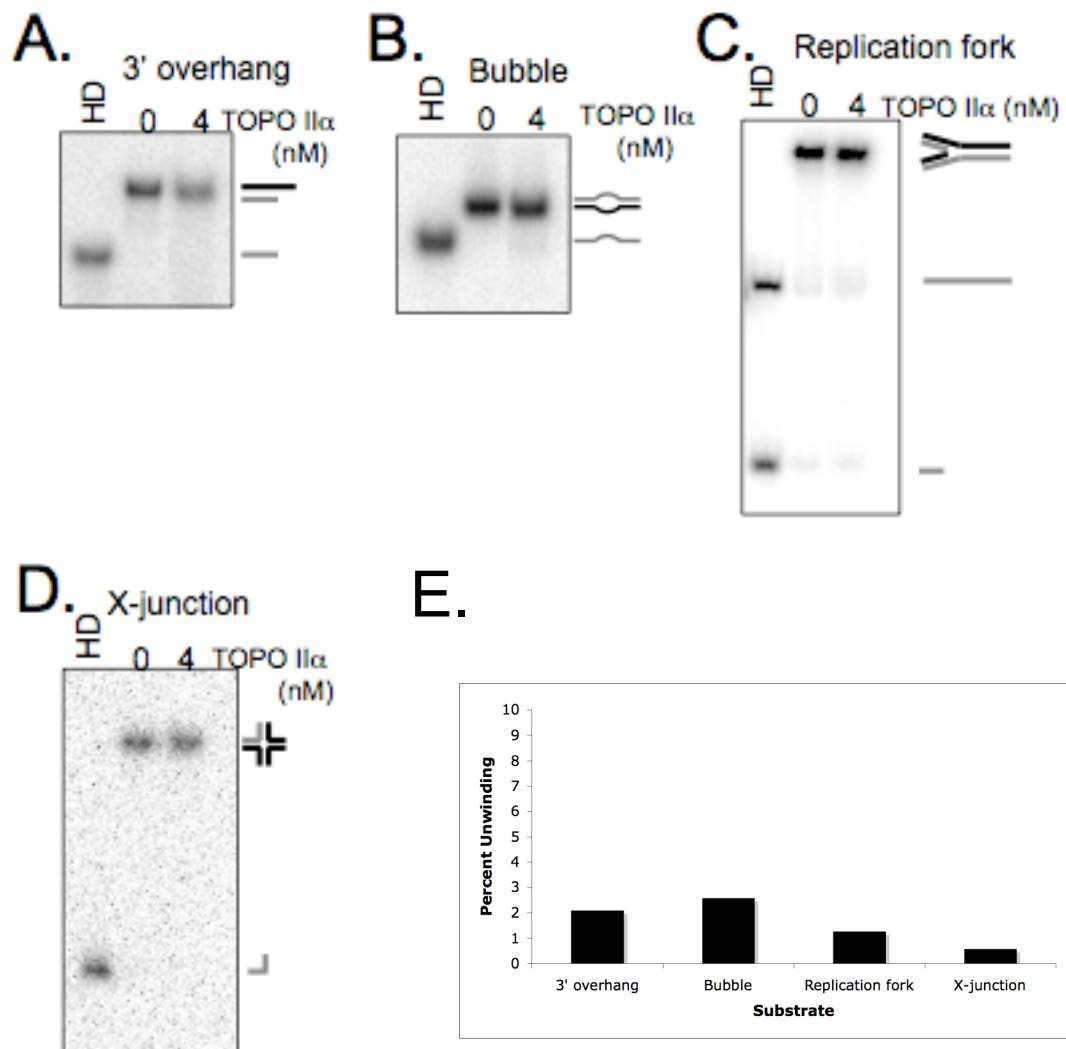
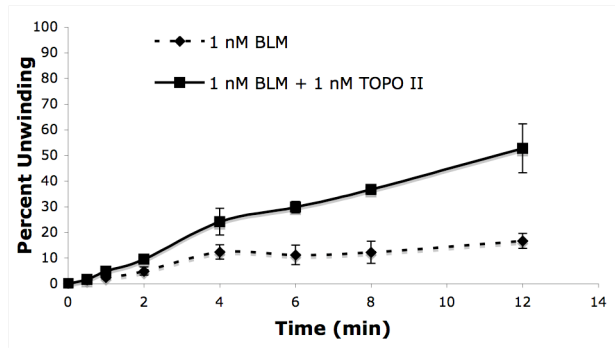
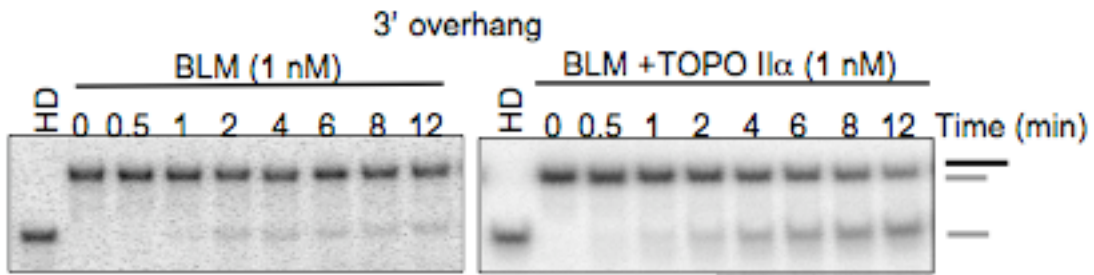
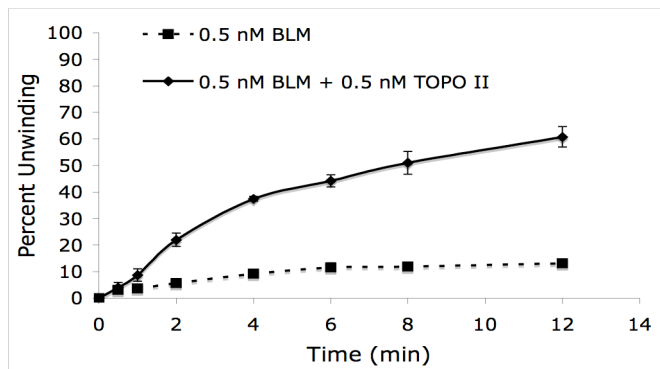
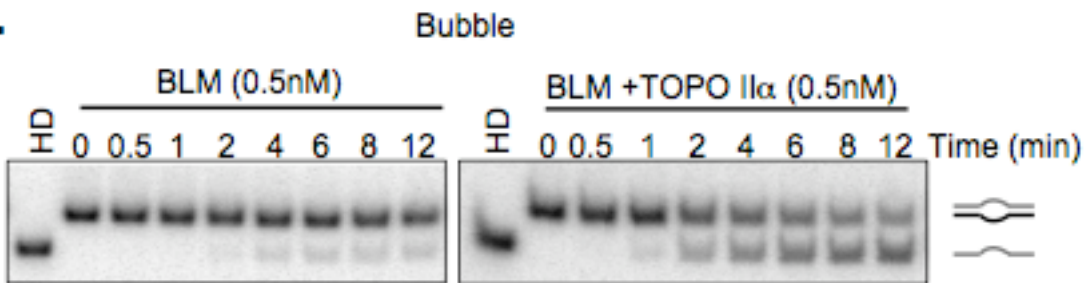


Figure 13. Topoisomerase II α alone does not have unwinding activity. Helicase assays were carried out with 4nM topoisomerase II α and A. two fmoles of the 3' overhang substrate, B. two fmoles of the bubble substrate, C. two fmoles of the model replication fork substrate, or D. two fmoles of the X-junction substrate. Heat denatured (HD) controls show the migration of the released radiolabeled strand (gray). A no protein control (0) is used to subtract any possible background due to spontaneous substrate disassociation. E. Percent unwinding for 4 nM topoisomerase II α for each of the substrates after background subtraction.

A.

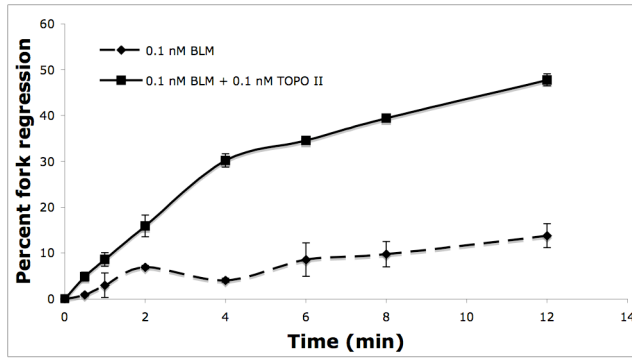
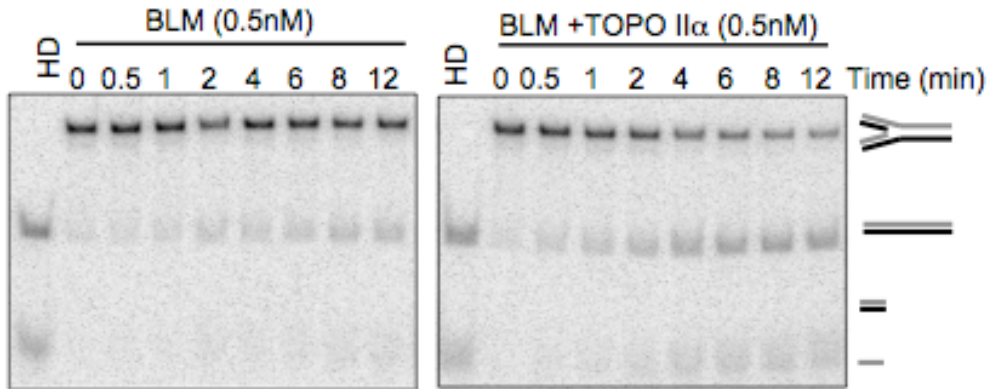


B.



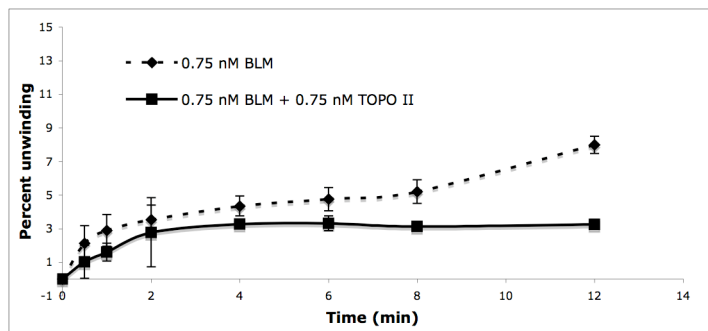
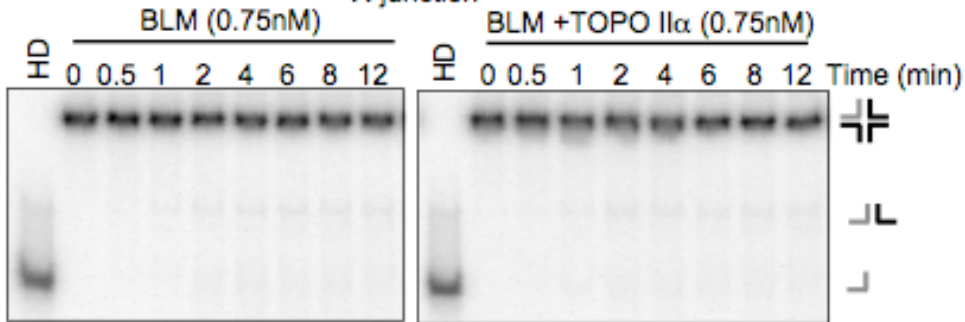
C.

Model replication fork



D.

X-junction



E

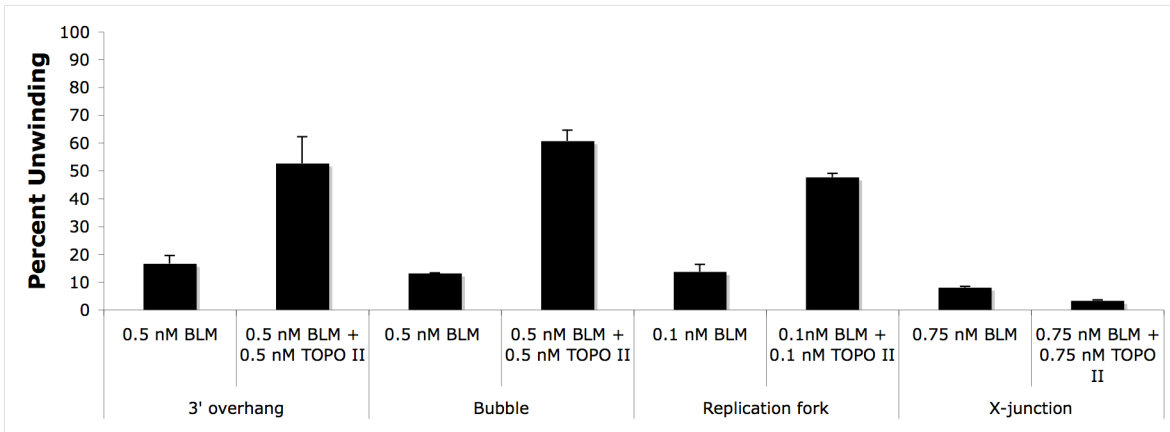


Figure 14. BLM unwinding activity is enhanced by topoisomerase II α using a 3' overhang, bubble and a model replication fork substrates, but not with an X-junction substrate. A. Autoradiograph of a time- course helicase assay shows enhanced BLM unwinding activity by topoisomerase II α . Helicase assays were carried out with 2 fmoles of 3' overhang substrate and 1 nM BLM to obtain 10% unwinding at 12 min (left panel). Topoisomerase II α (1 nM) was pre-incubated with substrate before starting the reaction by addition of BLM (1 nM). DNA products were resolved by non-denaturing PAGE. Lower panel represents graphical quantification of the percent unwinding by BLM alone or with equimolar amounts of topoisomerase II α . The dotted line represents the amount of unwinding as a function of time with 1 nM BLM and 2 fmoles of 3' overhang substrate. The solid line represents the percent unwinding by equimolar equimolar amounts (1 nM) of BLM and topoisomerase II α with 2 fmoles of 3' overhang substrate. Radiolabeled strand (gray). B. Experiment was carried out as in A with bubble substrate and 0.5 nM BLM and equimolar concentrations of topoisomerase II α . C. Experiment was carried out as in A with model replication fork substrate and 0.1 nM BLM and equimolar concentrations of topoisomerase II α . D. Experiment was carried out as in A with X-junction substrate and 0.75 nM BLM and equimolar concentrations of topoisomerase II α . E. Histogram showing the percent unwinding of indicated substrates by BLM, and BLM with topoisomerase II α at equimolar concentrations.

Table 2. Specific activity of BLM and BLM/TOPO II α on recombination substrates.

Substrate	Specific activity (fmol·min ⁻¹ ·nM ⁻¹)	
	BLM	BLM and TOPO II α
3' overhang	0.02768	0.08787
Bubble	0.04374	0.20245
Replication fork	0.22976	0.79583
X-junction	0.01774	0.00725

IV. Conclusions.

The data obtained in this chapter demonstrate that mammalian BLM and topoisomerase II α associate via a physical interaction mapped to residues 489-587 of BLM. The interaction is cell cycle-specific increasing in S and G₂ phases and peaking in mitosis. This evidence led us to test biochemically the effect that one protein may be having on the catalytic activity of the other. Taking into account that the most prominent association takes place in mitosis, we first assayed the effect BLM had on the decatenation activity of topoisomerase II α . Decatenation assays with purified 6xHis-tagged BLM or a helicase dead mutant, BLM^{D795A}, ranging in concentrations from 0.1 to 100 nM did not have an affect on the decatenation activity of topoisomerase II α . On the other hand, when the ability of topoisomerase II α to alter the helicase activity of BLM was assayed, BLM specific activity was enhanced 3- and 5-fold on the 3' overhang and bubble substrates, respectively, in the presence of topoisomerase II α . Interestingly, a 2-fold decrease in specific activity of BLM was observed with the X-junction substrate in the presence of topoisomerase II α . These data suggest that topoisomerase II α modulates BLM unwinding activity *in vitro* in a positive manner for DNA structures generated early in the process of HR suggesting that BLM and topoisomerase II α may enhance HR at early steps. Unwinding of DNA substrates occurring later, such as Holliday junctions, may be slightly inhibited probably allowing these intermediates to be processed by the BTB complex leading to non-crossover products.

CHAPTER FOUR. BLM and topoisomerase II α interaction is necessary to prevent chromosome breaks.

I. Introduction.

Cytogenetically, the hallmark of BS cells is excessive sister chromatid exchange (SCE), occurring at 5-10 fold higher frequency than in normal cells [8]. Telomere associations (TA) also occur at high frequency in BS cells [68] as do quadriradial structures (Qrs), the latter formed by unresolved recombination events between homologous chromosomes [8,9]. Chromosome breaks and gaps are common in BS cells [2,10] and include isochromatid breaks, associated displaced acentric fragments and telocentric chromosomal fragments. These chromosome fragments without spindle attachments then extrude from the nucleus as small extra nuclei known as micronuclei [119]. Not surprisingly, BS cells show an elevated number of micronuclei [11]. BS cells also display excessive levels of anaphase bridging [110], structures that represent incompletely segregated chromosomes possibly caused by unresolved recombination events and could give rise to chromosome breaks generated by the mitotic spindle forces [96].

The data presented in Chapter Three show that BLM and topoisomerase II α interact directly and present biochemical evidence that their interaction could potentially enhance the generation of early HR intermediates, therefore, carrying out a pro-recombinogenic role. In this chapter genetic tools are employed to determine whether the interaction of BLM and topoisomerase II α is necessary to prevent chromosome breakage, a feature common to both BS and topoisomerase-poisoned cells.

The data presented in this chapter show that *siRNA*-mediated gene knock-down of *BLM* or *TOPO II α* in normal cells increased chromosome breakage compared to non-treated, as

measured by comet assays. Breakage was not increased additively when both genes were knocked-down simultaneously, suggesting a common pathway for prevention of chromosome breakage. In order to assess if a physical interaction of the two proteins was necessary to prevent chromosome breakage, a vector expressing an EGFP-tagged mutant BLM protein was generated lacking the topoisomerase II α interaction domain determined in Chapter Three (*pEGFP-BLM^{A489-587}*). When transfected in 293T cells, the EGFP-BLM^{A489-587} mutant was unable to co-immunoprecipitate with topoisomerase II α unlike the expressed wild-type EGFP-BLM protein. The lack of association by immunoprecipitation was not due to incorrect compartmentalization of the mutant protein, as the mutant was able to localize to the nucleus in small punctate foci with PML and it also localized to the nucleolus. Introduction of the *pEGFP-BLM* and *pEGFP-BLM^{A489-587}* vectors in the GM08505 cell line (BLM^{-/-}) was used to determine if the mutant could rescue the breakage phenotype to the levels of wild-type BLM observed by γ H2AX foci formation. The interaction of the two proteins appeared necessary to reduce the number of γ H2AX foci, as expression of EGFP-BLM^{A489-587} mutant did not rescue the elevated levels of γ H2AX foci seen in wild-type BLM. Instead introduction of the EGFP-BLM^{A489-587} mutant seemed to exacerbate the number of γ H2AX foci observed in the BS cell tested. These results provide evidence that BLM and topoisomerase II α interact to participate in a common pathway that prevents chromosome breakage. These results suggest that in the presence of BLM, cells commit to repairing certain types of damage via a BLM dependent pathway. In the absence of BLM-interacting proteins that aid in this process, in this case topoisomerase II α , cells remain unable to complete the repair leading to the persistence of breaks.

II. Materials and Methods.

Cell lines and synchronization- 293T cells were obtained from the American Tissue Culture Collection (Rockville, MD). Both cell lines were cultured in DMEM (Invitrogen) containing 10% FBS and grown at 37°C in 5% CO₂.

Knock-down and comet assays- HeLa cells were transfected with 30 nM *BLM* and *TOP2 siRNA* (*BLM* siRNA ID: 146899, *TOP2* siRNA ID: 110840, Ambion) separately or in combination, or a scrambled control (AM4611, Ambion) using Lipofectamine 2000 (Invitrogen). Forty-eight hours post-transfection, the cells were harvested and lysed as described in the Immunoprecipitation section of the Materials and Methods in Chapter Three. BLM and topoisomerase II α proteins were visualized by western blotting with anti-BLM (ab476, Abcam) and anti-topoisomerase II α (Ab-1, Calbiochem) antibodies. Alkali comet assays were carried out two days post-transfection. Following harvesting of cells by trypsinization and a wash with PBS, cells were embedded in 1% low melting agarose (Sigma) and layered over a microscope slide. The cells were lysed in alkaline lysis solution (1.2M NaCl, 100 mM Na₂EDTA, 0.1% Na-lauryl sarcosinate, 0.26 M NaOH, pH > 13) at 4°C overnight followed by three 10 minutes washes in electrophoresis buffer (0.03 M NaOH, 2 mM Na₂EDTA, pH 12.3) and electrophoresis at 0.6 V/cm for 25 minutes. The DNA was stained with propidium iodine (25 μ g/ml) and the comets visualized with Axiovert 200M Carl Zeiss microscope with Axio Vision 4.5 software. Pictures of the comets were analyzed with CometScore (TriTek Corp.) software (http://autocomet.com/products_cometscore.php) to determine the percent DNA in each comet tail.

Generation of pEGFP-BLM^{A489-587} - pEGFP-BLM^{A489-587} was generated by sequential mutations of amino acids 488-489 and 587-588 into a *BspE1* restriction site in the *pEGFP-BLM* vector, using Quickchange (Invitrogen) PCR with the following primers: BLM489BspE1F (5'-CCAGGAAG AATCTTTTTGTCCGGACTTTATTCAATACCCATTTACAG-3') and BLM489BspE1R (5'-CTGTAAATGGGTATTCAATAAAGTCCGGACAAAAAGATTCTTCCTGG-3') for mutation of amino acid 489, and BLM587BspE1F (5'-CCACAGCCTGCCTATCAACCCATCCGGAAA GGTCGGCCAATTAAATCAG-3') and BLM587BspE1R (5'-CTGATTTAATTGGCCG\ACC TTTCCGGATGGGTTGATAGGCAGCTGTGG-3') for mutation of amino acid 587. Products of the Quickchange reactions were digested with *Dpn1* to remove the parental methylated vector and used to transform bacterial DH5 α cells. Vectors carrying mutations were mini-preped using the QIAGEN Plasmid Mini Kit and mutations confirmed by sequencing. The vector containing *BspE1* restriction sites at both residues 489 and 587 was subject to restriction enzyme digestion with *BspE1*, releasing the sequence coding for the topoisomerase II α -interaction domain. Following gel purification of linear *pEGFP-BLM^{A489-587}* vector and religation, correction of codons for amino acids 488 and 588 was carried out using Quickchange (Invitrogen) PCR with primers BLM488-588F (5'-CCAGGAAGAATCTTTTTGAAAGGGAAGGTCGGCCAATTAA ATCAG-3') and BLM488-588R (5'-CTGATTTAATTGGCCGACCTTCCCTTTCAAAAAGAT TCTTCCTGG-3'). The PCR reaction products were digested with *Dpn1* to remove the parental methylated vector and used to transform bacterial DH5 α cells. The vector carrying the final mutations was maxi-preped using the QIAGEN EndoFree Plasmid maxi Kit the final product was confirmed by sequencing.

Immunoprecipitations- 293T cells were transfected with 4 μg of *pEGFP-BLM* or *pEGFP-BLM^{A489-587}* expression vectors using Lipofectamine 2000 (Invitrogen) in Opti-MEM media for 5 hours at 37°C and 5% CO₂. Nuclear extracts were prepared by fractionation as described in the Immunoprecipitations section of the Materials and Methods in Chapter Three. Nuclear extracts (1 mg) in Buffer Z were immunoprecipitated using 2 μg of an antibody specific for GFP (T-19, Santa Cruz Biotechnologies) as described in immunoprecipitations section of the Materials and Methods in Chapter Three, and visualized by western blotting with an anti-GFP antibody (T-19, Santa Cruz Biotechnologies) and anti-topoisomerase II α antibody (Ab-1, Calbiochem).

Immunofluorescence- GM08505 (*BLM^{-/-}*) cells were grown on glass coverslips. Cells were transfected with 2 μg of *pEGFP-BLM* or *pEGFP-BLM^{A489-587}* vectors using Lipofectamine 2000 (Invitrogen). Two to three days post-transfection, cells were fixed with 4% formalin, permeabilized and stained with antibodies specific for γH2AX (Millipore) (1:500) or PML (PG-M3 Santa Cruz Biotechnology) as described in the Immunofluorescence section of the Materials and Methods in Chapter Three. Nuclei were stained with DAPI and viewed using an Axiovert 200M Zeiss microscope and Axio Vision 4.5 software.

III. Results.

BLM and topoisomerase II α prevent chromosome breakage in a common pathway.

Chromosome breakage is a distinguishing feature of BS cells [10], most likely caused by the inappropriate resolution of recombination intermediates in the absence of BLM. Our experiments have demonstrated that BLM and topoisomerase II α interact directly and function synergistically in the resolution of HR intermediates *in vitro*. As their action may also be

necessary during the *in vivo* HR process, we determined the individual and combined contributions of BLM and topoisomerase II α to levels of chromosome breakage in the cell.

siRNA-mediated knock-down of each protein alone or in combination was accomplished in HeLa cells. Western analyses confirmed the knock-down of BLM and topoisomerase II α at 48-hours post-transfection. No change in BLM or topoisomerase II α protein levels was observed in cells transfected with a scrambled control *siRNA* (Figure 15A). Representative comet assays of cells transfected with *siRNA* to *BLM*, *TOP2*, both in combination or a scrambled control are shown in Figure 15B along with hydrogen peroxide treated cells (positive control for comet formation) and untreated cells (negative control). Figure 15C show quantification of the percent of DNA in the comet tail of at least 100 cells per transfection or treatment. The hydrogen peroxide treatment resulted in 72.2% of DNA in the tail; untreated controls and scrambled control-transfected cells resulted in 10.5 and 14.0% of DNA in the tail, respectively. BLM, topoisomerase II α and BLM/topoisomerase II α knock-downs resulted in a higher percentage of DNA in the comet tail, (36.5, 38.8 and 41.9, respectively) than the negative controls. The difference between the BLM, topoisomerase II α and BLM/topoisomerase II α knock-downs was not statistically significant as determined by ANOVA test. These data suggest that BLM and topoisomerase II α function in a common pathway to prevent chromosome breakage.

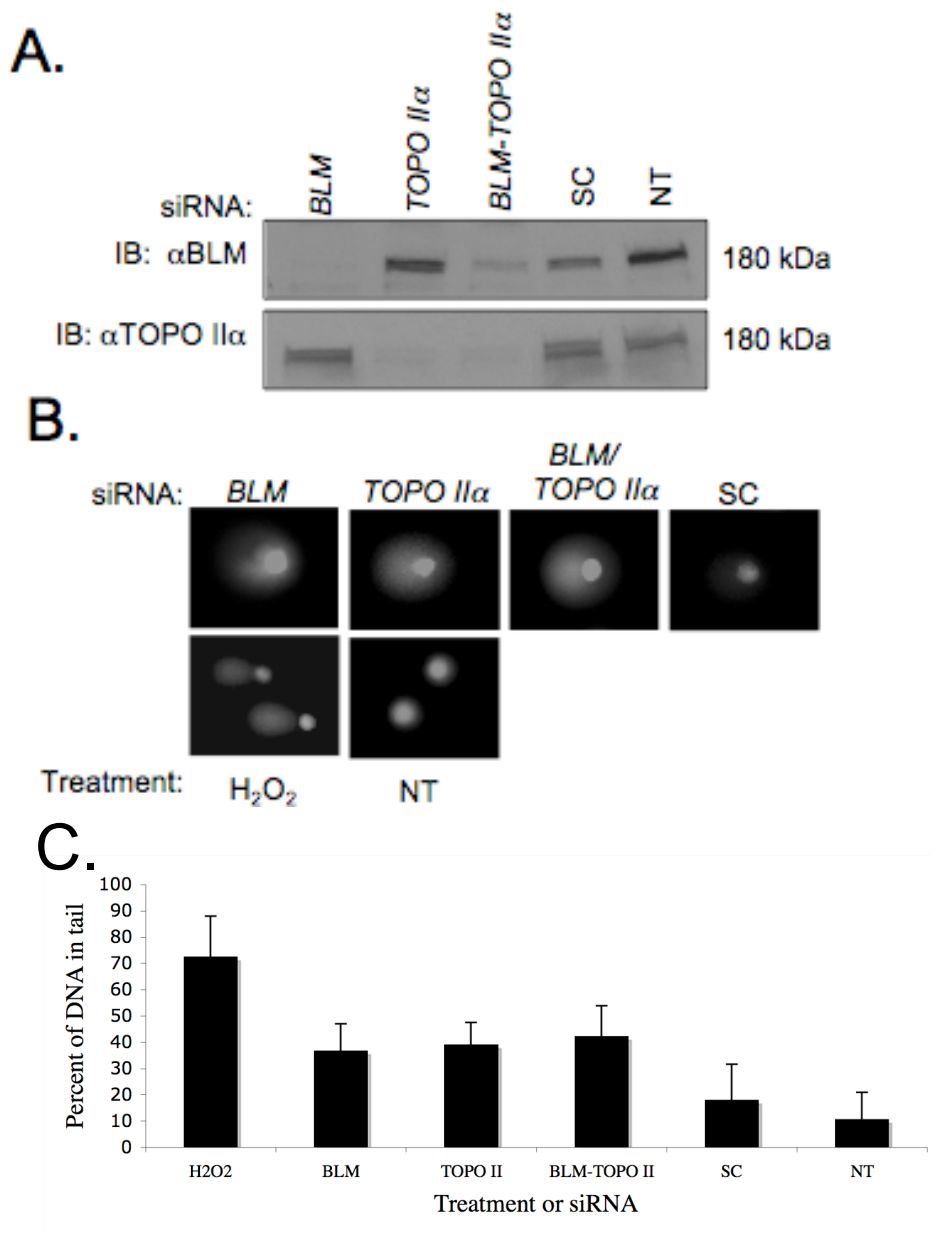


Figure 15. Comet tail size does not change following *siRNA*-mediated knock-down of BLM, topoisomerase II α , and both in combination. **A.** Western blot analysis of BLM and topoisomerase II α in HeLa nuclear extracts prepared from cells transfected with *siRNAs* targeting *BLM*, and *TOP2 α* or a scrambled control (SC). A non-treated control (NT) shows normal levels of the two proteins in this cell line. **B.** Representative comet assays of cells transfected with the indicated *siRNAs*. Hydrogen peroxide (H₂O₂) treated and untreated cells are shown as positive and negative controls, respectively. **C.** Histogram showing the percent of DNA in the comet tails for the indicated *siRNA* transfections or treatments. Comets were analyzed 24 hours post-transfection or 1 hour after H₂O₂ treatment, and analyzed using CometScore (TriTek Corp.). Histograms represent the average of 100 comet tails measured per sample from at least three different assays.

Amino acids 489-587 are necessary for binding topoisomerase II α .

In order to test whether a direct interaction of BLM and topoisomerase II α is required to prevent chromosome breakage, a deletion construct of *pEGFP-BLM* was generated without the region of BLM identified in Chapter Three required for topoisomerase II α -interaction (*pEGFP-BLM^{Δ489-587}*). 293T cells were transfected with *pEGFP-BLM* or *pEGFP-BLM^{Δ489-587}* and co-immunoprecipitations were performed to determine whether the BLM deletion mutant binds topoisomerase II α . Western blot analysis of nuclear extracts (IN) from *pEGFP-BLM^{Δ489-587}* transfected cells with an anti-GFP antibody revealed a protein with a slightly faster electrophoretic mobility than that seen in the *pEGFP-BLM* transfected cells (Figure 16A). This observation suggests that the BLM mutant is smaller than the wild-type protein, as expected. Immunoprecipitations with anti-GFP antibodies using lysates from 293T *pEGFP-BLM*- or *pEGFP-BLM^{Δ489-587}*-transfected cells show a marked decrease in co-immunoprecipitated topoisomerase II α in cells transfected with the mutant versus wild-type BLM (Figure 16A).

In order to verify that the lack of co-immunoprecipitation of topoisomerase II α by the *EGFP-BLM^{Δ489-587}* mutant was not due to lack of co-localization to the nucleus, 293T cells were transfected with *pEGFP-BLM^{Δ489-587}*. GFP fluorescence of transfected 293T cells demonstrates expression of *EGFP-BLM^{Δ489-587}* in small nuclear foci (Figure 16B a-b) and within the nucleolus (Figure 16B c-d), similar to what is normally observed for normal BLM protein [11,48]. Furthermore, co-localization with PML (Figure 16C) shows that this mutant is capable of correct compartmentalization suggesting that the lack of co-immunoprecipitation observed is due to the absence of the topoisomerase II α interaction domain.

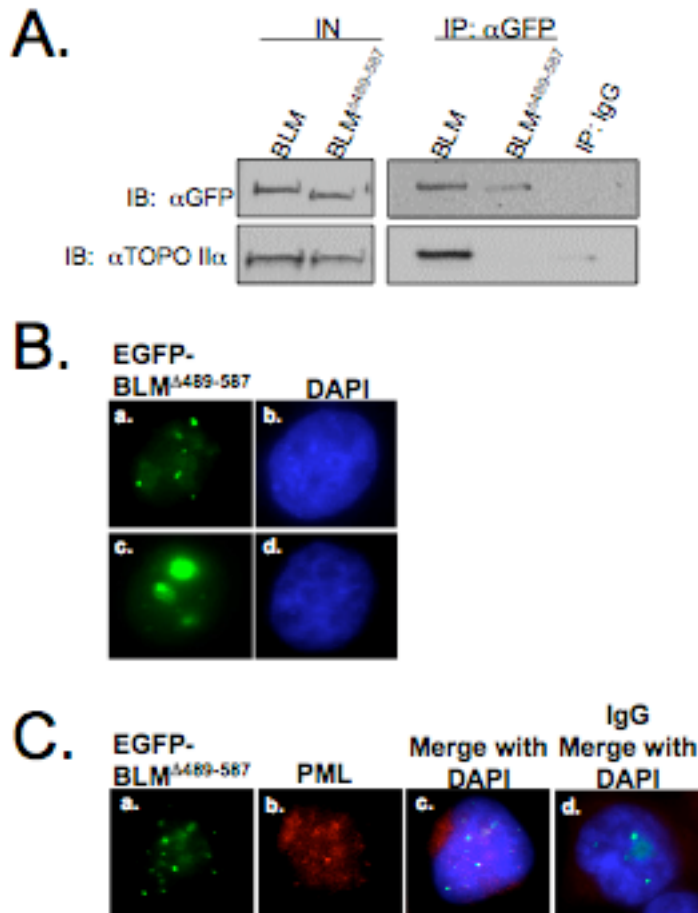


Figure 16. N-terminal amino acids 489-587 of BLM are necessary for topoisomerase II α binding. A. 293T cells were transfected with *pEGFP-BLM* or *pEGFP-BLM^{Δ489-587}* vectors. Twenty-four hours post-transfection, wild-type and mutant BLM proteins were immunoprecipitated from nuclear extracts with mouse anti-GFP antibody or mouse IgG control. Immunoprecipitated proteins were separated using SDS-PAGE and analyzed by western blotting with anti-GFP or anti-topoisomerase II α antibodies. B. 293T cells were transfected with the *pEGFP-BLM^{Δ489-587}* vector. Twenty-four hours post-transfection, cells were fixed and stained with anti-topoisomerase II α antibodies, and DAPI for nuclear staining. a. shows asynchronous cells with EGFP-BLM^{Δ489-587} punctate staining, c. shows asynchronous cells with EGFP-BLM^{Δ489-587} nucleolar staining and b,c. show that the EGFP expression is contained in the nucleus. C. 293T cells were transfected with the *pEGFP-BLM^{Δ489-587}* vector. Twenty-four hours post-transfection cells were fixed and stained with anti-topoisomerase II α antibodies, PML and DAPI for nuclear staining. a. shows cells with EGFP-BLM^{Δ489-587} punctate staining, b. shows cells stained for PML, c. shows merged images of EGFP-BLM^{Δ489-587}, PML and DAPI staining and d. shows merged images of EGFP-BLM^{Δ489-587}, IgG and DAPI staining.

The topoisomerase II α interaction domain of BLM is required for correction of increased chromosome breakage in BS cells.

Having verified that the EGFP-BLM^{A489-587} mutant protein is unable to bind topoisomerase II α , and its ability to correctly localize to PML bodies and the nucleolus, the effect of the loss of the BLM-topoisomerase II α interaction on chromosome breakage was analyzed. BS cells show endogenous γ H2AX activation [120] that can be partially rescued by the reintroduction of wild-type BLM. The BS cell line GM08505 was either left untransfected, or transfected with *pEGFP-BLM* or *pEGFP-BLM*^{A489-587}. Representative cells stained for γ H2AX are shown in Figure 17A. Cells showing both nucleolar and punctate EGFP protein expression are shown. The majority of non-transfected GM08505 cells displayed between 10 and 20 γ H2AX foci (57.14%), 11.44% of the cells had fewer than 10 foci, 20% of the cells showed 21 to 30 and 11.4% showed more than 30 foci (Figure 17B). Transfection with *pEGFP-BLM* doubled the percentage of cells with less than 10 foci to 24.24% and cells with 10-20 foci to 62.12%. Transfection with wild-type BLM decreased the percentage of cells with 21-30 foci by half, to 10.6% and the percentage of cells with greater than 30 foci was reduced to 3.03% compared to the untransfected cells. These observations suggest that re-introduction of wild-type BLM can partially correct the breakage phenotype of BS cells. In contrast, transfection of BS cells with *pEGFP-BLM*^{A489-587} seemed to exacerbate the breakage phenotype observed in the untransfected BS cells. No cells were observed that contained less than 10 γ H2AX foci while the number of cells with 10-20 foci was greatly reduced (16.66%), compared to untransfected cells. This reduction was accompanied by a dramatic increase in cells containing more than 30 foci to 64.58%, whereas the percentage of cells with 21-30 foci remained at relatively similar levels to untransfected cells (18.75%). Interestingly, although this experiment was not designed to assay

micronuclei formation, another measure of DNA breakage, 14.58% of cells transfected with *pEGFP-BLM^{A489-587}* displayed micronuclei, whereas only 6.06% of BS cells corrected with *pEGFP-BLM* showed micronuclei (data not shown). These results show that in a BLM mutant lacking the topoisomerase II α interaction domain, breakage that would normally be repaired by the action of a BLM dependent pathway does not take place resulting in increased breakage.

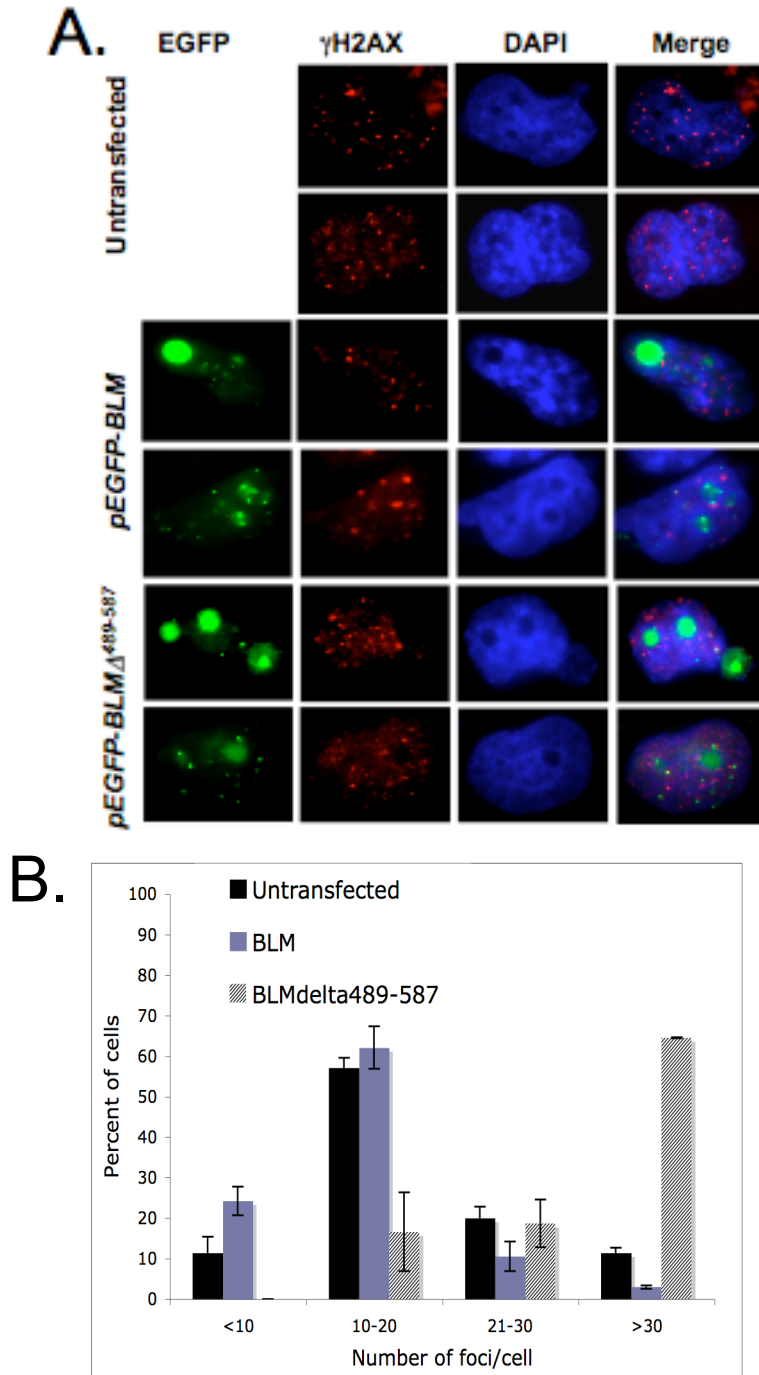


Figure 17. The interaction of BLM and topoisomerase II α is necessary to revert the breakage phenotype of BS cells. A. GM08505 cells (BLM $^{-/-}$) were untransfected or transfected with pEGFP-BLM or pEGFP-BLM $^{\Delta 489-587}$ vectors. Seventy-two hours post-transfection, cells were fixed and stained with an anti- γ H2AX antibody, and DAPI for nuclear staining. Two representative cells for each transfection condition are shown. B. Histogram showing the percentage of cells with the indicated number of γ H2AX foci. Percentages represent the average of at least 50 cells from three separate experiments.

IV. Conclusions.

The data obtained in this chapter provide evidence that BLM and topoisomerase II α function in a common pathway that prevents chromosome breakage. *siRNA*-mediated gene knock-down of *BLM* or *TOPO II α* in normal cells led to a level of chromosome breakage that was not increased additively when both genes were knocked-down simultaneously. The generation of the mutant BLM protein, EGFP-BLM^{A489-587}, lacking the topoisomerase II α interaction domain, showed that this region is needed to co-immunoprecipitate topoisomerase II α . Transfection of a BS cell line with a vector expressing wild-type BLM protein partially rescued the level of γ H2AX focus formation, an affect that was not observed when BS cells were transfected with the mutant vector (*pEGFP-BLM^{A489-587}*). Instead, expression of the EGFP-BLM^{A489-587} mutant, exacerbated the number of γ H2AX foci in cells compared to untransfected cells. These data suggest that in the presence of BLM, cells commit to BLM dependent pathways of double strand break repair. The inability of the EGFP-BLM^{A489-587} mutant to bind topoisomerase II α locks the cells in such pathways without the ability to completely or correctly finish DNA repair leading to the observed increase in γ H2AX focus formation. Taken together, these data suggest an involvement of BLM and topoisomerase II α in a pathway that prevents chromosome breakage.

CHAPTER FIVE. Thesis Summary and Discussion.

BS is a rare autosomal recessive disorder in which affected individuals show pre- and post-natal growth retardation, sun-sensitive facial erythema, immunodeficiency, male infertility and female subfertility. BS individuals are predisposed to a plethora of cancers often occurring in individuals by the age of 25 [3]. Cytogenetically, the hallmark of BS cells is excessive sister chromatid exchanges (SCE), [8], quadriradial structures (QRs) [8], telomere associations (TA) [9] and chromosome breaks [2,10]. The chromosomal abnormalities found in BS cells are caused by the lack of BLM protein and propose a role for BLM in processes such as homologous recombination (HR), telomere maintenance and double strand break repair (DSBR). The BLM protein is an ATP- and Mg^{2+} - dependent structure specific helicase with 3'-5' directionality [32]. Its substrates include model replication forks [44], X-junctions [40], double Holliday junctions [41], G4 DNA, or G tetraplex DNA [37], DNA duplexes containing a bubble [25], D-loops [39], and DNA duplexes with a 3' overhang [32], DNA structures appearing as intermediates in HR and telomeres.

In vivo, characteristics of BS cells such as slow DNA replication fork progression, abnormal distribution of DNA intermediates [98], and high sensitivity to HU and other DNA replication inhibiting drugs [80,82] suggest a role for BLM in the restart of DNA replication during S-phase, a process that can occur through recombination pathways. BLM exerts an anti-recombinogenic role through processing of early HR intermediates allowing repair to follow by other non-recombination pathways [95]. Once the cells are committed to repair by HR, biochemical evidence supports a pro-recombinogenic role for BLM by the processing of early HR intermediates that allow proficient generation of a 3' overhang used for strand invasion [72],

and proficient strand displacement activity that allows polymerase replication within structures that are forked [60].

Other evidence suggests that BLM may also play a role in chromosome segregation. BS cells display excessive levels of anaphase bridging and lagging chromosomes [110], structures that represent incompletely segregated chromosomes and could give rise to chromosome breaks generated by the mitotic spindle forces [96]. In fact, chromosome breakage was one of the first distinguishing cytological characteristics observed in BS cells [10]. In the budding yeast, *S. cerevisiae*, the BLM ortholog Sgs1, binds to a type II topoisomerase and their action is required for proper chromosome segregation [76].

Together, these observations suggested that we test whether the BLM helicase interacts directly or indirectly with the mammalian type II topoisomerase, topoisomerase II α , and whether their interaction is necessary for chromosome segregation or any aspect of HR repair, both of which could lead to chromosome breakage if not properly processed.

The data in Chapter Three show that the interaction between BLM and topoisomerase II α is conserved in mammalian cells in a cell cycle-dependent manner. The association of BLM and topoisomerase II α occurred in S-, G₂/M- and most prominent in M-phase (Figures 7 and 8). These observations suggest that the association of BLM and topoisomerase II α could be necessary to carry out processes in these phases of the cell-cycle, and perhaps most importantly in M-phase.

In vitro binding assays using distinct segments of BLM were employed to determine the topoisomerase II α interaction domain within BLM. This interaction occurs via BLM amino acids 489-587, a small segment in the N-terminus directly preceding the helicase domain (Figure 9). Its proximity to the helicase domain may allow topoisomerase II α to mediate changes in the

activity of BLM, providing further support for testing the effect of topoisomerase II α on the helicase activity of BLM. This small fragment falls within a larger fragment previously identified in yeast Sgs1 ortholog [76].

The biochemical data obtained provide evidence that BLM and topoisomerase II α may be involved in processing early HR intermediates but not those that occur later HR (Figure 14). Topoisomerase II α increased the specific activity of BLM on a 3' overhang more than three fold and on a bubble substrate almost five fold (Table 2). BLM and topoisomerase II α interaction may enhance the generation of the 3' overhang needed for strand invasion. In this model, BLM-topoisomerase II α and an exonuclease would work synergistically in the processing and generation of the 3' overhang. An interaction between BLM and EXO1 has been reported to stimulate EXO1 resection of DNA ends to enable DNA strand exchange by RAD51 [72], therefore, we propose that the action of BLM and topoisomerase II α could enhance the activity of EXO1 (Figure 18B). The biochemical data also show that topoisomerase II α enhances the unwinding of a bubble substrate. Following RAD51 strand exchange, BLM-topoisomerase II α could be involved in the processing of the ends of the D-loop structure (the same as one end of a bubble or a forked DNA structure), facilitating melting of the D-loop to allow replication from the invading strand. This is supported by the ability of BLM to stimulate DNA Pol η DNA synthesis on substrates that resemble one end of the D-loop [61]. Additionally, BLM was reported to interact with p12, the small subunit of DNA Pol δ , and this interaction enhances DNA Pol δ strand displacement activity allowing replication through DNA structures that are forked [60]. It still needs to be determined if the BLM-topoisomerase II α complex can enhance the activities of EXO1 or DNA Pol δ *in vitro*. Additionally, co-immunoprecipitation of EXO1 and DNA Pol δ with BLM and topoisomerase II α in situations of replication stress (HU

treatment) or double strand breaks (IR treatment) will help strengthen this model and should be considered in the future. Preliminary co-immunoprecipitation experiments show that under replication stress, the BLM-topoisomerase II α interaction remains (data not shown).

The data obtained with the model replication fork were unfortunately inconclusive as fork regression did not take place (Figure 14C), but are consistent with other data obtained. We propose that the biochemical activity taking place in Figure 14C is BLM unwinding of the 70 lead and 70 lag strands (a forked substrate) instead of fork regression. The increase in specific activity upon the addition of topoisomerase II α would represent an enhancement of a forked substrate, similar to one end of the bubble substrate. If fork regression had occurred in this assay, the change in specific activity of BLM in the presence of topoisomerase II α would most likely be absent, since the “chicken foot” intermediate is most similar to the X-junction substrate.

Although the biochemical data presented here suggest that topoisomerase II α may not influence the activity of BLM on intermediates produced later in the process of HR, the combined action of BLM and topoisomerase II α on the dissolution of double Holliday junction is worth examining. Double Holliday junctions are catenated structures [121], and the main activity of topoisomerase II α is decatenation, therefore BLM and topoisomerase II α may be involved in the dissolution of these structures. If not resolved properly, these structures are proposed to remain during mitosis leading to the fine anaphase bridges [110].

Evidence of a prominent interaction between BLM and topoisomerase II α in mitosis prompted the determination of what effect BLM has on the activity of topoisomerase II α . The main role of topoisomerase II α is chromosome decatenation, which needs to be completed before the onset of anaphase. Failure to fully decatenate chromosomes prior to or in mitosis is associated with increased DNA breakage [111]. The *in vitro* decatenation assays did not provide

any evidence that BLM is able to change the decatenation activity of topoisomerase II α (Figure 11). This does not, however, preclude a role for BLM and topoisomerase II α in mitotic decatenation as our *in vitro* assay conditions may have been suboptimal. Failure of our decatenation assays to show any change in catalytic activity of topoisomerase II α may be related to unknown post-translational modifications of either protein or the lack of other proteins in the assay. Indeed, other proteins have been reported to co-localize with BLM to fine anaphase bridges including topoisomerase III α , BLAP75 and the PICH protein, that links centromeric regions [110]. Additionally, BLM is modified in mitosis, by MPS1 phosphorylation at residue S144, which in turn, allows its interaction with PLK1. Phosphorylation at BLM S144 is necessary for PLK1 interaction and for accurate chromosome segregation [77]. The identification of a mitotic BLM complex that includes topoisomerase II α may help more fully define the role of BLM in mitotic chromosome segregation.

The co-localization and direct interaction of BLM and topoisomerase II α and their synergistic effect on resolution of *in vitro* HR intermediates lead to the examination of their interaction as related to chromosome breakage, as defects in the process of HR lead to the accumulation of DSBs. *siRNA*-mediated knock-down of either *BLM* or *TOPO II α* increased chromosome breakage as shown by comet assays compared to wild type cells; breakage was not increased above these levels when the two were knocked-down simultaneously (Figure 15). These results suggest that BLM and topoisomerase II α function in a common pathway to prevent chromosome breakage.

To determine if the prevention of chromosome breakage was mediated by a direct interaction of BLM and topoisomerase II α , a deletion construct of *pEGFP-BLM* lacking the previously mapped topoisomerase II α -interaction domain was generated (*pEGFP-BLM* ^{Δ 489-587}).

This deletion mutant was unable to co-immunoprecipitate topoisomerase II α from 293T nuclear lysates (Figure 16). Because the lack of interaction could potentially be due to the inappropriate targeting of the mutant protein to the nucleus, immunofluorescence was used to determine the cellular compartmentalization of the mutant protein. Results in Figure 17 show that this mutant protein is localized to the nucleus in small punctate foci with PML and also in the nucleolus, similarly to wild-type BLM. Therefore, the lack of topoisomerase II α co-immunoprecipitation is most likely due to the loss interaction. These results not only validate the strategy used to map the interaction domain, but also strengthen the idea that the *in vivo* association of BLM and topoisomerase II α is mediated via a physical interaction rather than via a larger protein complex.

The BS cell line GM08505 was used to determine whether the ablation of the BLM-topoisomerase II α interaction affected levels of chromosome breakage. BS cells show endogenous γ H2AX activation [120] that can be partially rescued by the reintroduction of wild-type BLM, a phenomenon also observed with partial reduction of SCE in BS cells by the reintroduction of wild-type BLM [122]. Non-transfected GM08505 cells showed high levels of γ H2AX foci formation (Figure 17). Transfection with a wild-type *BLM* reduced the average number of γ H2AX foci per cell. Conversely, transfection with a vector expressing the topoisomerase II α -binding mutant did not reduce the average number of γ H2AX foci per cell, but instead exacerbated it. These data are consistent with a model in which the presence of BLM commits cells to BLM dependent pathways repair. The inability of the EGFP-BLM ^{Δ 489-587} mutant to bind topoisomerase II α locks the cells in such pathways without the ability to completely or correctly finish DNA repair leading to the observed increase in γ H2AX focus formation.

Micronuclei, small extra nuclei containing chromosomal fragments extruded from the nucleus, are a general feature of BS cells [11]. Experiments in Figure 17 showed some cells that had excluded micronuclei. The percentage of cells excluding micronuclei in the *pEGFP-BLM^{A489-587}*-transfected cells was more than the *pEGFP-BLM*-transfected cells. Unpublished results from our laboratory show that a phosphorylation site mutant of BLM (BLM^{T547A}) is unable to reduce micronuclei in BS cells (Keirse et al., unpublished results). This site is a putative ATM/ATR phosphorylation site within our mapped topoisomerase II α -binding domain. Two other BLM phosphorylation sites that fall within the topoisomerase II α -binding domain have been identified. S517 and S579 have been verified by mass spectrometry and site-directed mutagenesis as phosphorylated *in vitro* by CHK1 and CHK2 (Keirse et al., unpublished results). Future experiments will determine how phosphorylation of BLM during the damage response affects topoisomerase II α binding and how these phosphorylation site mutants affect the function of BLM and topoisomerase II α in chromosome breakage.

As a whole, the data presented in this work suggest an involvement of BLM and topoisomerase II α in a pathway that prevents chromosome breakage via the regulation of HR intermediates that occur at an early stage. Figure 18A proposes that in situations of DSBs, cells lacking BLM can repair the damage by using other pathways such as NHEJ or SSA [91]. HR could also occur, albeit inefficiently leading to the observable basal levels of breakage in BS cells. The presence of BLM leads to efficient repair of DSB via HR, but commits cells to such a pathway. The inability of BLM to bind topoisomerase II α leads to lack of or incomplete repair increasing the amount of γ H2AX foci observed. The involvement of BLM and topoisomerase II α in repair could lead to EXO1 enhanced resection of DNA ends to enable DNA strand exchange by RAD51, and/or the enhancement of DNA Pol δ strand displacement activity

allowing replication of the invading strand through DNA structures that are forked (Figure 18B). These results suggest a pro-recombinogenic role for BLM and topoisomerase II α . Although evidence supports both pro-and anti-recombinogenic roles of BLM, at the current time it is unclear how exactly these biochemical activities of BLM come together physiologically. It is clear however, that a combination of these is necessary for the maintenance of genomic integrity.

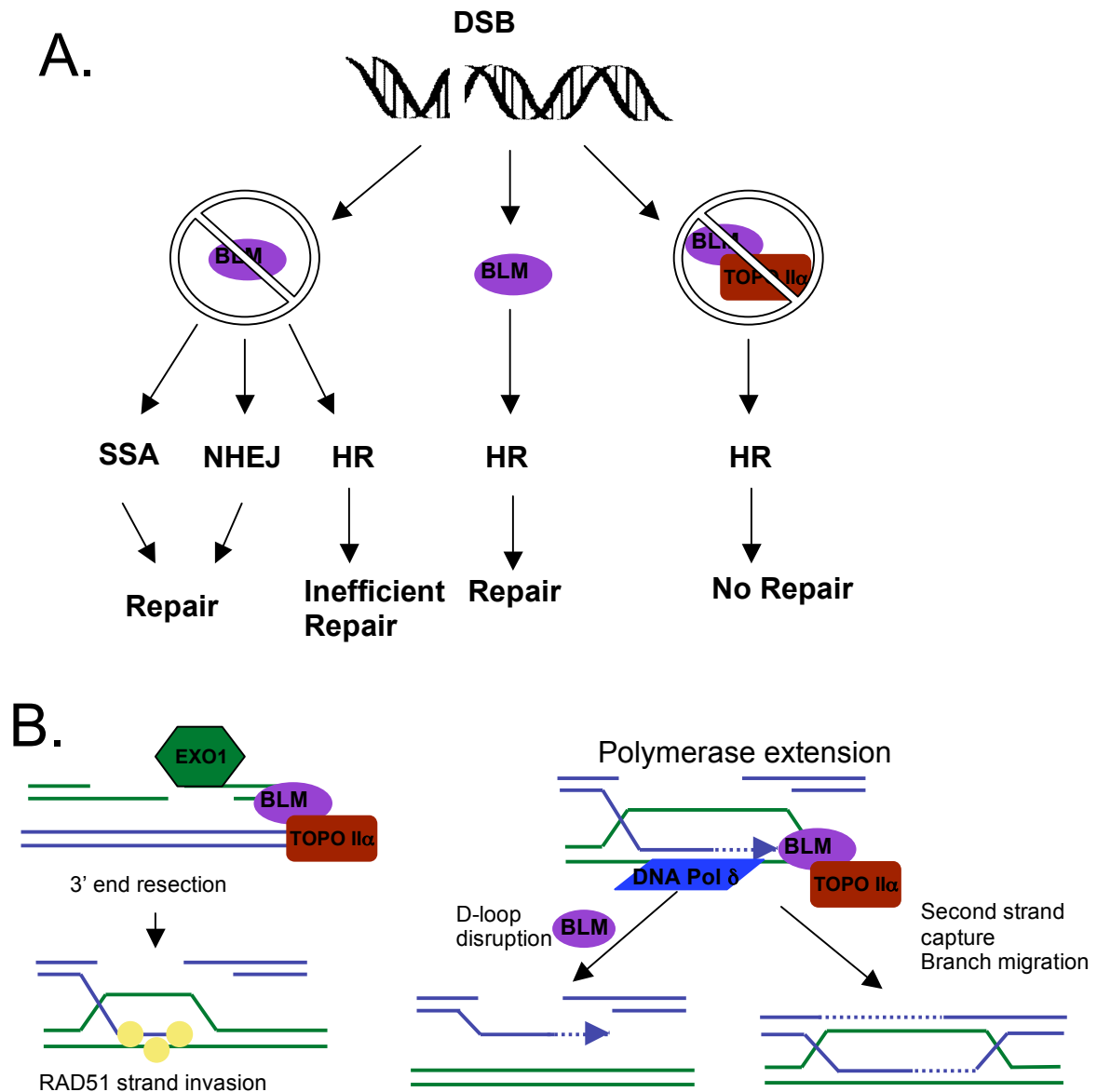


Figure 18. Model for BLM and topoisomerase II α involvement in double strand break repair. **A.** In situations of DSBs, cells lacking BLM can repair the damage by using other pathways such as NHEJ or SSA. HR could also occur, albeit inefficiently leading to the observable basal levels of breakage in BS cells. The presence of BLM leads to efficient repair of DSB via HR, but commits cells to such a pathway. The inability of BLM to bind topoisomerase II α leads to lack of, or incomplete repair. **B.** The interaction of BLM and topoisomerase II α is proposed to enhance EXO1 resection of DNA ends to enable DNA strand exchange by RAD51 (represented as yellow circles), and/or could enhance DNA Pol δ strand displacement activity allowing replication of the invading strand through DNA structures that are forked. Normal functions of BLM in the resolution of the intermediates that form would then follow.

CHAPTER SIX. Bibliography.

1. Bloom, D. (1954) Congenital telangiectatic erythema resembling lupus erythematosus in dwarfs. *Am J Dis Child*, **88**, 754.
2. German, J. (1964) Cytological Evidence for Crossing-over in Vitro in Human Lymphoid Cells. *Science*, **144**, 298-301.
3. German, J. (1993) Bloom syndrome: a mendelian prototype of somatic mutational disease. *Medicine (Baltimore)*, **72**, 393-406.
4. German, J., Sanz, M.M., Ciocci, S., Ye, T.Z., Ellis, N.A. (2007) Syndrome-causing mutations of the BLM gene in persons in the Bloom's syndrome registry. *Hum Mutat*, **28**, 743-753.
5. Ellis, N.A. (1997) DNA helicases in inherited human disorders. *Curr Opin Genet Dev*, **7**, 354-63.
6. Kondo, N., Ozawa, T., Kato, Y., Motoyoshi, F., Kasahara, K., Kameyama, T. and Orii, T. (1992) Reduced secreted mu mRNA synthesis in selective IgM deficiency of Bloom's syndrome. *Clin Exp Immunol*, **88**, 35-40.
7. Hutteroth, T.H., Litwin, S.D. and German, J. (1975) Abnormal immune responses of Bloom's syndrome lymphocytes in vitro. *J Clin Invest*, **56**, 1-7.
8. Chaganti, R.S., Schonberg, S. and German, J. (1974) A manyfold increase in sister chromatid exchanges in Bloom's syndrome lymphocytes. *Proc Natl Acad Sci U S A*, **71**, 4508-12.
9. German, J. and Crippa, L.P. (1966) Chromosomal breakage in diploid cell lines from Bloom's syndrome and Fanconi's anemia. *Annales de Genetique*, **9**, 143-153.
10. German, J., Archibald, R. and Bloom, D. (1965) Chromosomal Breakage in a Rare and Probably Genetically Determined Syndrome of Man. *Science*, **148**, 506-7.
11. Yankiwski, V., Marciniak, R.A., Guarente, L. and Neff, N.F. (2000) Nuclear structure in normal and Bloom syndrome cells. *Proc Natl Acad Sci U S A*, **97**, 5214-9.
12. Hand, R. and German, J. (1975) A retarded rate of DNA chain growth in Bloom's syndrome. *Proc Nat Acad Sci U S A*, **72**, 758-762.
13. Ellis, N.A., Groden, J., Ye, T.Z., Straughen, J., Lennon, D.J., Ciocci, S., Proytcheva, M. and German, J. (1995) The Bloom's syndrome gene product is homologous to RecQ helicases. *Cell*, **83**, 655-66.
14. McDaniel, L.D. and Schultz, R.A. (1992) Elevated sister chromatid exchange phenotype of Bloom syndrome cells is complemented by human chromosome 15. *Proc Natl Acad Sci U S A*, **89**, 7968-72.
15. German, J., Roe, A.M., Leppert, M.F. and Ellis, N.A. (1994) Bloom syndrome: an analysis of consanguineous families assigns the locus mutated to chromosome band 15q26.1. *Proc Natl Acad Sci U S A*, **91**, 6669-73.
16. Straughen, J., Ciocci, S., Ye, T.Z., Lennon, D.N., Proytcheva, M., Alhadeff, B., Goodfellow, P., German, J., Ellis, N.A. and Groden, J. (1996) Physical mapping of the bloom syndrome region by the identification of YAC and P1 clones from human chromosome 15 band q26.1. *Genomics*, **35**, 118-28.
17. Straughen, J.E., Johnson, J., McLaren, D., Proytcheva, M., Ellis, N., German, J. and Groden, J. (1998) A rapid method for detecting the predominant Ashkenazi Jewish mutation in the Bloom's syndrome gene. *Hum Mutat*, **11**, 175-8.

18. Watt, P.M., Louis, E.J., Borts, R.H. and Hickson, I.D. (1995) Sgs1: a eukaryotic homolog of E. coli RecQ that interacts with topoisomerase II in vivo and is required for faithful chromosome segregation. *Cell*, **81**, 253-60.
19. Stewart, E., Chapman, C.R., Al-Khodairy, F., Carr, A.M. and Enoch, T. (1997) rqh1+, a fission yeast gene related to the Bloom's and Werner's syndrome genes, is required for reversible S phase arrest. *Embo J*, **16**, 2682-92.
20. Karow, J.K., Wu, L. and Hickson, I.D. (2000) RecQ family helicases: roles in cancer and aging. *Curr Opin Genet Dev*, **10**, 32-8.
21. Dietschy, T., Shevelev, I. and Stagljar, I. (2007) The molecular role of the Rothmund-Thomson-, RAPADILINO- and Baller-Gerold-gene product, RECQL4: recent progress. *Cell Mol Life Sci*, **64**, 796-802.
22. Mohaghegh, P. and Hickson, I.D. (2001) DNA helicase deficiencies associated with cancer predisposition and premature ageing disorders. *Hum Mol Genet*, **10**, 741-6.
23. Siitonen, H.A., Kopra, O., Kaariainen, H., Haravuori, H., Winter, R.M., Saamanen, A.M., Peltonen, L. and Kestila, M. (2003) Molecular defect of RAPADILINO syndrome expands the phenotype spectrum of RECQL diseases. *Hum Mol Genet*, **12**, 2837-44.
24. van Brabant, A.J., Stan, R. and Ellis, N.A. (2000) DNA helicases, genomic instability, and human genetic disease. *Annu Rev Genomics Hum Genet*, **1**, 409-59.
25. Mohaghegh, P., Karow, J.K., Brosh Jr, R.M., Jr., Bohr, V.A. and Hickson, I.D. (2001) The Bloom's and Werner's syndrome proteins are DNA structure-specific helicases. *Nucleic Acids Res*, **29**, 2843-9.
26. Hickson, I.D. (2003) RecQ helicases: caretakers of the genome. *Nat Rev Cancer*, **3**, 169-78.
27. Popuri, V., Bachrati, C.Z., Muzzolini, L., Mosedale, G., Costantini, S., Giacomini, E., Hickson, I.D. and Vindigni, A. (2008) The Human RecQ helicases, BLM and RECQ1, display distinct DNA substrate specificities. *J Biol Chem*, **283**, 17766-76.
28. Wu, L., Chan, K.L., Ralf, C., Bernstein, D.A., Garcia, P.L., Bohr, V.A., Vindigni, A., Janscak, P., Keck, J.L. and Hickson, I.D. (2005) The HRDC domain of BLM is required for the dissolution of double Holliday junctions. *Embo J*, **24**, 2679-87.
29. Shimamoto, A., Nishikawa, K., Kitao, S. and Furuichi, Y. (2000) Human RecQ5beta, a large isomer of RecQ5 DNA helicase, localizes in the nucleoplasm and interacts with topoisomerases 3alpha and 3beta. *Nucleic Acids Res*, **28**, 1647-55.
30. Nakayama, H. (2002) RecQ family helicases: roles as tumor suppressor proteins. *Oncogene*, **21**, 9008-21.
31. Orren, D.K., Machwe, A., Karmakar, P., Piotrowski, J., Cooper, M.P. and Bohr, V.A. (2001) A functional interaction of Ku with Werner exonuclease facilitates digestion of damaged DNA. *Nucleic Acids Res*, **29**, 1926-34.
32. Karow, J.K., Chakraverty, R.K. and Hickson, I.D. (1997) The Bloom's syndrome gene product is a 3'-5' DNA helicase. *J Biol Chem*, **272**, 30611-4.
33. Karow, J.K., Newman, R.H., Freemont, P.S. and Hickson, I.D. (1999) Oligomeric ring structure of the Bloom's syndrome helicase. *Curr Biol*, **9**, 597-600.
34. Lohman, T.M. and Bjornson, K.P. (1996) Mechanisms of helicase-catalyzed DNA unwinding. *Annu Rev Biochem*, **65**, 169-214.
35. Brosh, R.M., Jr., Li, J.L., Kenny, M.K., Karow, J.K., Cooper, M.P., Kurekattil, R.P., Hickson, I.D. and Bohr, V.A. (2000) Replication protein A physically interacts with the

- Bloom's syndrome protein and stimulates its helicase activity. *J Biol Chem*, **275**, 23500-8.
36. Garcia, P.L., Bradley, G., Hayes, C.J., Krintel, S., Soultanas, P. and Janscak, P. (2004) RPA alleviates the inhibitory effect of vinylphosphonate internucleotide linkages on DNA unwinding by BLM and WRN helicases. *Nucleic Acids Res*, **32**, 3771-8.
 37. Sun, H., Karow, J.K., Hickson, I.D. and Maizels, N. (1998) The Bloom's syndrome helicase unwinds G4 DNA. *J Biol Chem*, **273**, 27587-92.
 38. Brosh, R.M., Jr., Majumdar, A., Desai, S., Hickson, I.D., Bohr, V.A. and Seidman, M.M. (2001) Unwinding of a DNA triple helix by the Werner and Bloom syndrome helicases. *J Biol Chem*, **276**, 3024-30.
 39. van Brabant, A.J., Ye, T., Sanz, M., German, I.J., Ellis, N.A. and Holloman, W.K. (2000) Binding and melting of D-loops by the Bloom syndrome helicase. *Biochemistry*, **39**, 14617-25.
 40. Karow, J.K., Constantinou, A., Li, J.L., West, S.C. and Hickson, I.D. (2000) The Bloom's syndrome gene product promotes branch migration of holliday junctions. *Proc Natl Acad Sci U S A*, **97**, 6504-8.
 41. Wu, L. and Hickson, I.D. (2003) The Bloom's syndrome helicase suppresses crossing over during homologous recombination. *Nature*, **426**, 870-4.
 42. Yin, J., Sobeck, A., Chang, X., Ruhikanta Meetei, A., Hoatlin, M., Li, L. and Wang, W. (2005) BLAP75, an essential component of Bloom's syndrome protein complexes that maintain genome integrity. *Embo J*, **24**, 1465-1467.
 43. Singh, T.R., Ali, A.M., Busygina, V., Raynard, S., Fan, Q., Du, C.H., Andreassen, P.R., Sung, P. and Meetei, A.R. (2008) BLAP18/RMI2, a novel OB-fold-containing protein, is an essential component of the Bloom helicase-double Holliday junction dissolvosome. *Genes Dev*, **22**, 2856-68.
 44. Machwe, A., Xiao, L., Groden, J. and Orren, D.K. (2006) The Werner and Bloom Syndrome Proteins Catalyze Regression of a Model Replication Fork. *Biochemistry*, **45**, 13939-13946.
 45. Turley, H., Wu, L., Canamero, M., Gatter, K.C. and Hickson, I.D. (2001) The distribution and expression of the Bloom's syndrome gene product in normal and neoplastic human cells. *Br J Cancer*, **85**, 261-5.
 46. Dutertre, S., Ababou, M., Onclercq, R., Delic, J., Chatton, B., Jaulin, C. and Amor-Gueret, M. (2000) Cell cycle regulation of the endogenous wild type Bloom's syndrome DNA helicase. *Oncogene*, **19**, 2731-8.
 47. Kaneko, H., Orii, K.O., Matsui, E., Shimosawa, N., Fukao, T., Matsumoto, T., Shimamoto, A., Furuichi, Y., Hayakawa, S., Kasahara, K. and Kondo, N. (1997) BLM (the causative gene of Bloom syndrome) protein translocation into the nucleus by a nuclear localization signal. *Biochem Biophys Res Commun*, **240**, 348-53.
 48. Bischof, O., Kim, S.H., Irving, J., Beresten, S., Ellis, N.A. and Campisi, J. (2001) Regulation and localization of the Bloom syndrome protein in response to DNA damage. *J Cell Biol*, **153**, 367-80.
 49. Gharibyan, V. and Youssoufian, H. (1999) Localization of the Bloom syndrome helicase to punctate nuclear structures and the nuclear matrix and regulation during the cell cycle: comparison with the Werner's syndrome helicase. *Mol Carcinog*, **26**, 261-73.
 50. Dutertre, S., Sekhri, R., Tintignac, L.A., Onclercq-Delic, R., Chatton, B., Jaulin, C. and Amor-Gueret, M. (2002) Dephosphorylation and subcellular compartment change of the

- mitotic Bloom's syndrome DNA helicase in response to ionizing radiation. *J Biol Chem*, **277**, 6280-6.
51. Wang, Y., Cortez, D., Yazdi, P., Neff, N., Elledge, S.J. and Qin, J. (2000) BASC, a super complex of BRCA1-associated proteins involved in the recognition and repair of aberrant DNA structures. *Genes Dev*, **14**, 927-39.
 52. Meetei, A.R., Sechi, S., Wallisch, M., Yang, D., Young, M.K., Joenje, H., Hoatlin, M.E. and Wang, W. (2003) A multiprotein nuclear complex connects Fanconi anemia and Bloom syndrome. *Mol Cell Biol*, **23**, 3417-26.
 53. Wu, L., Bachrati, C.Z., Ou, J., Xu, C., Yin, J., Chang, M., Wang, W., Li, L., Brown, G.W. and Hickson, I.D. (2006) BLAP75/RMI1 promotes the BLM-dependent dissolution of homologous recombination intermediates. *Proc Natl Acad Sci U S A*, **103**, 4068-73.
 54. Raynard, S., Bussen, W. and Sung, P. (2006) A double Holliday junction dissolvosome comprising BLM, topoisomerase III α , and BLAP75. *J Biol Chem*, **281**, 13861-4.
 55. Yin, J., Sobek, A., Xu, C., Meetei, A.R., Hoatlin, M., Li, L. and Wang, W. (2005) BLAP75, an essential component of Bloom's syndrome protein complexes that maintain genome integrity. *Embo J*, **24**, 1465-76.
 56. Bhattacharyya, S., Keirse, J., Russell, B., Kavecansky, J., Lillard-Wetherell, K., Tahmaseb, K., Turchi, J.J. and Groden, J. (2009) Telomerase-associated Protein 1, HSP90, and Topoisomerase II α Associate Directly with the BLM Helicase in Immortalized Cells Using ALT and Modulate Its Helicase Activity Using Telomeric DNA Substrates. *J Biol Chem*, **284**, 14966-77.
 57. Wu, L., Davies, S.L., Levitt, N.C. and Hickson, I.D. (2001) Potential role for the BLM helicase in recombinational repair via a conserved interaction with RAD51. *J Biol Chem*, **276**, 19375-81.
 58. Pichierri, P., Franchitto, A. and Rosselli, F. (2004) BLM and the FANC proteins collaborate in a common pathway in response to stalled replication forks. *Embo J*, **23**, 3154-63.
 59. Jiao, R., Bachrati, C.Z., Pedrazzi, G., Kuster, P., Petkovic, M., Li, J.L., Egli, D., Hickson, I.D. and Stagljar, I. (2004) Physical and functional interaction between the Bloom's syndrome gene product and the largest subunit of chromatin assembly factor 1. *Mol Cell Biol*, **24**, 4710-9.
 60. Selak, N., Bachrati, C.Z., Shevelev, I., Dietschy, T., van Loon, B., Jacob, A., Hubscher, U., Hoheisel, J.D., Hickson, I.D. and Stagljar, I. (2008) The Bloom's syndrome helicase (BLM) interacts physically and functionally with p12, the smallest subunit of human DNA polymerase delta. *Nucleic Acids Res*, **36**, 5166-79.
 61. Bugreev, D.V., Yu, X., Egelman, E.H. and Mazin, A.V. (2007) Novel pro- and anti-recombination activities of the Bloom's syndrome helicase. *Genes Dev*, **21**, 3085-94.
 62. Yang, Q., Zhang, R., Wang, X.W., Linke, S.P., Sengupta, S., Hickson, I.D., Pedrazzi, G., Perrera, C., Stagljar, I., Littman, S.J., Modrich, P. and Harris, C.C. (2004) The mismatch DNA repair heterodimer, hMSH2/6, regulates BLM helicase. *Oncogene*, **23**, 3749-56.
 63. Langland, G., Kordich, J., Creaney, J., Goss, K.H., Lillard-Wetherell, K., Bebenek, K., Kunkel, T.A. and Groden, J. (2001) The Bloom's syndrome protein (BLM) interacts with MLH1 but is not required for DNA mismatch repair. *J Biol Chem*, **276**, 30031-5.
 64. Pedrazzi, G., Perrera, C., Blaser, H., Kuster, P., Marra, G., Davies, S.L., Ryu, G.H., Freire, R., Hickson, I.D., Jiricny, J. and Stagljar, I. (2001) Direct association of Bloom's

- syndrome gene product with the human mismatch repair protein MLH1. *Nucleic Acids Res*, **29**, 4378-86.
65. Pedrazzi, G., Bachrati, C.Z., Selak, N., Studer, I., Petkovic, M., Hickson, I.D., Jiricny, J. and Stajlgjar, I. (2003) The Bloom's syndrome helicase interacts directly with the human DNA mismatch repair protein hMSH6. *Biol Chem*, **384**, 1155-64.
 66. Stavropoulos, D.J., Bradshaw, P.S., Li, X., Pasic, I., Truong, K., Ikura, M., Ungrin, M. and Meyn, M.S. (2002) The Bloom syndrome helicase BLM interacts with TRF2 in ALT cells and promotes telomeric DNA synthesis. *Hum Mol Genet*, **11**, 3135-44.
 67. Opresko, P.L., von Kobbe, C., Laine, J.P., Harrigan, J., Hickson, I.D. and Bohr, V.A. (2002) Telomere-binding protein TRF2 binds to and stimulates the Werner and Bloom syndrome helicases. *J Biol Chem*, **277**, 41110-9.
 68. Lillard-Wetherell, K., Machwe, A., Langland, G.T., Combs, K.A., Behbehani, G.K., Schonberg, S.A., German, J., Turchi, J.J., Orren, D.K. and Groden, J. (2004) Association and regulation of the BLM helicase by the telomere proteins TRF1 and TRF2. *Hum Mol Genet*, **13**, 1919-32.
 69. Sengupta, S., Linke, S.P., Pedeux, R., Yang, Q., Farnsworth, J., Garfield, S.H., Valerie, K., Shay, J.W., Ellis, N.A., Wasyluk, B. and Harris, C.C. (2003) BLM helicase-dependent transport of p53 to sites of stalled DNA replication forks modulates homologous recombination. *Embo J*, **22**, 1210-22.
 70. von Kobbe, C., Karmakar, P., Dawut, L., Opresko, P., Zeng, X., Brosh, R.M., Jr., Hickson, I.D. and Bohr, V.A. (2002) Colocalization, physical, and functional interaction between Werner and Bloom syndrome proteins. *J Biol Chem*, **277**, 22035-44.
 71. Sharma, S., Sommers, J.A., Wu, L., Bohr, V.A., Hickson, I.D. and Brosh, R.M., Jr. (2004) Stimulation of flap endonuclease-1 by the Bloom's syndrome protein. *J Biol Chem*, **279**, 9847-56.
 72. Nimonkar, A.V., Ozsoy, A.Z., Genschel, J., Modrich, P. and Kowalczykowski, S.C. (2008) Human exonuclease 1 and BLM helicase interact to resect DNA and initiate DNA repair. *Proc Natl Acad Sci U S A*, **105**, 16906-11.
 73. Beamish, H., Kedar, P., Kaneko, H., Chen, P., Fukao, T., Peng, C., Beresten, S., Gueven, N., Purdie, D., Lees-Miller, S., Ellis, N., Kondo, N. and Lavin, M.F. (2002) Functional link between BLM defective in Bloom's syndrome and the ataxia-telangiectasia-mutated protein, ATM. *J Biol Chem*, **277**, 30515-23.
 74. Sengupta, S., Robles, A.I., Linke, S.P., Sinogeeva, N.I., Zhang, R., Pedeux, R., Ward, I.M., Celeste, A., Nussenzweig, A., Chen, J., Halazonetis, T.D. and Harris, C.C. (2004) Functional interaction between BLM helicase and 53BP1 in a Chk1-mediated pathway during S-phase arrest. *J Cell Biol*, **166**, 801-13.
 75. Tripathi, V., Kaur, S. and Sengupta, S. (2008) Phosphorylation-dependent interactions of BLM and 53BP1 are required for their anti-recombinogenic roles during homologous recombination. *Carcinogenesis*, **29**, 52-61.
 76. Watt, P.M., Louis, E.J., Borts, R.H. and Hickson, I.D. (1995) Sgs1: A Eukaryotic Homolog of E. coli RecQ That Interacts with Topoisomerase II In Vivo and Is Required for Faithful Chromosome Segregation. *Cell*, **81**, 253-260.
 77. Leng, M., Chan, D.W., Luo, H., Zhu, C., Qin, J. and Wang, Y. (2006) MPS1-dependent mitotic BLM phosphorylation is important for chromosome stability. *Proc Natl Acad Sci U S A*, **103**, 11485-90.

78. Ababou, M., Dutertre, S., Lecluse, Y., Onclercq, R., Chatton, B. and Amor-Gueret, M. (2000) ATM-dependent phosphorylation and accumulation of endogenous BLM protein in response to ionizing radiation. *Oncogene*, **19**, 5955-63.
79. Ababou, M., Dumaire, V., Lecluse, Y. and Amor-Gueret, M. (2002) Bloom's syndrome protein response to ultraviolet-C radiation and hydroxyurea-mediated DNA synthesis inhibition. *Oncogene*, **21**, 2079-88.
80. Franchitto, A. and Pichierri, P. (2002) Bloom's syndrome protein is required for correct relocalization of RAD50/MRE11/NBS1 complex after replication fork arrest. *J Cell Biol*, **157**, 19-30.
81. Li, W., Kim, S.M., Lee, J. and Dunphy, W.G. (2004) Absence of BLM leads to accumulation of chromosomal DNA breaks during both unperturbed and disrupted S phases. *J Cell Biol*, **165**, 801-12.
82. Davies, S.L., North, P.S., Dart, A., Lakin, N.D. and Hickson, I.D. (2004) Phosphorylation of the Bloom's syndrome helicase and its role in recovery from S-phase arrest. *Mol Cell Biol*, **24**, 1279-91.
83. Abraham, R.T. (2001) Cell cycle checkpoint signaling through the ATM and ATR kinases. *Genes Dev*, **15**, 2177-96.
84. Aurias, A., Antoine, J.L., Assathiany, R., Odievre, M. and Dutrillaux, B. (1985) Radiation sensitivity of Bloom's syndrome lymphocytes during S and G2 phases. *Cancer Genet Cytogenet*, **16**, 131-6.
85. Eladad, S., Ye, T.Z., Hu, P., Leversha, M., Beresten, S., Matunis, M.J. and Ellis, N.A. (2005) Intra-nuclear trafficking of the BLM helicase to DNA damage-induced foci is regulated by SUMO modification. *Hum Mol Genet*, **14**, 1351-65.
86. Valerie, K. and Povirk, L.F. (2003) Regulation and mechanisms of mammalian double-strand break repair. *Oncogene*, **22**, 5792-812.
87. Khanna, K.K. and Jackson, S.P. (2001) DNA double-strand breaks: signaling, repair and the cancer connection. *Nat Genet*, **27**, 247-54.
88. Elliott, B. and Jasin, M. (2002) Double-strand breaks and translocations in cancer. *Cell Mol Life Sci*, **59**, 373-85.
89. van Gent, D.C., Hoeijmakers, J.H. and Kanaar, R. (2001) Chromosomal stability and the DNA double-stranded break connection. *Nat Rev Genet*, **2**, 196-206.
90. Haber, J.E. (2000) Partners and pathways repairing a double-strand break. *Trends Genet*, **16**, 259-64.
91. Iijima, K., Ohara, M., Seki, R., Tauchi, H (2008) Dancing on damaged chromatin: Functions of ATM and the RAD50/MRE11/NBS1 complex in cellular responses to DNA damage. *J. Radiat. Res.*, **49**, 451-464.
92. D'Amours, D. and Jackson, S.P. (2002) The Mre11 complex: at the crossroads of dna repair and checkpoint signalling. *Nat Rev Mol Cell Biol*, **3**, 317-27.
93. San Filippo, J., Sung, P. and Klein, H. (2008) Mechanism of Eukaryotic Homologous Recombination. *Annu Rev Biochem*, **77**, 229-257.
94. Haber, J.E. (1999) DNA recombination: the replication connection. *Trends Biochem Sci*, **24**, 271-5.
95. Adams, M.D., McVey, M. and Sekelsky, J.J. (2003) Drosophila BLM in double-strand break repair by synthesis-dependent strand annealing. *Science*, **299**, 265-7.
96. Payne, M. and Hickson, I.D. (2009) Genomic instability and cancer: lessons from analysis of Bloom's syndrome. *Biochem Soc Trans*, **37**, 553-9.

97. Cheok, C.F., Wu, L., Garcia, P.L., Janscak, P. and Hickson, I.D. (2005) The Bloom's syndrome helicase promotes the annealing of complementary single-stranded DNA. *Nucleic Acids Res*, **33**, 3932-41.
98. Lonn, U., Lonn, S., Nylén, U., Winblad, G. and German, J. (1990) An abnormal profile of DNA replication intermediates in Bloom's syndrome. *Cancer Res*, **50**, 3141-5.
99. Davies, S.L., North, P.S. and Hickson, I.D. (2007) Role for BLM in replication-fork restart and suppression of origin firing after replicative stress. *Nat Struct Mol Biol*, **14**, 677-9.
100. Davalos, A.R. and Campisi, J. (2003) Bloom syndrome cells undergo p53-dependent apoptosis and delayed assembly of BRCA1 and NBS1 repair complexes at stalled replication forks. *J Cell Biol*, **162**, 1197-209.
101. Davalos, A.R., Kaminker, P., Hansen, R.K. and Campisi, J. (2004) ATR and ATM-dependent movement of BLM helicase during replication stress ensures optimal ATM activation and 53BP1 focus formation. *Cell Cycle*, **3**, 1579-86.
102. Langland, G., Elliott, J., Li, Y., Creaney, J., Dixon, K. and Groden, J. (2002) The BLM helicase is necessary for normal DNA double-strand break repair. *Cancer Res*, **62**, 2766-70.
103. Gaymes, T.J., North, P.S., Brady, N., Hickson, I.D., Mufti, G.J. and Rassool, F.V. (2002) Increased error-prone non homologous DNA end-joining--a proposed mechanism of chromosomal instability in Bloom's syndrome. *Oncogene*, **21**, 2525-33.
104. Henson, J.D., Neumann, A.A., Yeager, T.R. and Reddel, R.R. (2002) Alternative lengthening of telomeres in mammalian cells. *Oncogene*, **21**, 598-610.
105. Huang, P., Pryde, F.E., Lester, D., Maddison, R.L., Borts, R.H., Hickson, I.D. and Louis, E.J. (2001) SGS1 is required for telomere elongation in the absence of telomerase. *Curr Biol*, **11**, 125-9.
106. Li, J.L., Harrison, R.J., Reszka, A.P., Brosh, R.M., Jr., Bohr, V.A., Neidle, S. and Hickson, I.D. (2001) Inhibition of the Bloom's and Werner's syndrome helicases by G-quadruplex interacting ligands. *Biochemistry*, **40**, 15194-202.
107. Schawalder, J., Paric, E. and Neff, N.F. (2003) Telomere and ribosomal DNA repeats are chromosomal targets of the bloom syndrome DNA helicase. *BMC Cell Biol*, **4**, 15.
108. Champoux, J.J. (2001) DNA topoisomerases: structure, function, and mechanism. *Annu Rev Biochem*, **70**, 369-413.
109. Wang, J.C. (2002) Cellular roles of DNA topoisomerases: a molecular perspective. *Nat Rev Mol Cell Biol*, **3**, 430-40.
110. Chan, K.-L., North, P.S. and Hickson, I.D. (2007) BLM is required for faithful chromosome segregation and its location defines a class of ultrafine anaphase bridges. *Embo J*, 1-13.
111. Holm, C., Stearns, T. and Botstein, D. (1989) DNA topoisomerase II must act at mitosis to prevent nondisjunction and chromosome breakage. *Mol. Cell. Biol.*, **9**, 159-168.
112. Stewart, G.S., Maser, R.S., Stankovic, T., Bressan, D.A., Kaplan, M.I., Jaspers, N.G., Raams, A., Byrd, P.J., Petrini, J.H. and Taylor, A.M. (1999) The DNA double-strand break repair gene hMRE11 is mutated in individuals with an ataxia-telangiectasia-like disorder. *Cell*, **99**, 577-87.
113. Young, B.R. and Painter, R.B. (1989) Radioresistant DNA synthesis and human genetic disease. *Hum Genet*, **82**, 113-117.

114. Wang, W. (2007) Emergence of a DNA-damage response network consisting of Fanconi anaemia and BRCA proteins. *Nat Rev Genet*, **8**, 735-48.
115. Rahman, N., Seal, S., Thompson, D., Kelly, P., Renwick, A., Elliott, A., Reid, S., Spanova, K., Barfoot, R., Chagtai, T., Jayatilake, H., McGuffog, L., Hanks, S., Evans, D.G., Eccles, D., Easton, D.F. and Stratton, M.R. (2007) PALB2, which encodes a BRCA2-interacting protein, is a breast cancer susceptibility gene. *Nat Genet*, **39**, 165-7.
116. Bugreev, D.V., Yu, X., Egelman, E.H. and Mazin, A.V. (2007) Novel pro- and anti-recombination activities of the Bloom's syndrome helicase. *Genes and Development*.
117. Heck, M.M., Hittelman, W.N. and Earnshaw, W.C. (1988) Differential expression of DNA topoisomerase I and II during the eukarotic cell cycle. *Proc Natl Acad Sci U S A*, **85**, 1086-1090.
118. Machwe, A., Xiao, L., Lloyd, R.G., Bolt, E. and Orren, D.K. (2007) Replication fork regression in vitro by the Werner syndrome protein (WRN): holliday junction formation, the effect of leading arm structure and a potential role for WRN exonuclease activity. *Nucleic Acids Res*, **35**, 5729-47.
119. Savage, J.R. (1976) Classification and relationships of induced chromosomal structural changes. *J Med Genet*, **13**, 103-122.
120. Rao, V.A., Conti, C., Guirouilh-Barbat, J., Nakamura, A., Miao, Z.-H., Davies, S.L., Sacca, B., Hickson, I.D., Bensimon, A. and Pommier, Y. (2007) Endogenous gammaH2AX-ATM-Chk2 Checkpoint Activation in Bloom's Syndrome Helicase-Deficient Cells Is Related to DNA Replication Arrested Forks. *Mol Cancer Res*, **5**, 713-724.
121. Fu, T.J., Tse-Dinh, Y.C. and Seeman, N.C. (1994) Holliday junction crossover topology. *J Mol Biol*, **236**, 91-105.
122. Ellis, N.A., Proytcheva, M., Sanz, M.M., Ye, T.Z. and German, J. (1999) Transfection of BLM into cultured bloom syndrome cells reduces the sister-chromatid exchange rate toward normal. *Am J Hum Genet*, **65**, 1368-74.